

SUSPENSION FIRING OF RESIDUE/COAL MIXTURES:
NO_x FORMATION AND CONTROL

by

Hossein Sadeghi Zamani

B.S., Kansas State University, 1980

A MASTER'S THESIS

Submitted in partial fulfillment of the
requirements for the degree

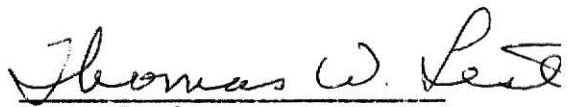
MASTER OF SCIENCE

Department of Nuclear Engineering

KANSAS STATE UNIVERSITY

Manhattan, Kansas

1983


Major Professor

LD
2668
.TY
1983
Z35
c.2

ALL202 575117

TABLE OF CONTENTS

	<u>Page</u>
LIST OF FIGURES.	ii
LIST OF TABLES	vi
1.0 INTRODUCTION.	1
1.1 General Considerations	1
1.2 Oxidation of Coal Nitrogen	4
2.0 SYSTEM DESIGN AND CONSTRUCTION.	12
2.1 Combustion Chamber	12
2.2 Air Supply System.	20
2.3 Solid Fuel Feeding Mechanism	24
2.4 Cooling System	27
2.5 Natural Gas Supply System.	27
2.6 Safety Systems	33
2.7 Burner Design.	39
2.8 Sample Collecting System	42
2.8.1 Gas Sampling System	42
2.8.2 Solid Sampling System	48
3.0 EXPERIMENTAL PROCEDURE.	51
3.1 Introduction	51
3.2 Unstaged Furnace Operation	52
3.3 Sampling During Unstaged Combustion.	55
3.4 Staged Furnace Operation	57
3.5 Sampling During Staged Combustion.	58
3.6 Miscellaneous Experimental Observations.	58
4.0 RESULTS AND DISCUSSION.	60
4.1 Unstaged Combustion.	60
4.1.1 Flue Gas Analysis	60
4.1.2 Axial Gas Analysis.	76
4.1.3 Axial Solids and Gas-Phase Compositions	76
4.2 Staged Combustion Gas Analysis	93
4.3 Summary.	104
REFERENCES	107
APPENDIX A. Probe Sampling Flowrate Calculations.	109
APPENDIX B. Energy Balance on Furnace System.	114
APPENDIX C. Calculation of Air Flowrate through the Funnel.	126
APPENDIX D. Flame Safeguard Unit.	128
APPENDIX E. Furnace Operation Procedure	131
ACKNOWLEDGEMENTS	138

LIST OF FIGURES

<u>Figure</u>		<u>Page</u>
1.1	Simplified Diagram of the Coal Nitrogen Conversion to NO_x (from Sarofim and Beér ⁶)	5
1.2	(a) % Char Nitrogen Converted to NO_x vs Fuel/Oxygen Equivalence Ratio (b) and Percent of Coal Nitrogen Converted to NO_x Against Fuel/Oxygen Equivalence Ratio (after Sarofim and Beér ⁶)	7
1.3	Percent of Volatile Nitrogen Converted to NO_x and % of Total NO_x Contributed by Volatile Nitrogen Versus Fuel/Oxygen Equivalence Ratio for Two Different Temperatures (after Sarofim and Beér ⁶)	8
2.1	Kansas State University Suspension Phase Furnace . .	13
2.2	Schematic Presentation of Combustion Facility. . . .	14
2.3	Cross-Sectional View of Combustion Chamber	15
2.4	Cross-Sectional View of the Staging Section.	18
2.5	Second Stage Combustion Air Supply Schematic	19
2.6	Air Piping Schematic	21
2.7	Solid Fuel Transport System Schematic.	23
2.8	Pre-Heater Electrical Service Hook-up.	25
2.9	Feeder Calibration Curve for Colorado Coal	28
2.10	Feeder Calibration Curve for Mo-Kan Coal	29
2.11	Feeder Calibration Curve for Illinois-6 Coal	30
2.12	Feeder Calibration Curve for Corn Stover	31
2.13	Feeder Calibration Curve for Wheat Straw	32
2.14	Gas Piping Schematic	34
2.15	Pilot Assembly	35
2.16	Main Gas Injector.	36
2.17	Concentric Burner.	40

<u>Figure</u>		<u>Page</u>
2.18	Solid Fuel Injector.	41
2.19	Sampling Probe Cross-Section	43
2.20	Gas Collection System Schematic.	44
2.21	Solid Collection System Schematic.	49
3.1	Temperature Profiles During Warm-up.	53
4.1	Flue NO _x Concentration for Colorado, Wheat Straw, and Mixtures vs. % Excess Oxygen.	61
4.2	NO _x Emissions and Estimated % Conversion of Fuel Nitrogen vs. % Excess Oxygen for Colorado Coal.	62
4.3	NO _x Emissions and Estimated % Conversion of Fuel Nitrogen vs. % Excess Oxygen for the Colorado/25% Wheat Straw Mixture.	63
4.4	NO _x Emissions and Estimated % Conversion of Fuel Nitrogen vs. % Excess Oxygen for the Colorado/50% Wheat Straw Mixture.	64
4.5	NO _x Emissions and Estimated % Conversion of Fuel Nitrogen vs. % Excess Oxygen for Wheat Straw	65
4.6	Flue NO _x Concentration for Colorado, Corn Stover, and Mixtures vs. % Excess Oxygen	66
4.7	NO _x Emissions and Estimated % Conversion vs. % Excess Oxygen for Corn Stover.	67
4.8	NO _x Emissions and Estimated % Conversion vs. % Excess Oxygen for the Colorado/25% Corn Stover Mixture	68
4.9	NO _x Emissions and Estimated % Conversion for Mo-Kan Coal.	69
4.10	Axial Temperature Profiles for Fuels Tested.	72
4.11	Ammonia Conversion to NO _x in Propane/NH ₃ Flame, and Char/Propane/NH ₃ Flame (after Pershing et al. ¹⁴)	74
4.12	Axial NO _x Distribution for Colorado, Wheat Straw, and Colorado/Wheat Straw Mixture.	77
4.13	Axial NO _x Distribution from Corn Stover.	78

<u>Figure</u>		<u>Page</u>
4.14	Axial NO_x Distribution from Mo-Kan Coal.	79
4.15	Axial % Burnout of Hydrogen, Nitrogen, and Carbon for Colorado Coal	81
4.16	Axial % Burnout of Hydrogen, Nitrogen, and Carbon for the Colorado/50% Wheat Straw Mixture.	82
4.17	Axial % Burnout of Hydrogen, Nitrogen, and Carbon for the Mo-Kan Coal.	83
4.18	Axial % Burnout of Hydrogen, Nitrogen and Carbon for Wheat Straw.	84
4.19	Axial % Burnout of Hydrogen, Nitrogen, and Carbon for Corn Stover.	85
4.20	Comparison of NO_x Emissions vs % Fuel Nitrogen (DAF) with Pershing, et al. ¹⁴	87
4.21	Axial Gas-Phase Composition for Colorado Coal	88
4.22	Axial Gas Phase Composition for the Colorado/50% Wheat Straw Mixture	89
4.23	Axial Gas Phase Composition for Wheat Straw	90
4.24	Axial Gas Phase Composition for Corn Stover	91
4.25	Axial Gas Phase Composition for Mo-Kan Coal	92
4.26	NO_x Emissions vs. First Stage Stoichiometric Ratio (SR_1) for Colorado Coal	94
4.27	NO_x Emissions vs. First Stage Stoichiometric Ratio (SR_1) for the Colorado/50% Wheat Straw Mixture	95
4.28	NO_x Emissions vs. First Stage Stoichiometric Ratio (SR_1) for Wheat Straw	96
4.29	NO_x Emissions vs. First Stage Stoichiometric Ratio (SR_1) for the Colorado/25% Corn Stover Mixture	97
4.30	NO_x Emissions vs. First Stage Stoichiometric Ratio (SR_1) for Corn Stover	98
4.31	Gas-Phase Distribution of Volatile Nitrogen Species at the Exit of the First Stage for a High Volatile B Bituminous Coal and a Lignite A (after Pershing, et al. ¹⁴).	100

LIST OF TABLES

<u>Table</u>		<u>Page</u>
2.1	Components of Gas Sampling System.	45
2.2	Calibration Gases.	46
3.1	Analysis of Fuels (Wt%).	54
A.1	Sampling Flowrates for Fuels Tested.	113
B.1	Layer Geometry and Thermal Conductivities.	118
B.2	Thermochemical Data.	121
B.3	Calculated Heating Values.	125

1. INTRODUCTION

1.1 General Considerations

Approximately 2000 municipal utilities in the Great Plains use natural gas as a boiler fuel. Now as a consequence of Federal legislation, the escalating price of natural gas, inadequate interconnections to the main power grid, and fierce local opposition to becoming wholly dependent on a distant utility, municipal governments have been motivated to search for alternative methods of maintaining their municipal electric utilities. The utilization of crop residue as a supplementary boiler fuel to pulverized coal has come under increasing inquiry as a possible solution to this problem. The use of these agricultural materials as supplementary fuels could have substantial impact on industries and small utilities which normally would have to use coal exclusively.

Very little work has been performed on assessing the environmental impact of using agricultural residues as supplementary boiler fuels. Specifically, environmental constraints may arise in two areas, agronomic and air quality. The first topic has been addressed in several recent, interdisciplinary studies at Kansas State University.⁽¹⁾ In the later study, an investigation into the feasibility of employing crop residues as boiler fuels for local utilities in communities with populations of six to twenty thousand people was conducted. This project focused especially on the use of wheat straw and cornstover as supplementary fuels and initiated the study of the NO_x emissions from the combustion of these fuels in a scale combustion chamber (5 K/g fuel/hr).

It was found that the amount of biomass available in the Great Plains depends strongly on the crop and soil conditions. Nevertheless, twenty percent of the material left in the field after grain, rice, and sugar cane harvesting could be used as a source of biomass. For instance, this implies that for an average crop yield in the United States, crop residue with an energy content of about 1.05×10^{15} KJ/yr could be collected and used for energy production without exceeding current soil erosion standards.⁽²⁾

Kansas farmers have planted in excess of 12 million acres of wheat per year, from which they have produced from 350 to nearly 450 million bushels of wheat annually. About 9 kilograms of wheat straw per bushel can be removed without serious damage to the soil. In the Kansas State studies, it was concluded that if approximately 4.99×10^5 T of wheat straw is needed to provide 20% of the heat input for a 35 MW(e) power plant having a capacity factor of 50%, adequate amounts of excess straw residue from area farms in Kansas would be available within a 25 mile radius of a number of municipal power plants. In total, the excess straw could provide five percent of the total energy requirements (1.7×10^{15} KJ) for Kansas.⁽³⁾

The other substitute fuel, coal, has been burned in utility boilers for steam electric-power generation since the early 1900s. In 1980 about 58 percent of the steam generated electrical energy was produced by burning coal.⁽⁴⁾ The U.S. Department of Energy (DOE) estimates that coal-fired electric utility generating capacity should more than double by 1995. Attendant to this increased use of coal and biomass are a plethora of environmental concerns. Of major impact are nitrogen oxide emissions from combustion, which are projected by DOE to be twice as

high in 2000 as in 1975.⁽²⁾ This concern is well founded, even though natural sources of nitrogen dioxide (from bacterial processes, fires, and volcanic activity) are estimated to be ten- to fifteen-fold greater than those from anthropogenic sources on a global basis. More so than SO_2 , NO_2 is known to be toxic at relatively high concentrations.⁽²⁾ However, very few studies have been conducted on the toxicity of urban levels of NO_2 , and as in most epidemiological studies of air pollution, the results are not conclusive.⁽²⁾ In the atmosphere, much of the NO_x may be converted to the very toxic intermediate, peroxyacetyl nitrate (PAN), and the most likely final product is nitric acid, a powerful oxidizing agent and strong acid. Nitric acid and its salts are therefore of concern with respect to health effects of inhaled particulates and as contributors to acid rain.

The term acid rain is somewhat a misnomer because it excludes other means whereby acids fall to earth, acid snow, sleet and hail and even fog. Moreover, pollutants in dry form fall to earth awaiting some future precipitation or other moisture to transform them into the same acids found in acid rain. The U.S. Environmental Protection Agency (EPA) estimates that nitric acid comprises about 25 to 30% of acidity in the precipitation in the Eastern United States, but may constitute as much as 80% of a localized rain's acidity in the Western United States.⁽⁵⁾

The suppression of nitric oxide emissions from stationary and mobile sources has been the subject of intense research for the past decade and a half. Particularly aggressive research programs have been conducted by the EPA's Combustion Research Branch and the DOE's Basic

Energy Sciences Program. To understand the processing of fuel nitrogen to NO_x , let us consider some of the research conducted under the auspices of these programs.

1.2 Oxidation of Coal Nitrogen

Work by Sarofim and Beér⁶ over the last decade has been concerned about the evaluation of fuel nitrogen during the heating of coal. When a pulverized coal particle is injected into a flame, it decomposes and the fuel bound nitrogen is split between the char and the volatile fractions. These volatile fractions are composed of tars and light gases, and it is assumed that tars further decompose after ejection from the coal particle producing gas-phase nitrogen compounds and soot.

In order to determine what fraction of total NO_x from fuel nitrogen is attributable to volatile oxidation and in order to determine the efficiency of conversion to NO_x of the nitrogen in char and the volatiles, Sarofim conducted a series of oxidation experiments in a laminar flow reactor where the temperature and excess air could be varied independently. A simplified diagram of his hypothesized conversion scheme is shown in Fig. 1.1. Based on this diagram the overall conversion of coal nitrogen is given by:

$$\eta^* = \alpha \eta_1 + (1-\alpha) \gamma \eta_2 \quad , \quad (1.1)$$

where

η^* = overall fuel nitrogen to NO_x ,

α = fraction of coal nitrogen released as volatiles,

η_1 = fraction of volatile nitrogen converted to NO_x ,

$(1-\alpha)$ = fraction of fuel nitrogen in the char,

**THIS BOOK
CONTAINS
NUMEROUS PAGES
WITH DIAGRAMS
THAT ARE CROOKED
COMPARED TO THE
REST OF THE
INFORMATION ON
THE PAGE.**

**THIS IS AS
RECEIVED FROM
CUSTOMER.**

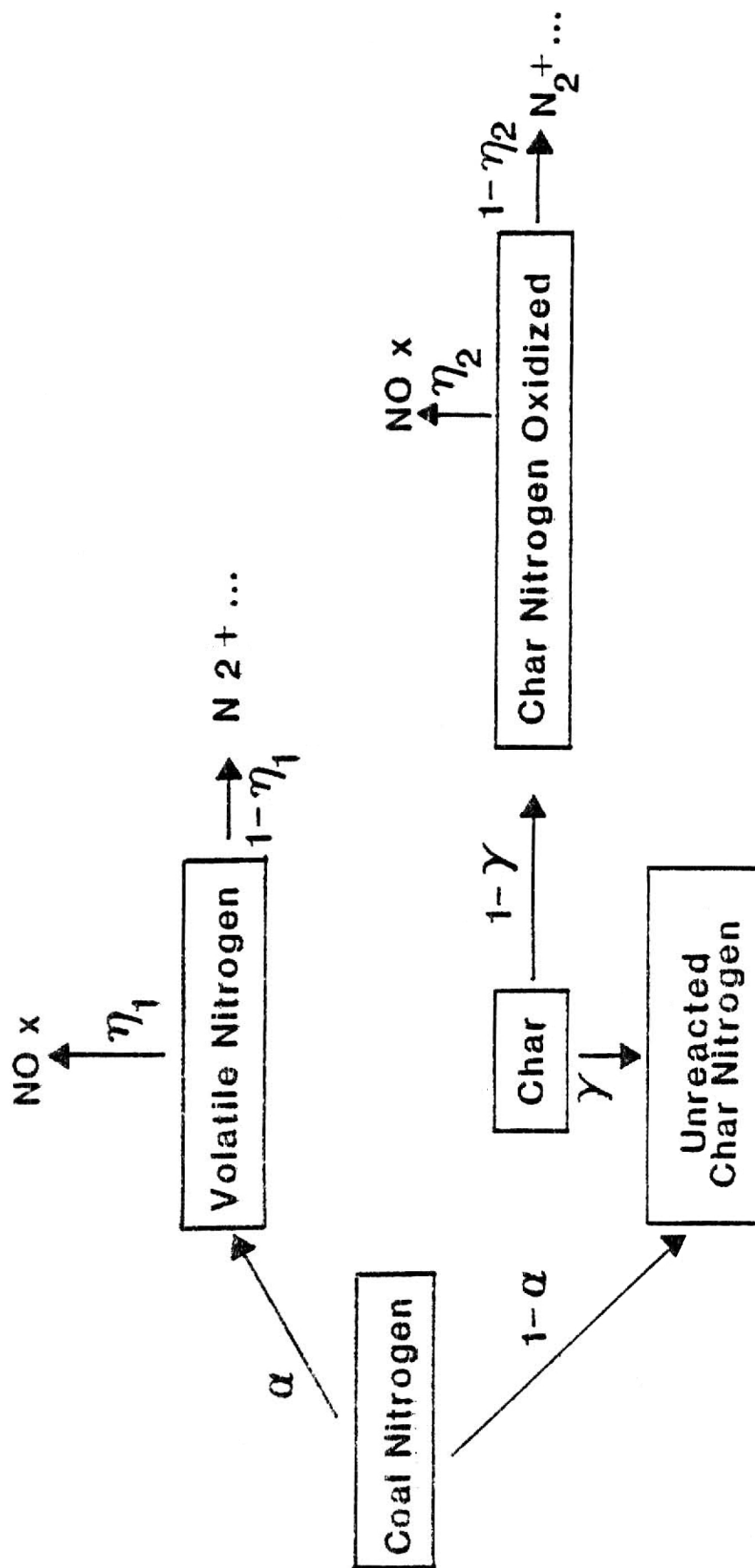


Fig. 1.1 Simplified Diagram of the Coal Nitrogen Conversion to NO_x (from Sarofim and Beér⁶)

γ = fraction of char nitrogen consumed,

$\gamma\eta_2$ = fraction of char nitrogen converted to NO_x .

In order to identify the contribution of the different pathways to NO_x conversion the following experiments were performed by Sarofim:

- 1) An oxidation experiment at the equivalence ratio and temperature of interest (1750 K) to determine the overall nitrogen conversion, η^* .
- 2) A devolatilization experiment at the same temperature to determine the fraction of the nitrogen, α , evolved as volatiles for a residence time corresponding to the combustion time.
- 3) The oxidation of char collected from the devolatilization experiments at the temperatures and equivalence ratio of interest in order to determine both the fraction γ of the char that burns, and the fractional conversion η_2 of the nitrogen in the char to NO_x .

The results obtained from above experiments are shown in Fig. 1.2. The conversion of coal nitrogen to nitric oxide falls from 40% under lean conditions to about 10% under slightly fuel rich conditions (Fig. 1.2.a). The percent of char nitrogen converted to NO_x decreases from 30% at lean flame conditions to less than 5% as the flame becomes richer. From the results of the above experiments, and similar experiments at 1250 K, the fraction of the total NO_x contributed by the oxidation of devolatilized nitrogen compounds ($\alpha\eta_1$) and the fraction of the volatile nitrogen are shown in the same Fig. 1.3. It can be seen that at the higher combustion temperature of 1750 K, the majority, but not all, of the NO_x is contributed by the volatiles, while at 1250 K,

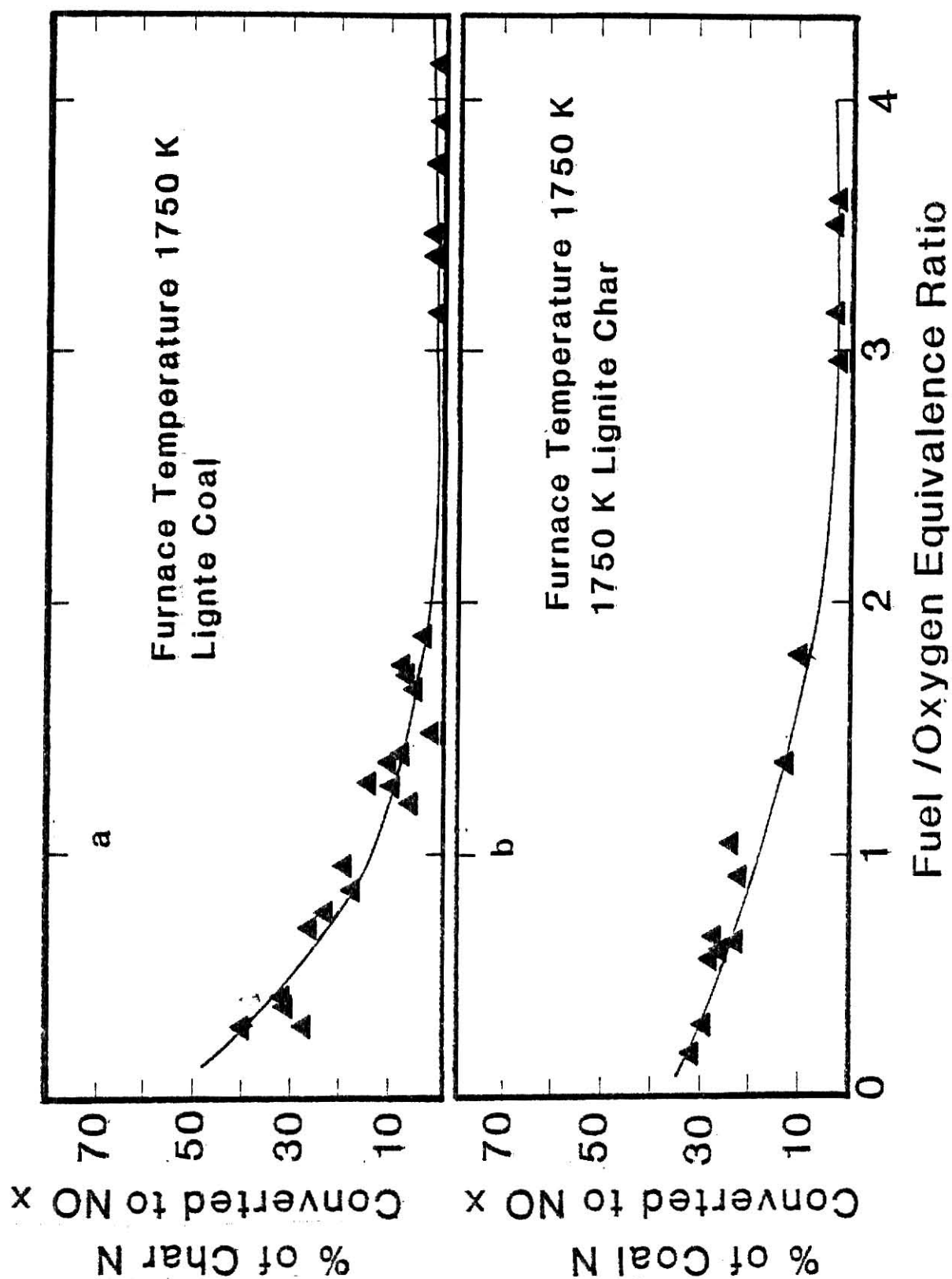


Fig. 1.2 (a) % Char Nitrogen Converted to NO_x vs Fuel/Oxygen Equivalence Ratio (b) and Percent of Coal Nitrogen Converted to NO_x Against Fuel/Oxygen Equivalence Ratio (after Sarofim and Beér⁶)

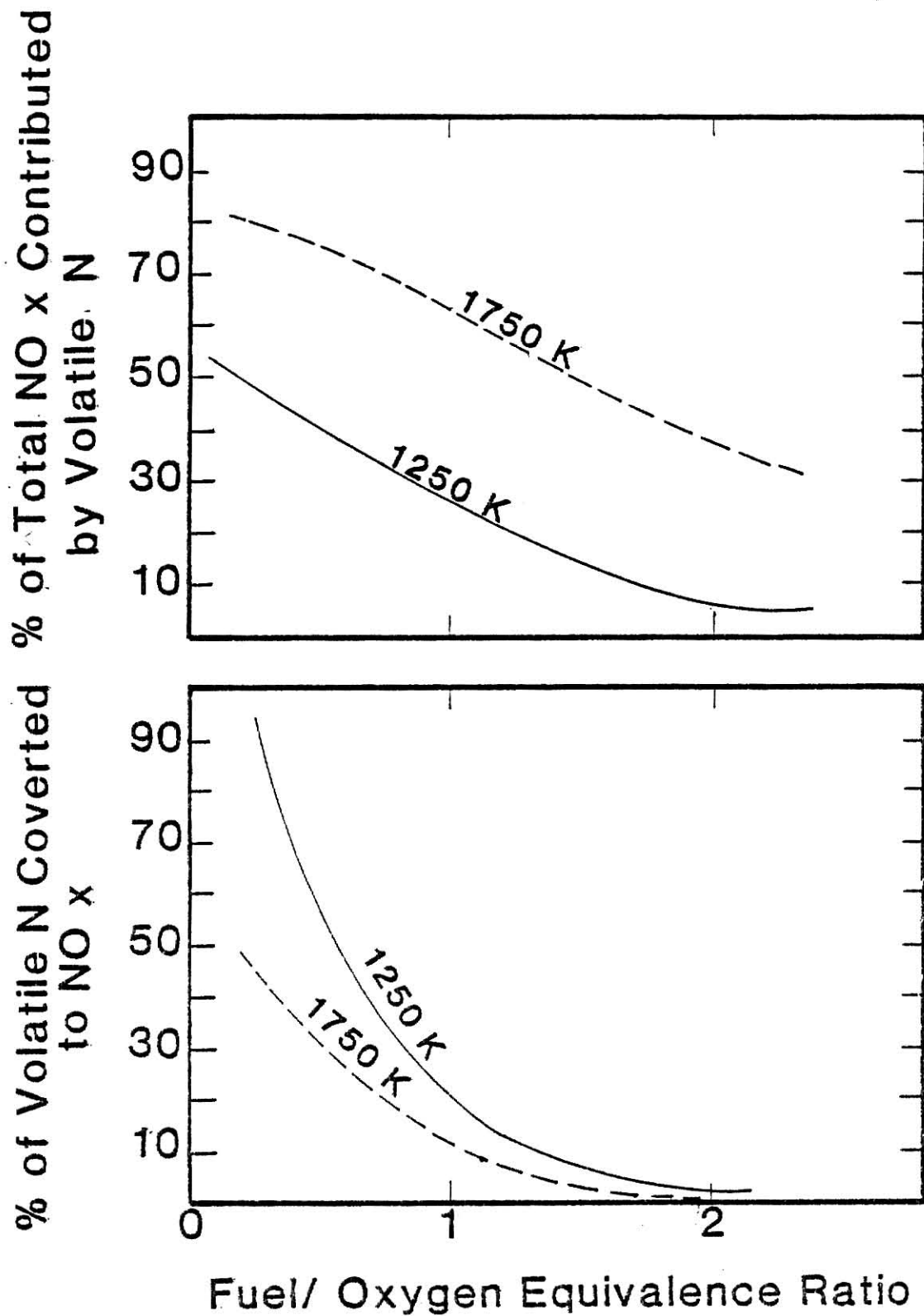


Fig. 1.3 Percent of Volatile Nitrogen Converted to NO_x and % of Total NO_x Contributed by Volatile Nitrogen vs. Fuel/Oxygen Equivalence Ratio for Two Different Temperatures (after Sarofim and Beér⁶)

the volatiles contribute less than half of the total NO_x . The conversion η_1 of the volatile nitrogen to NO_x decreases with increasing equivalence ratio and with decreasing temperature.

Not all the NO_x formed in the combustion arises from fuel nitrogen, however. The fixation of atmospheric nitrogen, termed thermal NO_x , is also important. The formation of thermal NO_x has been shown to follow the Zeldovich⁽⁷⁾ mechanism through which formation depends exponentially on temperature and has a reaction order of 1/2 with respect to oxygen⁽⁸⁾, i.e., is proportional to the square root of the oxygen concentration. The two reactions postulated by Zeldovich are:



where Glassman indicates that the chain is initiated either by the dissociation of O_2 or by H atom attack on O_2 . Pershing et al.⁽⁹⁾ used oxygen diluted with argon to determine that the fuel-bound nitrogen contributed approximately 80% of the total NO_x emissions from pulverized coal combustion, and that thermal NO_x constitutes the balance.

The effects of flame temperature, coal composition, and the burner configuration on NO_x formation, especially fuel NO_x , have been investigated by Pershing et al.,⁽⁹⁾ Wendt and Pershing,^(10,11) and Heap, et al.^(12,13) Their conclusions are:

- 1) NO_x control schemes aimed at lowering the flame temperature are effective in reducing thermal NO_x , but relatively ineffective in combating fuel NO_x ;

- 2) Fuel NO_x is most effectively reduced by forcing the ignition and early stages of combustion to proceed in a fuel rich atmosphere;
- 3) In staging, the total NO_x levels will depend upon the nitrogen content of the volatiles and the char, present at the exit of the first stage.

A major emphasis of this study is to ascertain the extent to which wheat straw and cornstover behave like coal in the production of NO_x . The fuel properties of agricultural residue are closest to lower rank fuels such as lignite (high volatile, low fixed carbon, and high oxygen content). Fuel NO_x formation as a function of percent nitrogen (on a dry ash-free basis), as determined by Pershing,⁽⁹⁾ is shown in Fig. 1.4. In general, fuel NO_x emissions increase with increasing fuel nitrogen content.

As noted above, one of the most successful NO_x control technologies available is staged combustion. In the staged combustion mode, fuel-rich and fuel-lean regions of combustion are segregated through externally divided air ports rather than through flame aerodynamic control. A fuel rich zone in the furnace allows partial oxidation of the fuel and, presumably, devolatilization of nitrogeneous species in an oxygen-deficient environment. This is followed by a fuel-lean zone in which the unburnt fuel is combusted, but in which the temperatures are sufficiently low so that thermal NO_x formation is insignificant.

The purpose of this project is to determine the firing and NO_x formation characteristics of the suspension firing of wheat straw and corn stover. Specifically under what conditions can the conversion of fuel-bound nitrogen in these agricultural materials to NO_x be minimized?

The test facility, a fully instrumented, scale model furnace can be fired both staged and unstaged, and is capable of simulating the conditions in the primary flame zone of a suspension fired furnace. Both on-line and batch sample analysis of the gas products can be performed to determine NO_x , O_2 , CO , CO_2 , and solid elemental composition in both the flue and at various axial locations of the furnace. Chapter 2 covers the details of the experimental facility. Chapter 3 and associated appendices detail the facility operation, and Chapter 4 discusses the experimental results.

2.0 SYSTEM DESIGN AND CONSTRUCTION

The design of this facility is patterned after the solid fuel furnaces constructed by Pershing.⁽⁹⁾ It is designed to fire a wide range of solid fuels in both staged and unstaged combustion. The furnace, shown in Fig. 2.1, has an overall length of 190 cm, an outer diameter of 40.64 cm and an inner diameter of 15.24 cm. The diameter at the staging choke is 5.08 cm.

The furnace has been designed to simulate as closely as possible the residence time in conventional scale facilities. The facility can be divided into eight components, as shown in Fig. 2.2. These are the combustion chamber, the air supply system, the solid fuel feeding mechanism, the cooling system, the natural gas supply system, the safety system, the sampling probe, and finally the burner configuration.

2.1 Combustion Chamber

The combustion chamber, shown in Fig. 2.3, is 152.4 cm in length and has a 15.24 cm inside diameter. It is mounted vertically with its bottom approximately 160 cm above the floor to permit insertion of a sampling probe from the bottom. Solid fuel is introduced from the top, and the combustion products exit through the flue located at the bottom of the combustion chamber. The feeding mechanism is described in detail in Section 2.3. The flue exit is 304 stainless steel pipe of about 11.4 cm inside diameter, and is centered 17.5 cm above the bottom of the chamber. At the end of each experiment, after the chamber is cool enough, the plug that is bolted to the bottom of the chamber is removed for the removal of ash and melted slag. To assure that there are no ash deposits along the horizontal section of the flue, a mirror is used for

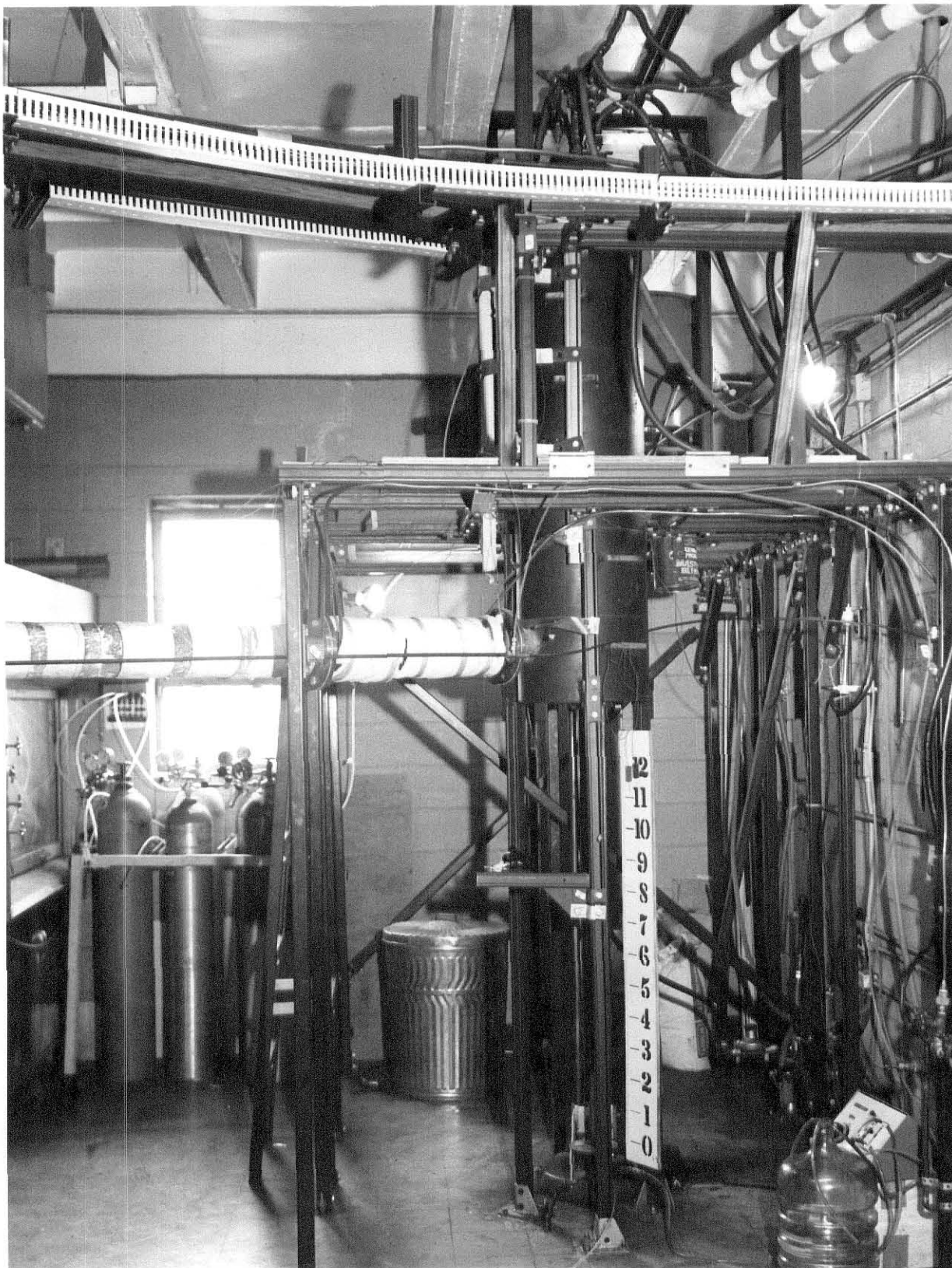


Fig. 2.1 Kansas State University Suspension Phase Furnace

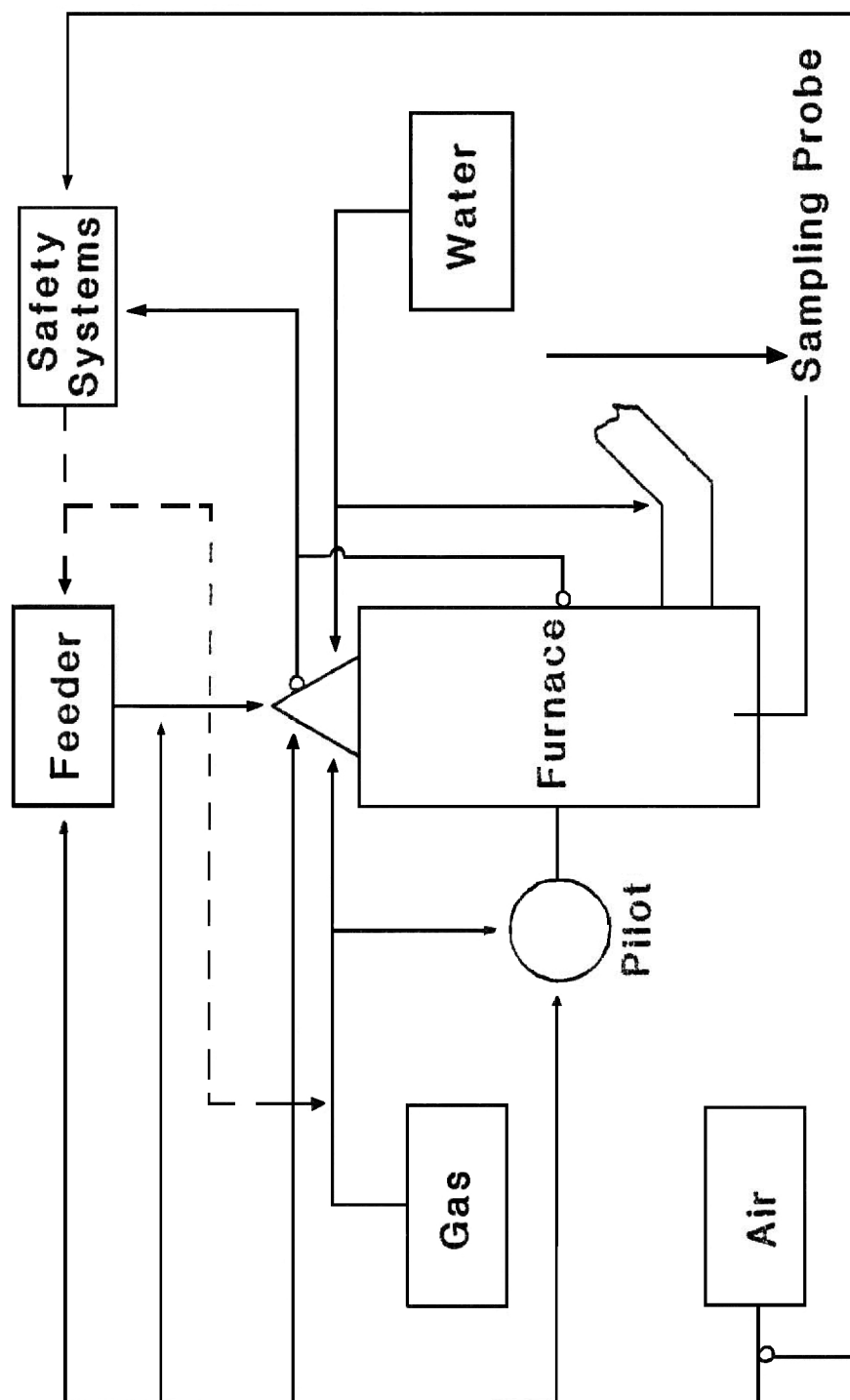


Fig. 2.2 Schematic Presentation of Combustion Facility

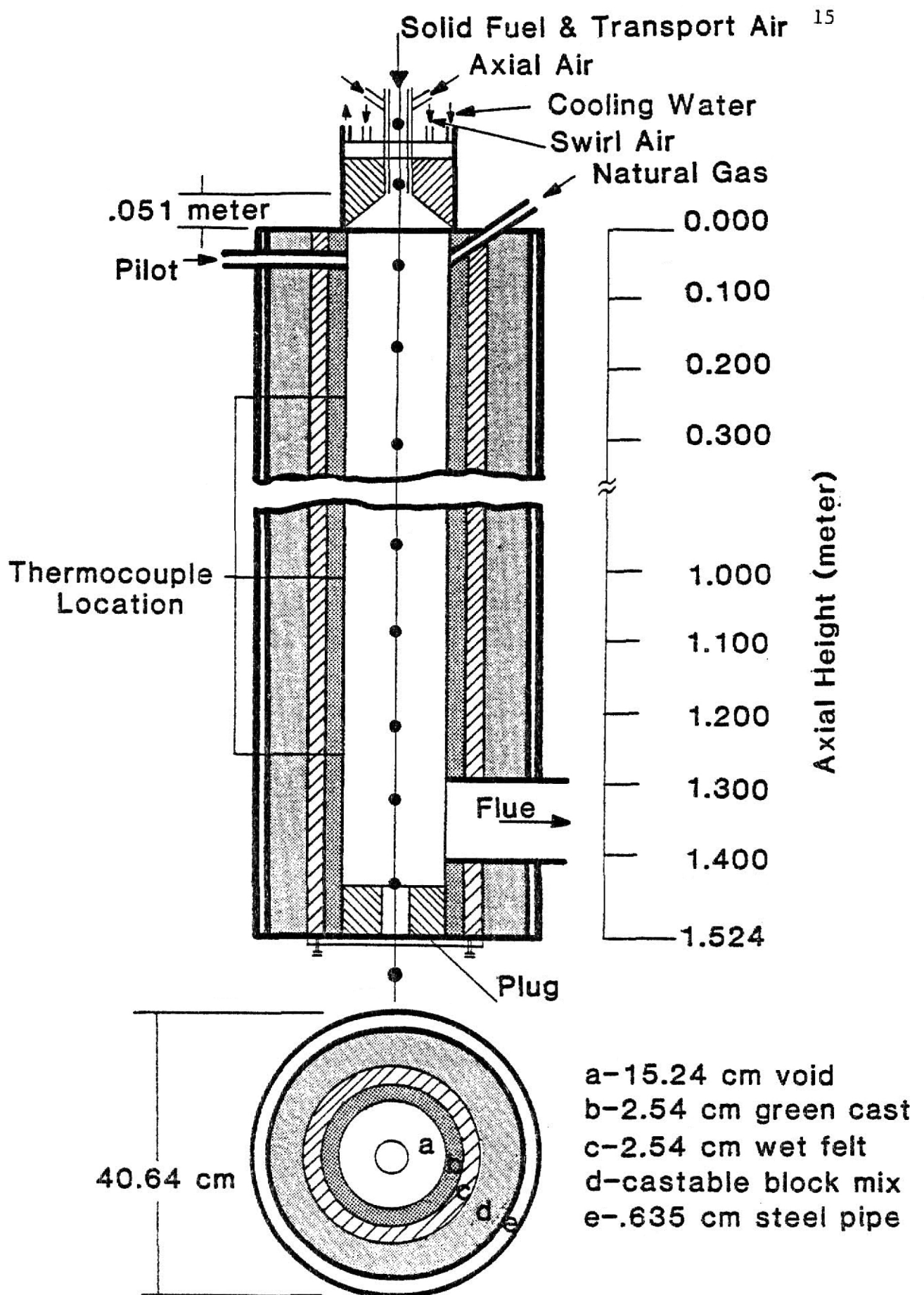


Fig. 2.3 Cross-Sectional View of Combustion Chamber

periodic inspection. The ash build-up is insignificant unless a very high ash coal, such as Missouri-Kansas coal, is used. Then cleaning must be performed using a flexible rod and rags to push the ash down on the floor of the combustion facility room. The flue is encircled with 0.64 cm i.d. soft copper tubing to facilitate heat removal from the combustion gases. The entire length of the flue is covered with Babcock and Wilcox Kaowool ceramic fiber insulation for the protection of laboratory personnel.

Fig. 2.3 also shows the furnace wall structure. The inner wall is constructed of 2.54 cm thick green cast with a 1600 K operating temperature. This is surrounded by a 2.54 cm thick layer of Babcock and Wilcox Kaowool ceramic fiber insulation which is rated to a temperature of 1450 K. Finally, a 6.98 cm thick layer of castable block from A. P. Green Refractory Company is used for insulation purposes. The outer wall of the furnace is made of 0.95 cm thick black steel pipe, divided into six sections of equal lengths of 25.40 cm. The refractory sections were formed individually. The joints were machined such that adjoining sections would interlock to minimize leaks from the furnace. During operation, the outer wall temperature is approximately 400 K. The heat transfer through the furnace wall is discussed in Appendix B.

An observation window of 2.54 cm diameter and located 5 cm from the top of the furnace, is kept free from soot and other deposits by a continuous purge of nitrogen gas of 1 liter/min. The flame can be seen through this window from the control room.

The inside wall temperature of the furnace is monitored using Pt/Pt-10% Rh thermocouples. Thermocouples are positioned every 25.4 cm along the length of the furnace (see Fig. 2.3), and penetrate into the

wall to a point within about 0.65 cm of the inside wall. The temperatures are displayed on an Omega Engineering model 2160A digital thermometer, and the thermocouple selection is made via an Omega Engineering model OSW5-24 24 Pole thermocouple selector switch, both mounted on the control panel.

An ultra-violet detector is located at the very top of the furnace where the flame is stabilized. It is mounted at a downward angle to help prevent accumulation of soot and particulate matter. The flame detector, which is an integral part of the furnace safety system, is discussed in more detail in Section 2.6.

There are two other openings at the top of the furnace. The pilot burner, which is located horizontally about 5.5 cm from the top of the chamber, and the main gas burner, which is located at the same height on the opposite wall, are discussed further in Section 2.5.

Staged combustion is accommodated by removing the midsection of the combustion chamber and replacing it by another section of the same height, but with an inner diameter of 5.08 cm. Fig. 2.4 shows the cross-sectional and the top views of the staged section. The structural materials used in this section are the same as those used in the other sections of the furnace wall. Second stage air is supplied through four 1.27 cm i.d. steel pipes (see Fig. 2.5). The pipes are of equal length to promote equal air flow rates. Four inlets of 0.64 cm i.d. are located 7.62 cm below the choke's exit. The inlets, which are reduced, provide most of the pressure drop in each leg and thus insure that the flow rate of the second stage air is equally distributed.

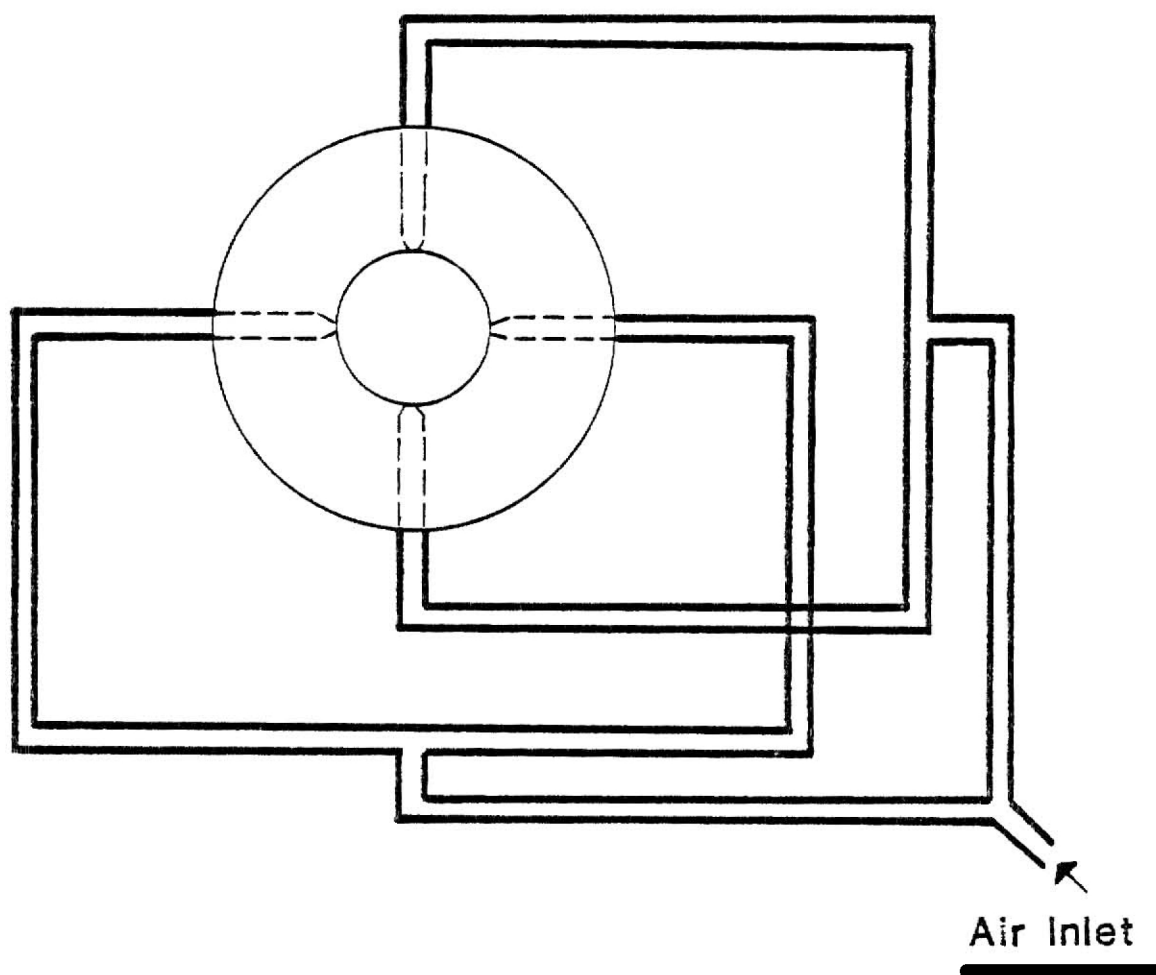


Fig. 2.5 Second Stage Combustion Air Supply Schematic

2.2 Air Supply System

Compressed air is used as the oxidizer in both the pilot and main flames, and serves as a control for the speed of the solid fuel feeder. The air system schematic is shown in Fig. 2.6. The source of compressed air is a Kellogg model 340 B air compressor rated to have a 1.37×10^4 cm^3/sec free air capacity at 652.6 KPa. The compressor is equipped with an inlet valve unloader that allows the motor to turn with no load whenever the pressure in the storage tank is above a predetermined level. This allows for cooler engine operation and a longer motor life than would be possible if the motor cycled with the tank at high pressures. A flexible insulated hose of 12.70 cm i.d. is used to supply the atmospheric air to the compressor. This supply is ducted off the Ward Hall air conditioning system. This configuration sharply reduces the water accumulation in the compressor tank and the combustion air supply line. The storage tank outlet is equipped with a manual valve at the entrance to the supply line. The air is filtered through a Schrader model 3536-1000 filter to remove oil, water, and other impurities. To collect any remaining moisture or oil in the supply air, a Beach Precision Parts Co. model 65-L filter is used. After filtering, the pilot air separates from the main air supply and passes through a normally closed 110 V solenoid valve and a Hoke model 5133F8A low pressure regulator, adjustable from 8.9 to 352 cm H_2O above atmospheric pressure, and finally to the pilot assembly.

A Ranco type 010 low pressure disconnect switch is located in the supply line immediately past the pilot air branch point. The operation of this device is explained in Section 2.6. Another branch separates

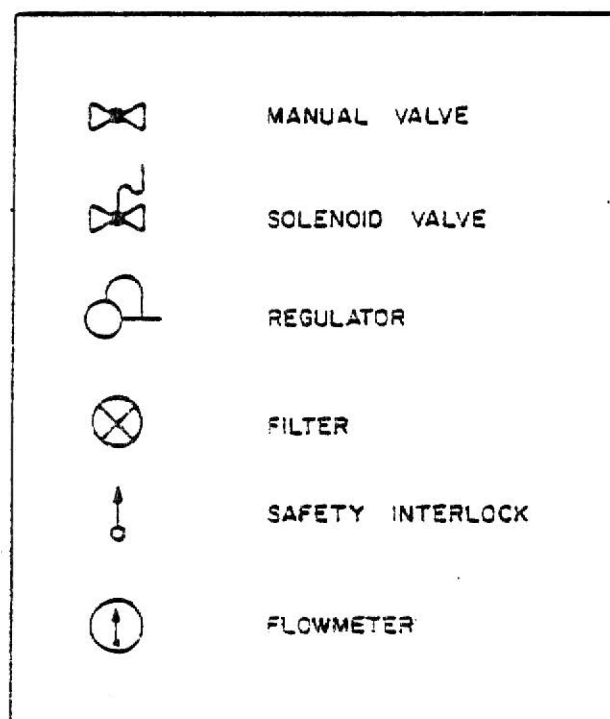
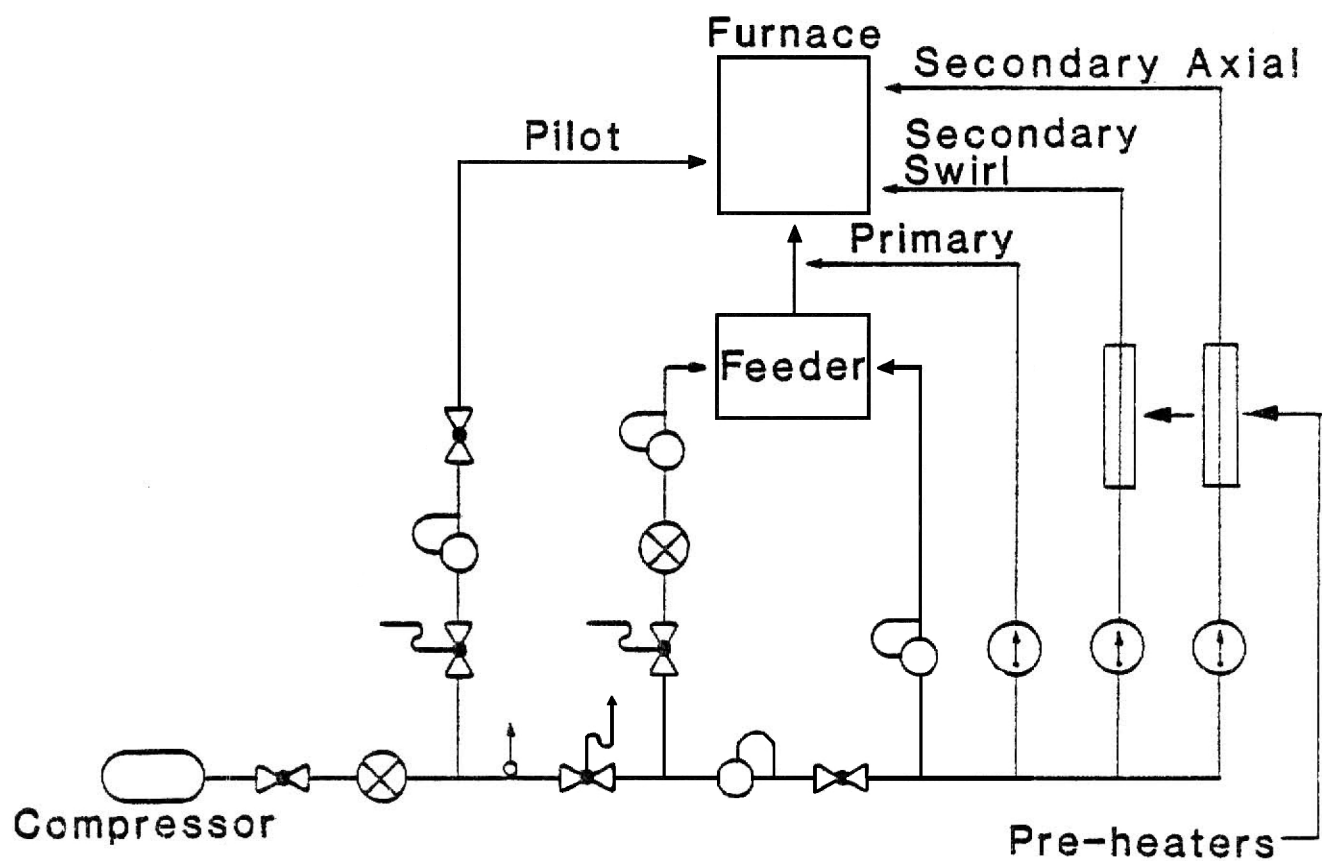


Fig. 2.6 Air Piping Schematic

downstream of the disconnect and passes through a normally closed solenoid valve to a Moore model 91F-60 adjustable air regulator and filter. The pressure of the line, which is maintained at 445.9 KPa, serves as the reference air pressure for the solid fuel feeder's pneumatic speed control. This will be explained further in Section 2.3.

The main air supply line pressure is reduced to 273.6 KPa by a Schrader model 3566-1000 variable air pressure regulator. The line terminates with a manual ball valve under the equipment control panel, after which four separate air lines diverge. One passes through a Watts model 362-2 variable air regulator and gauge positioned on the control panel, and proceeds to the solid fuel feeder where it serves as the control air line for the pneumatic speed regulator. The remaining three air lines supply combustion air to the furnace, and pneumatically transport the solid fuel to the combustion chamber.

The solid fuel transport mechanism is shown in Fig. 2.7. The solid fuels, at atmospheric pressure, fall into a funnel, which is soldered to a 1.27 cm i.d. copper tube. The other end of the tube is placed at the throat of a 2.54 cm i.d. copper tube, where the air velocity is maximum and pressure at its minimum. The solid fuel transport air is termed the primary air, and it is metered by a Dwyer RMB Ratemaster Flowmeter calibrated from 944 to 9440 cm^3/sec of air. Flow through the two secondary air lines is metered by a Dwyer RMC Ratemaster Flowmeter calibrated from 472 to 4720 cm^3/sec of air. In addition to the air flow through the flowmeters there is another source of combustion air, which is drawn in through the funnel by the passage of the primary air through the throat. The procedure for the calculation of that flow rate is detailed in Appendix C.

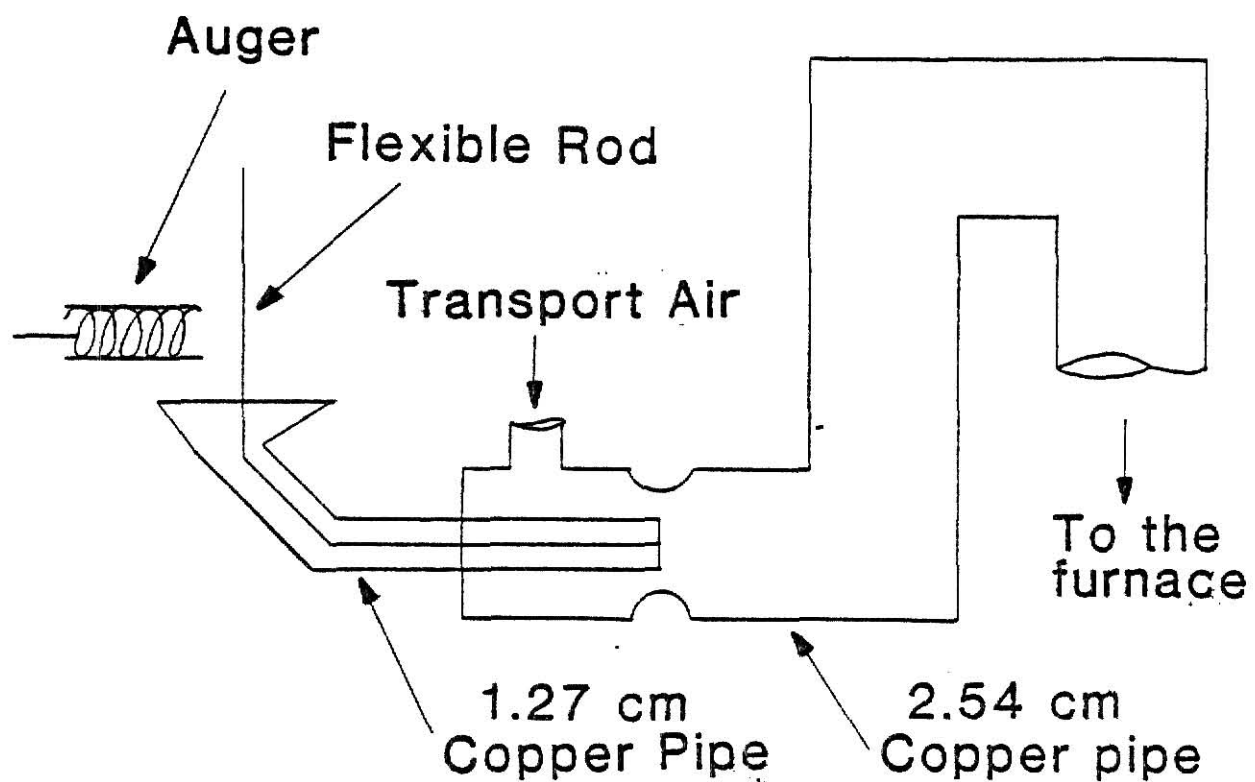


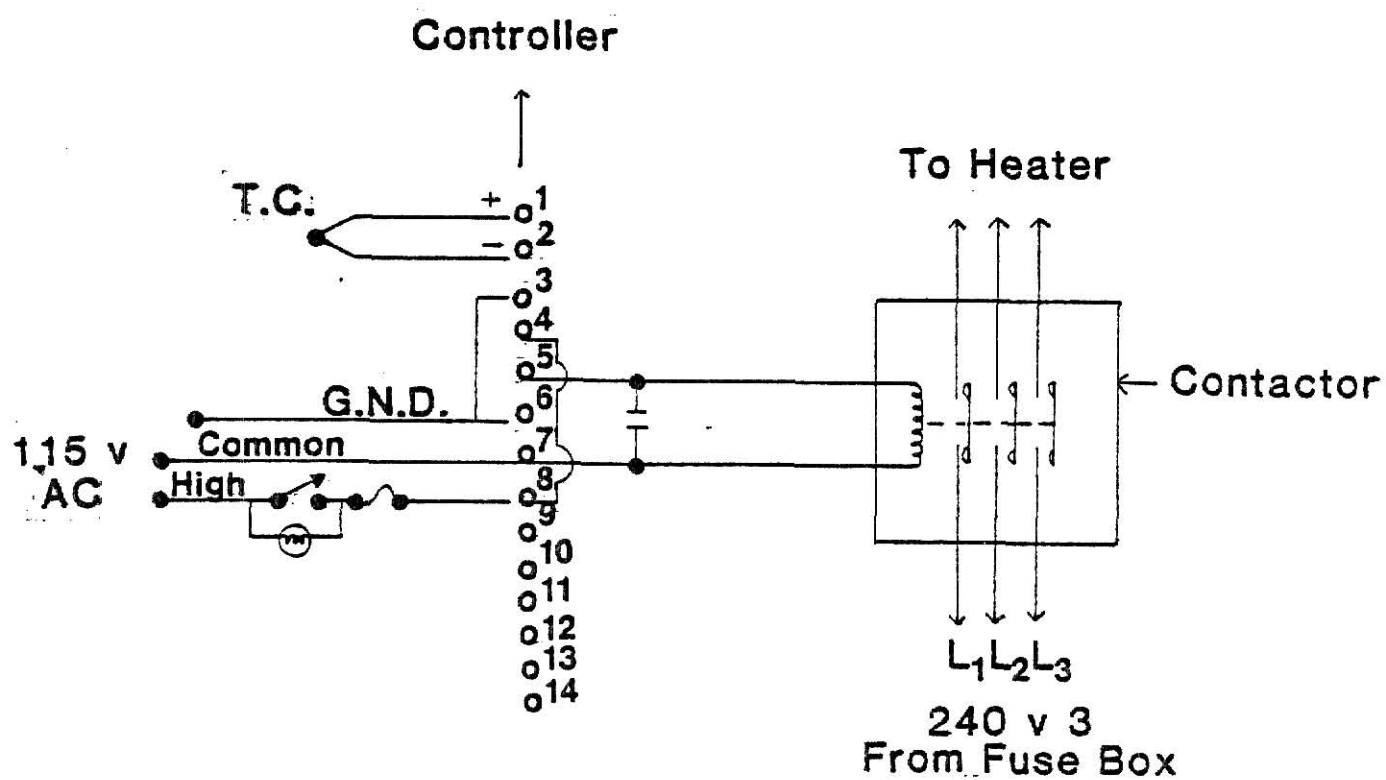
Fig. 2.7 Solid Fuel Transport System Schematic

Two air pre-heaters manufactured by Chromalox, model GCH-60905, were used to pre-heat the axial and swirl air. They are mounted vertically against the wall of the furnace room close to the burner, to minimize convective heat loss from the air supply lines. The maximum power output of the pre-heaters is 9 KW, and the temperature range is 422-644 K. A Chromalox on-off control, model J03 equipped with solid-state circuitry, is used to control the pre-heaters' temperatures. Figure 2.8 shows the electrical diagram of this controller.

Routine maintenance of the air system is required to insure reliable operation. To this end, daily procedure calls for the replacement of all air filter elements followed by drying in an oven for the next operating day, the checking of the compressor oil level, the draining of the condensate from the air storage tank, and the testing of the high pressure safety valve.

2.3 Solid Fuel Feeding Mechanism

The major components of the solid fuel mechanism are the screw feeder and the solid fuel transport system. The screw feeder is a pre-assembled unit manufactured by the Vibra Screw Company and generously offered to this research on an indefinite loan basis. It includes a $8.5 \times 10^4 \text{ cm}^3$ dust-sealed live-bin, so named because of the vibrating action designed to force all material to settle to the bottom of the bin, a 1.27 cm i.d. stainless steel pipe containing an auger of spring steel to transfer the pulverized fuel to the furnace, and a pneumatic speed control mechanism. The latter is comprised of a valve positioner with an internal diaphragm separating two chambers of different pressure. On the reference side of the diaphragm a pressure



Pre-Heater Hook-Up

Fig. 2.8 Pre-Heater Electrical Service Hook-up

of 445.9 KPa is maintained, while the pressure on the control side may be varied from 122.0 to 204.7 KPa. Adjustment of the control pressure causes the diaphragm and an attached piston to shift position. The piston causes the width of the groove of a variable width pulley to change, which effectively varies the diameter of the pulley. The bolt riding the pulley is forced to move either away from or toward the axis, and varies the feeder speed.

The electrical requirements of the feeder are 220 V three phase, which is provided through flexible conduit so that the vibratory motion does not damage the connection. The feeder also has an electrical tachometer mounted in an explosion-proof case at the equipment control panel.

The feeder is mounted on a 224 cm high scaffolding constructed of uni-strut structural steel material (see Fig. 2.1). The feeder is situated such that the end of its delivery tube is located above the funnel of the solid fuel transport system, as shown in Fig. 2.7.

The feeder delivery tube feeds the solid fuel directly into the funnel while a flexible rod of 0.32 cm diameter is rotated by an a.c. motor positioned above the axis of the funnel. The rod extends to the throat of the fuel transport system. The flexible rod is used to crush the chunks of solid fuel to prevent clogging in the funnel. The transport air, which is controlled on the control panel, passes through an air filter to absorb any moisture left in the line and then to the throat where the pressure is the smallest as predicted by the Bernoulli equation.

The solid fuel output rate of the feeder was found to vary with the fuel used and with the fuel conditions. It is sensitive especially to

high ash and moisture. Figures 2.9-2.13 show the calibration curves for different coals and biomass fuels. The measurements were made by collecting the solid at the exit of the feeder's delivery tube for approximately 60 seconds.

2.4 Cooling System

Water is used to cool the burners, the gas sampling probe, and to withdraw heat from the first section of the flue. The temperature within the combustion chamber usually exceeds 1400 K; therefore, if cooling were not provided to metallic parts, their thermal destruction would quickly result. The gas sampling probe in the flue is enclosed by a water jacket.

The water flow rate for the probe was not measured, but periodic checks of the exit water of the probe were made with a thermometer during the operation to provide some assurance that the probe was sufficiently cool to avoid structural damage.

The water flowrate to the main burner is ensured by both an electrical water flow control sensor, which is set for a specific flowrate, and a thermocouple located on top of the burner. If the water flowrate drops below the predetermined level, or the thermocouple records a burner temperature above a predetermined level, the flame immediately extinguishes before any thermal destruction of the burner takes place.

2.5 Natural Gas Supply System

Natural gas is used for both a main flame, which heats the combustion chamber in preparation for solid fuel firing, and as a stabilizing pilot flame for the solid fuel. In addition, the system is

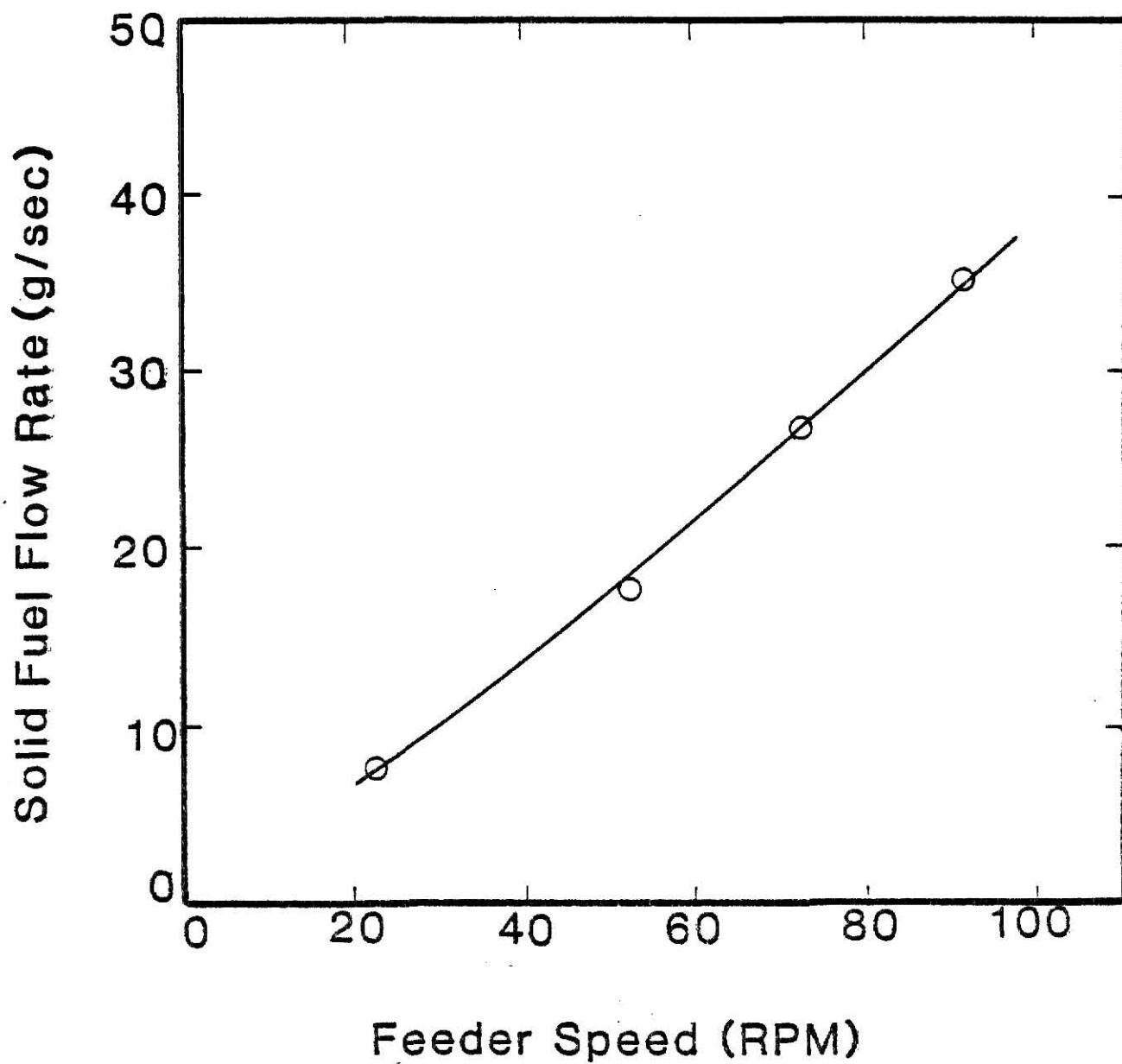


Fig. 2.9 Feeder Calibration Curve for Colorado Coal

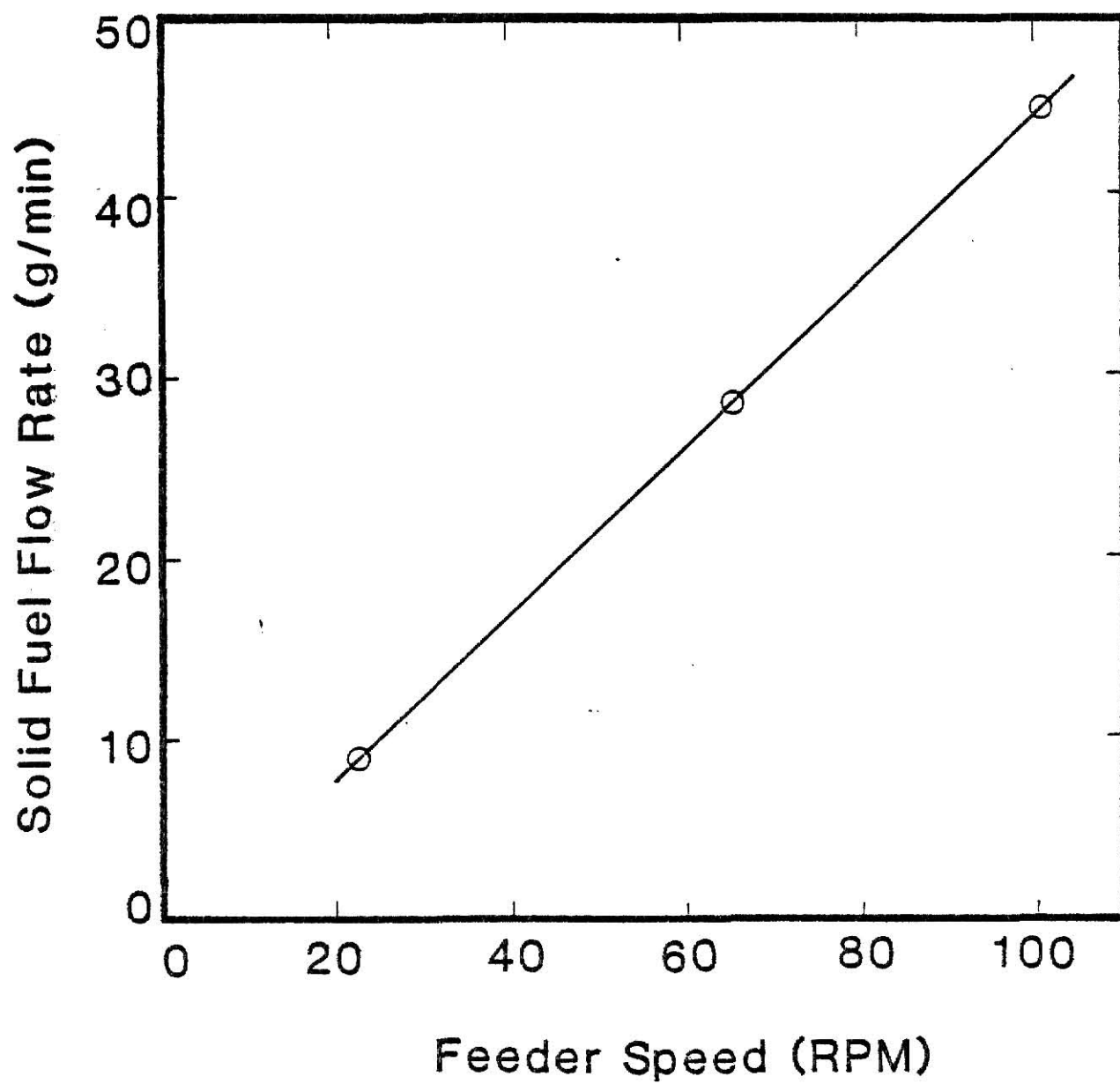


Fig. 2.10 Feeder Calibration Curve for Mo-Kan Coal

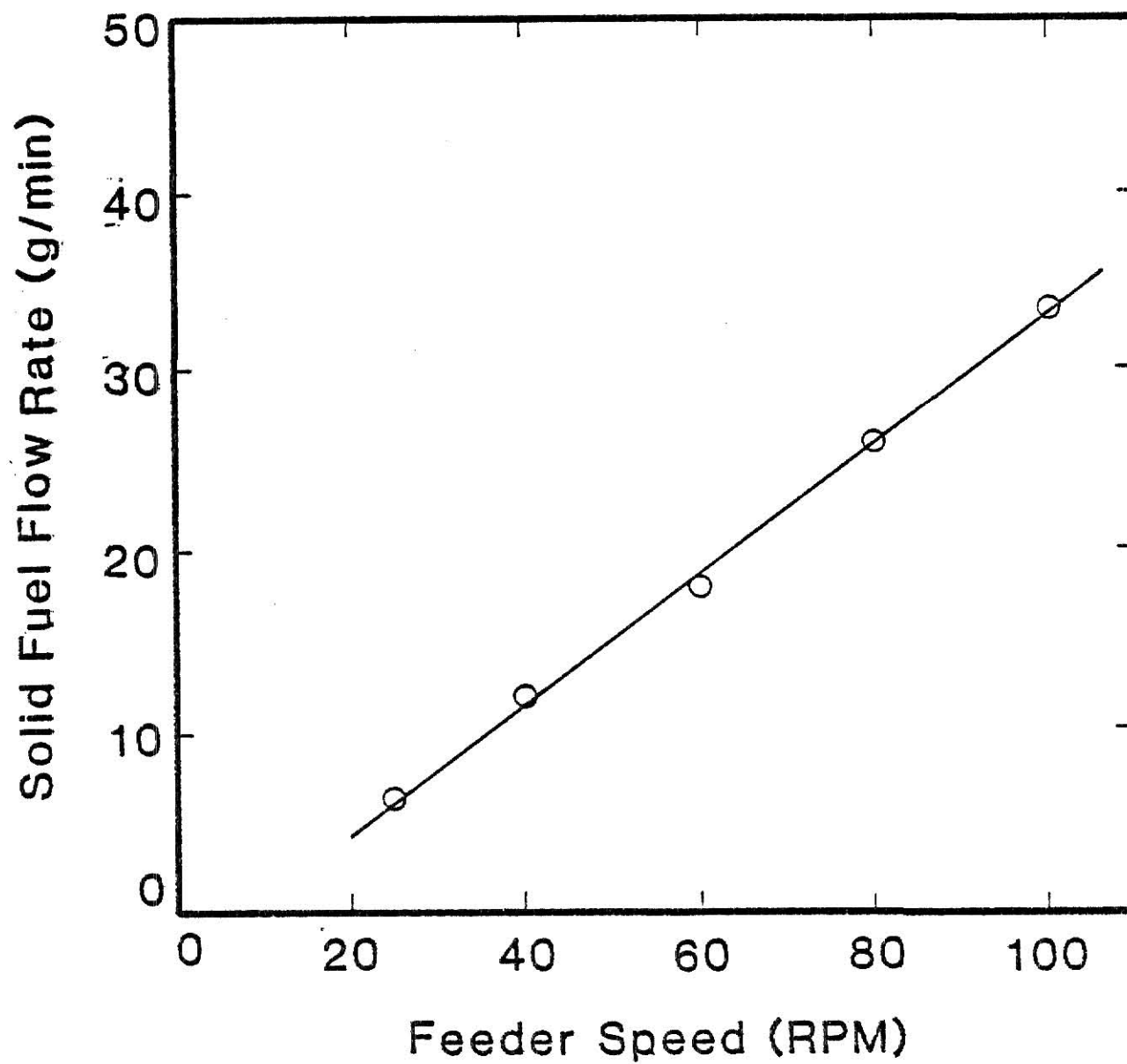


Fig. 2.11 Feeder Calibration Curve for Illinois-6 Coal

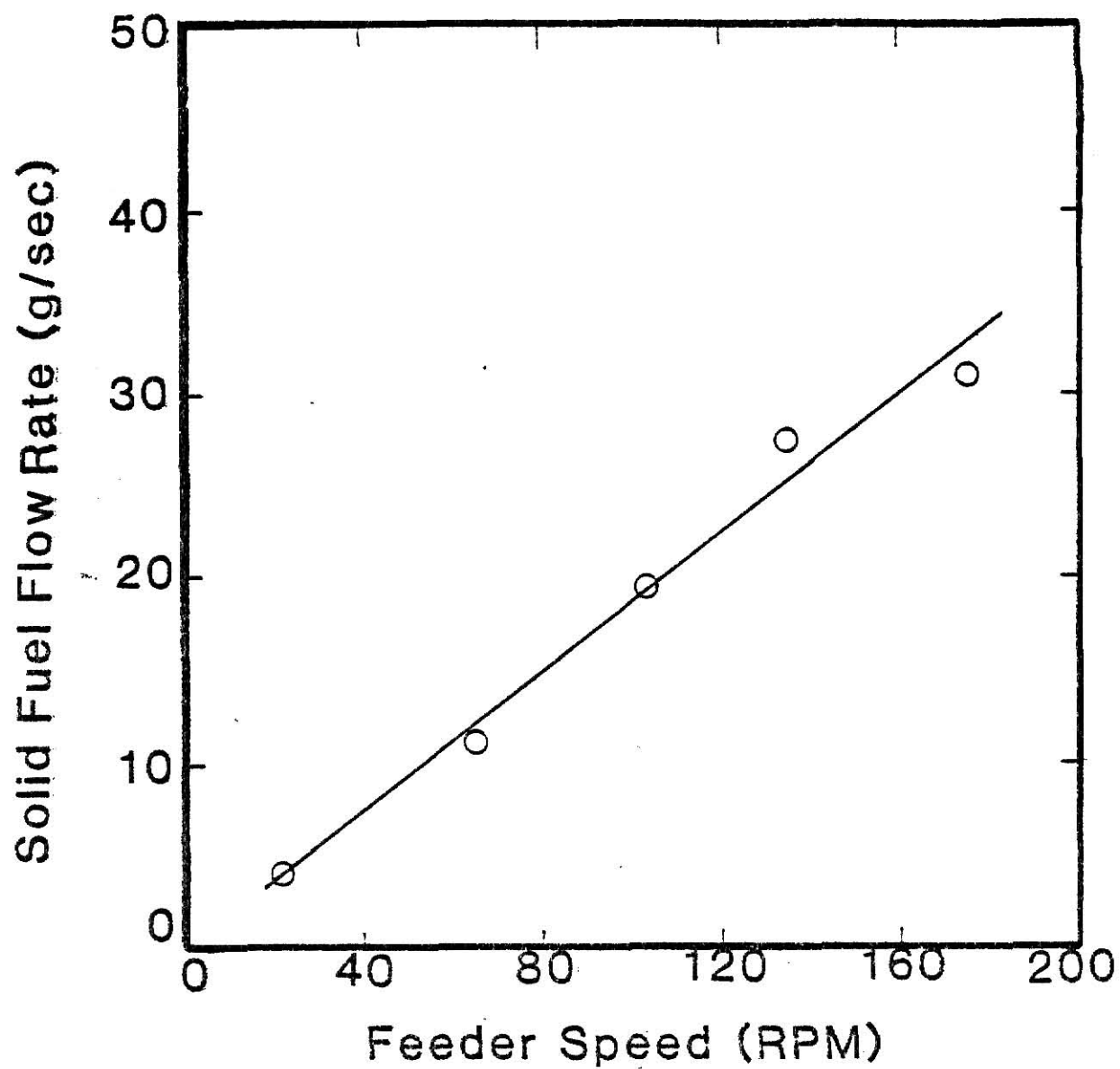


Fig. 2.12 Feeder Calibration Curve for Corn Stover

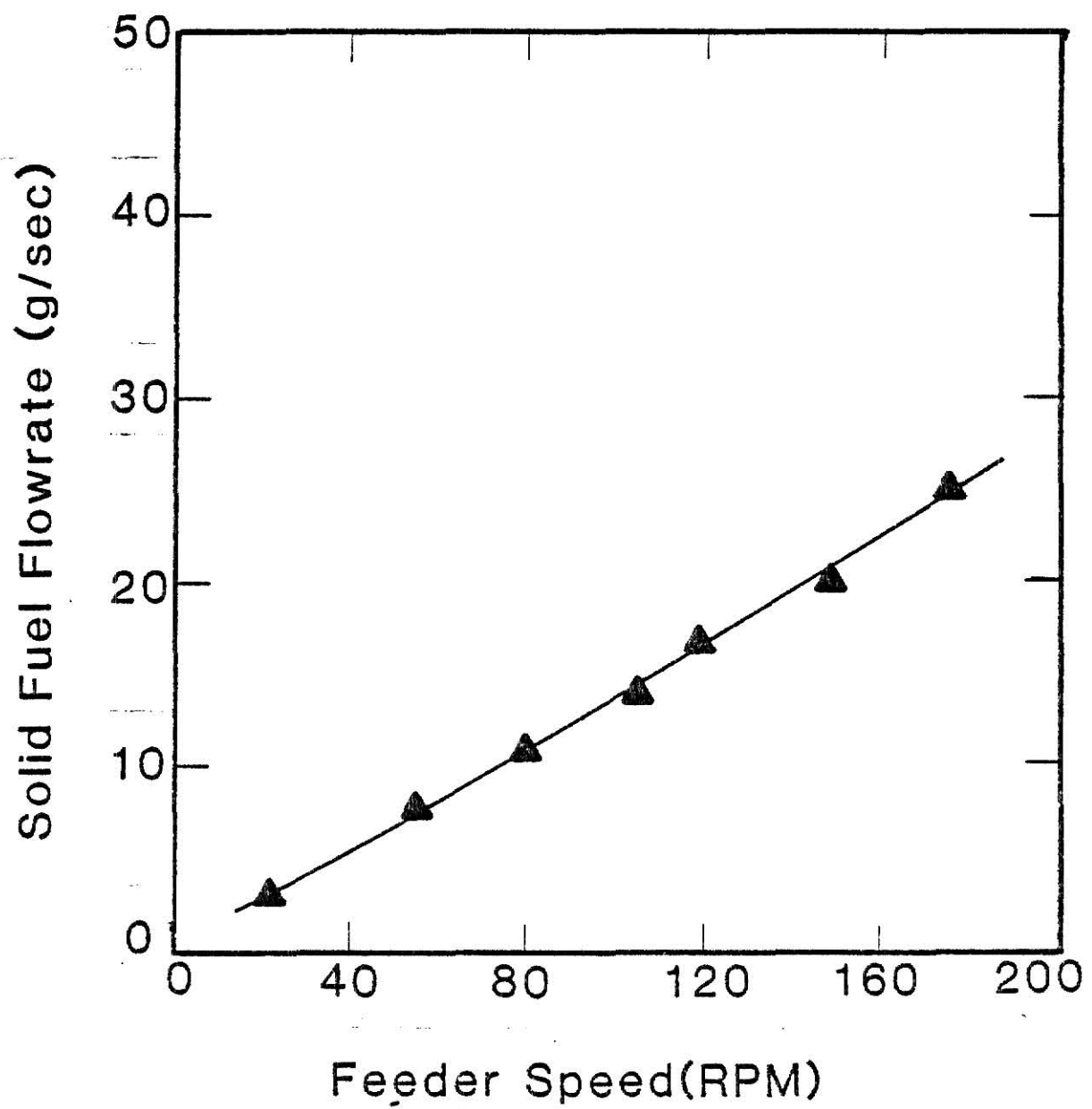


Fig. 2.13 Feeder Calibration Curve for Wheat Straw

set up such that natural gas can be doped with ammonia or hydrogen sulfide to assist in the calibration of detection instruments and to determine the importance of chemical reactions on the furnace wall and in the sampling probe.

Natural gas service is taken from the building supply through a 1.27 cm i.d. steel pipe equipped with a manual ball valve at the equipment control panel. The piping schematic is shown in Fig. 2.14. In addition to the manual valve, both the pilot and main gas lines feature 110 V solenoid valves that are normally closed. The pilot burner, an Eclipse model 3EPA-12 pilot with Eclipse model 131PM pilot mixer, is shown in Fig. 2.15. An internal spark plug supplies the ignition source, and the total gas flow and flame stoichiometry are controlled by an adjustable gas regulator, a needle-seat metering orifice, and ball valves in the gas and air lines. The spark plug requires a dc voltage for proper operation. This is provided by a Dongan model A06-506 6000 V ignition transformer.

The main gas supply is partly regulated by a maxitrol model RV42 gas pressure regulator which controls the line pressure at 19.0 cm of water above atmospheric pressure. The flow through the line is metered by a Dwyer RMC Ratemaster flowmeter calibrated for up to $1572 \text{ cm}^3/\text{sec}$ of air. The gas is connected to the burner through a 1.27 cm i.d. flexible natural gas hose. The injector used in this research is shown in Fig. 2.16.

2.6 Safety Systems

The facility is equipped with a number of safety interlocks that minimize the danger of a gas or dust explosion. A Honeywell model

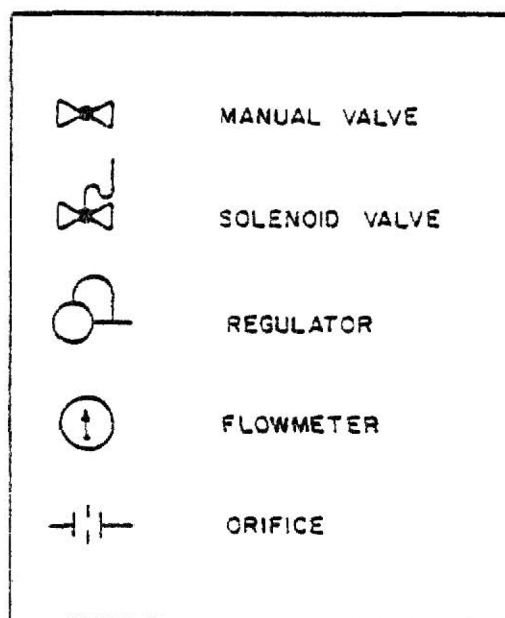
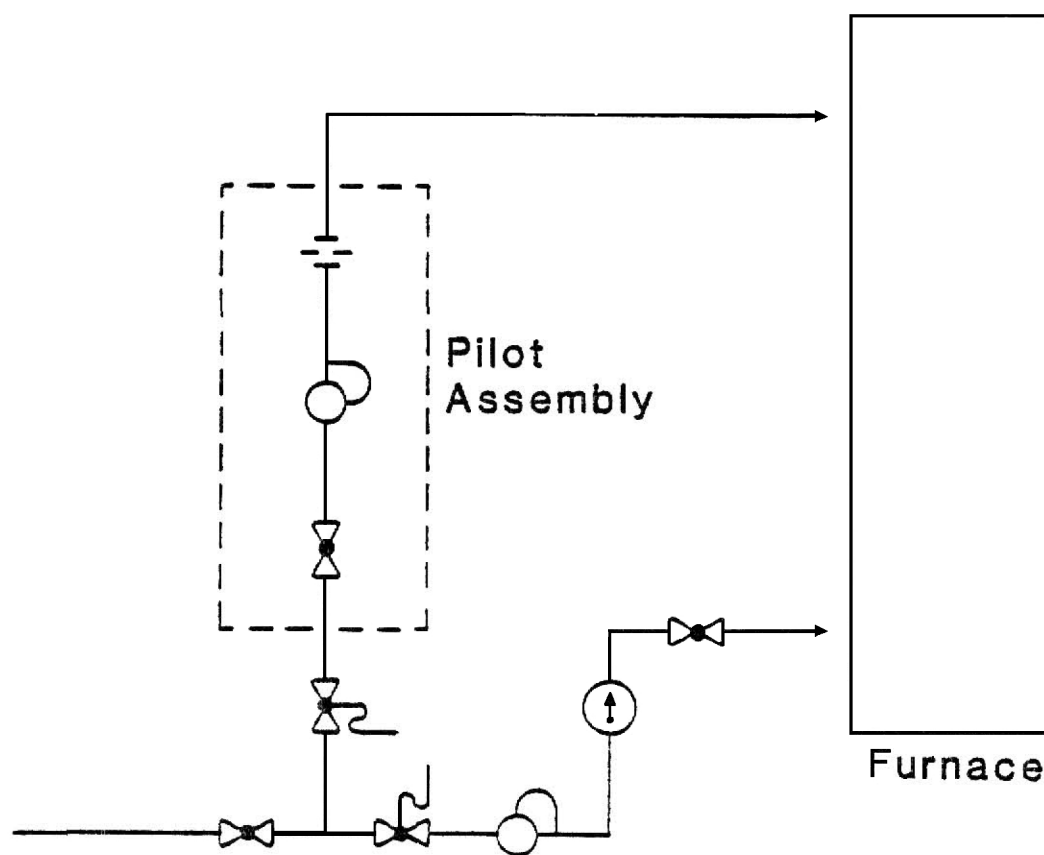


Fig. 2.14 Gas Piping Schematic

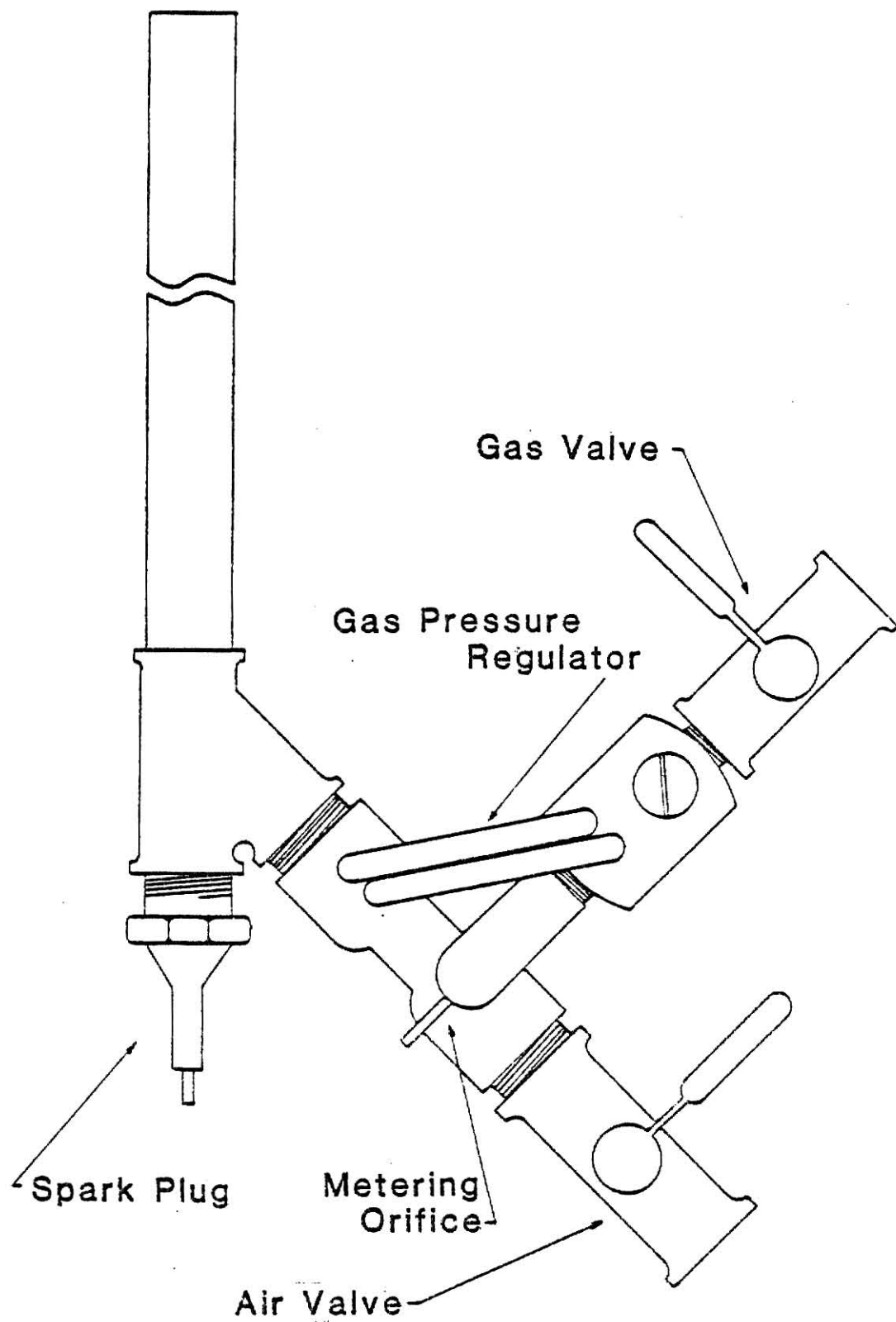


Fig. 2.15 Pilot Assembly

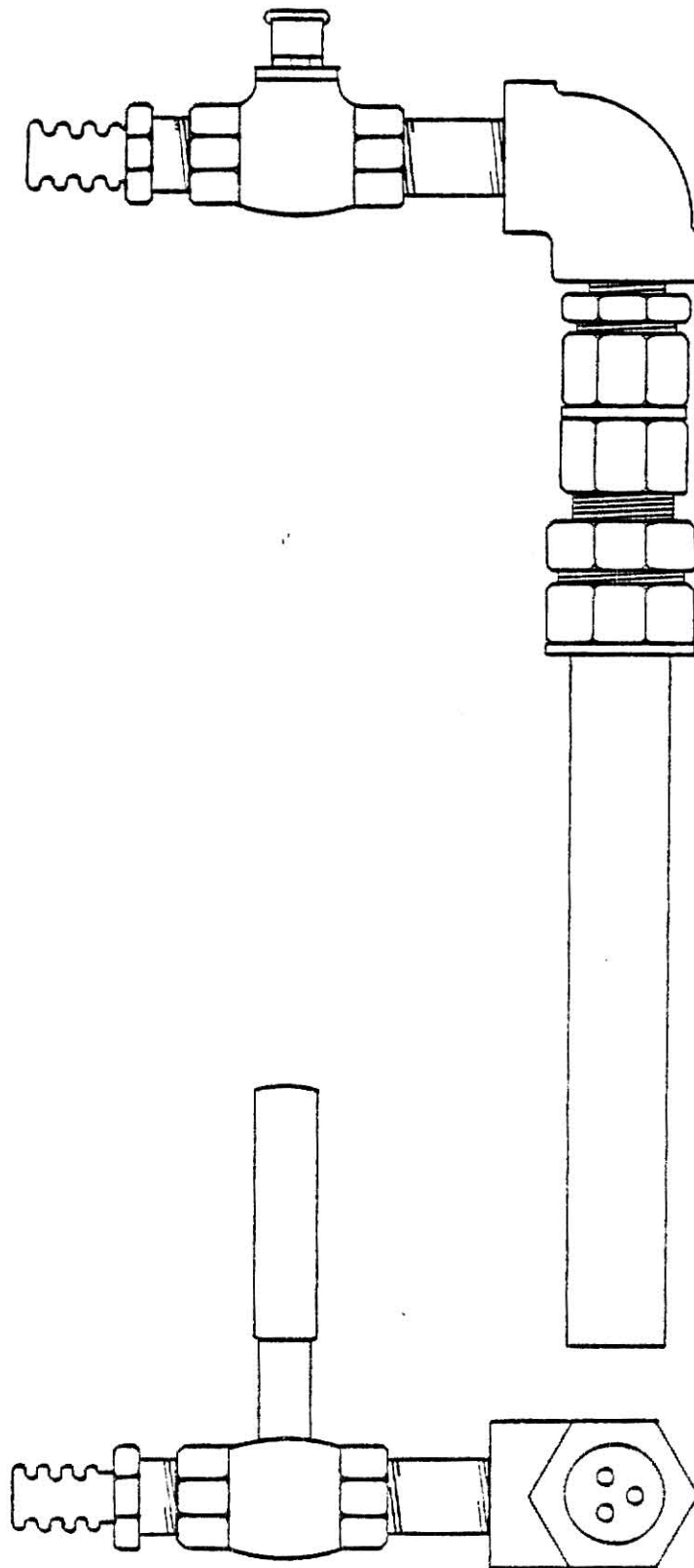


Fig. 2.16 Main Gas Injector

RA890G flame safeguard unit is used to monitor the gas and solid fuel flames and to control the distribution of power to all the solenoid valves in the gas lines, the solenoid valve in the feeder reference air supply line, the pilot air solenoid valve, the pilot assembly ignition circuit, and the feeder motor. In addition, the flow rate of the water to the burner is monitored by the flame safeguard unit to ensure a minimum flow rate of $420.5 \text{ cm}^3/\text{sec}$. The main air solenoid valves and compressor power are not controlled by the safeguard since a continuing supply of air is used to purge the combustion chamber in the event of an unanticipated shutdown. Furthermore, the flame safeguard unit automatically controls the initial startup process. Because of its importance to the overall system, this unit's operation is explained fully in Appendix D.

The interior of the combustion chamber is monitored by a Honeywell model C7027 Minipeeper ultraviolet flame detector. The detector's line of sight is aligned with the path of both the main and pilot flames. The detector provides a signal to the flame safeguard whenever there is a flame in its viewing range. The gas in the flame detector is ionized by ultraviolet photons from the flames; therefore, a weakly ionized plasma generates a closed circuit, signaling the presence of a flame. If this signal is not present at the safeguard, the fuel flow to the furnace is interrupted. Thus, the flame detector insures that the fuel burns properly and prevents the dangerous accumulation of gas or solid fuel within the furnace.

Two additional safety systems are provided that open the circuit feeding line voltage to the flame safeguard. The first, a Ranco type 010 low pressure power disconnect, opens whenever the air pressure in

the main air supply line drops below a preset level, which is usually maintained at 693.4 KPa. Since the compressor always keeps the pressure between 721.5 and 928.2 KPa during normal operation, this system effectively indicates either a compressor malfunction or a leak of serious proportions in the supply line. In either case, the flame is immediately extinguished before conditions allowing flashback into the fuel supply system can be realized.

The other safety monitor is a Penn series A19 temperature control located on the top side of the burner assembly. A copper sensing element, at the end of a 100 cm copper line, opens the circuit whenever the temperature of the sensor exceeds a preset level, between 311 and 389 K. The temperature is normally set at 323 K. Under normal operating conditions, the cooling water in the burner maintains the temperature at around 305 K; therefore, the activation of this control indicates either a flame above the furnace or the overheating of the burner assembly. In either case, fuel flow is interrupted.

Throughout the operation of the facility, the low pressure and the high temperature disconnects were never called upon except during simulated failures, e.g., turning the compressor off while the furnace was ignited. The water flow rate sensor to the burner dropped several times below the preset level, whereupon the circuit to the flame safeguard unit interrupted the flow of fuel to the furnace. The reason for this reduction of water flow rate was determined to be a pressure drop in the university water supply lines. The flame detector was checked occasionally to insure that soot or ash would not accumulate on the window and block its line of vision. Although an operator was

always present when a shutdown occurred, the greatest benefit of the safety systems was to allow the operator to leave the facility briefly during operation without fear of serious consequences.

2.7 Burner Design

The combustion facility is equipped with a concentric firing burner that simulates the conventional solid fuel burners used in utility boilers. The fuel and the primary air are premixed and emitted from an injector in the center of the burner, and the secondary air flows through an annulus surrounding the injector.

A cutaway diagram of the concentric firing burner is shown in Fig. 2.17. The secondary air that enters the burner through the top inlets and flows straight down along the outside of the injector is termed the secondary axial air. The air entering near the bottom and passing through the curved vanes is denoted the secondary swirl air since the vanes impart a tangential velocity to it.

The solid fuel injector is similar to those used in tangentially fired boilers. This injector is comprised of a 17.8 cm long 2.22 cm i.d. stainless steel pipe. The axial injector produces a long cone shaped flame since the feeding pattern produces a rather leisurely mixing of the fuel and air. The axial injector is shown in Fig. 2.18. In tangentially fired boilers, similar burners are placed in the corners of the combustion chamber and directed toward a point slightly off the center of the chamber so that the flame assumes a torodial shape when viewed from above.

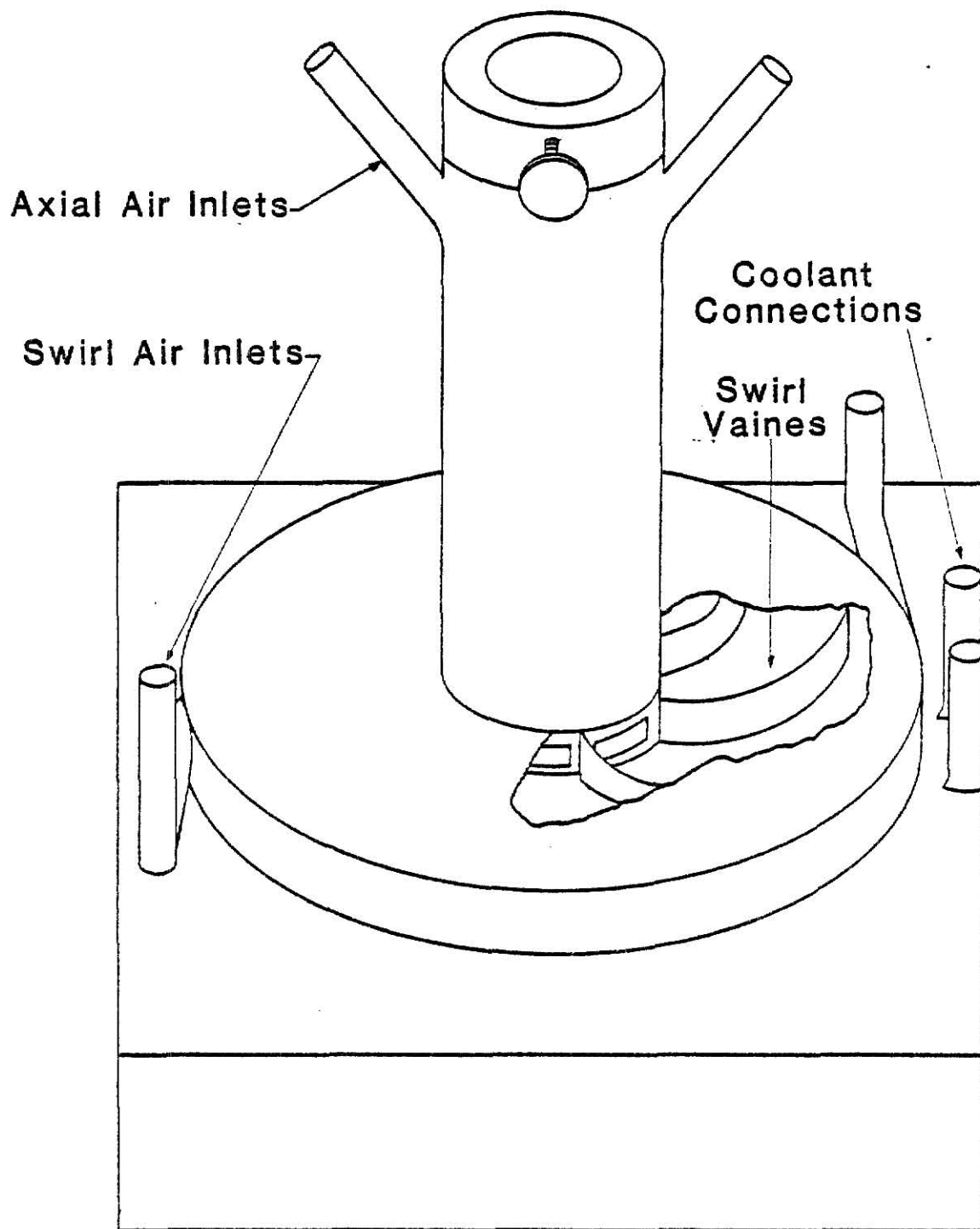


Fig. 2.17 Concentric Burner

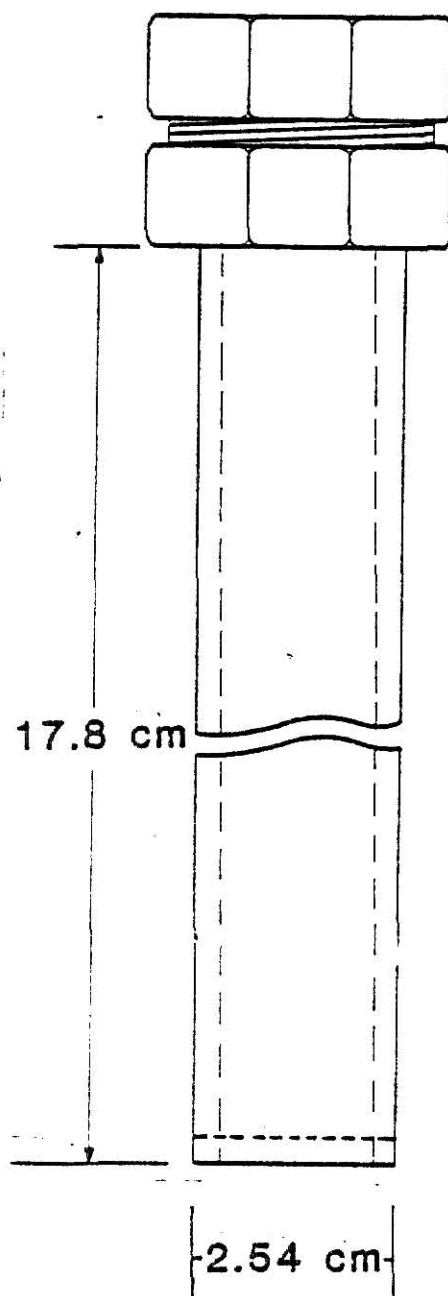


Fig. 2.18 Solid Fuel Injector

2.8 Sample Collecting System

This investigation involved the collection, identification, and quantification of gas and solid species both from the flue and from axial positions along the furnace. Figure 2.19 is a representation of the sample collecting probe. This probe, which is made of stainless steel, comprises a tubular shielding member and a dividing tube which separates the water inlet and outlet paths.

To collect the solid samples, a water quencher of 1.6 mm i.d. was used and located at the centerline of the probe. The quencher tip with 6 holes was placed 1.27 cm from the sample point to prevent splashing into the combustion chamber.

2.8.1 Gas Sampling System

The schematic in Fig. 2.20 represents the collection apparatus. The components' manufacturers and model numbers are listed in Table 2.1. Three of the sampling lines go directly to the oxygen, carbon dioxide and carbon monoxide analyzers. The fourth proceeds to a 3-way valve and through a molecular sieve dryer to ensure that there is no moisture in the gas passing through the nitrogen oxide analyzer. The exits of the four analyzers are connected to a 6-way manifold, which directs the sampled gases to the atmosphere. All four analyzers were calibrated prior to every operation. The calibration gases used and their purities are listed in Table 2.2.

The chemiluminizer or nitrogen oxide analyzer of Meloy Laboratories, Inc. model NA 510-2 is the most sensitive to the moisture content of the gas sample. An electrical discharge ozone generator, which was built by the manufacturer, produces a high concentration of

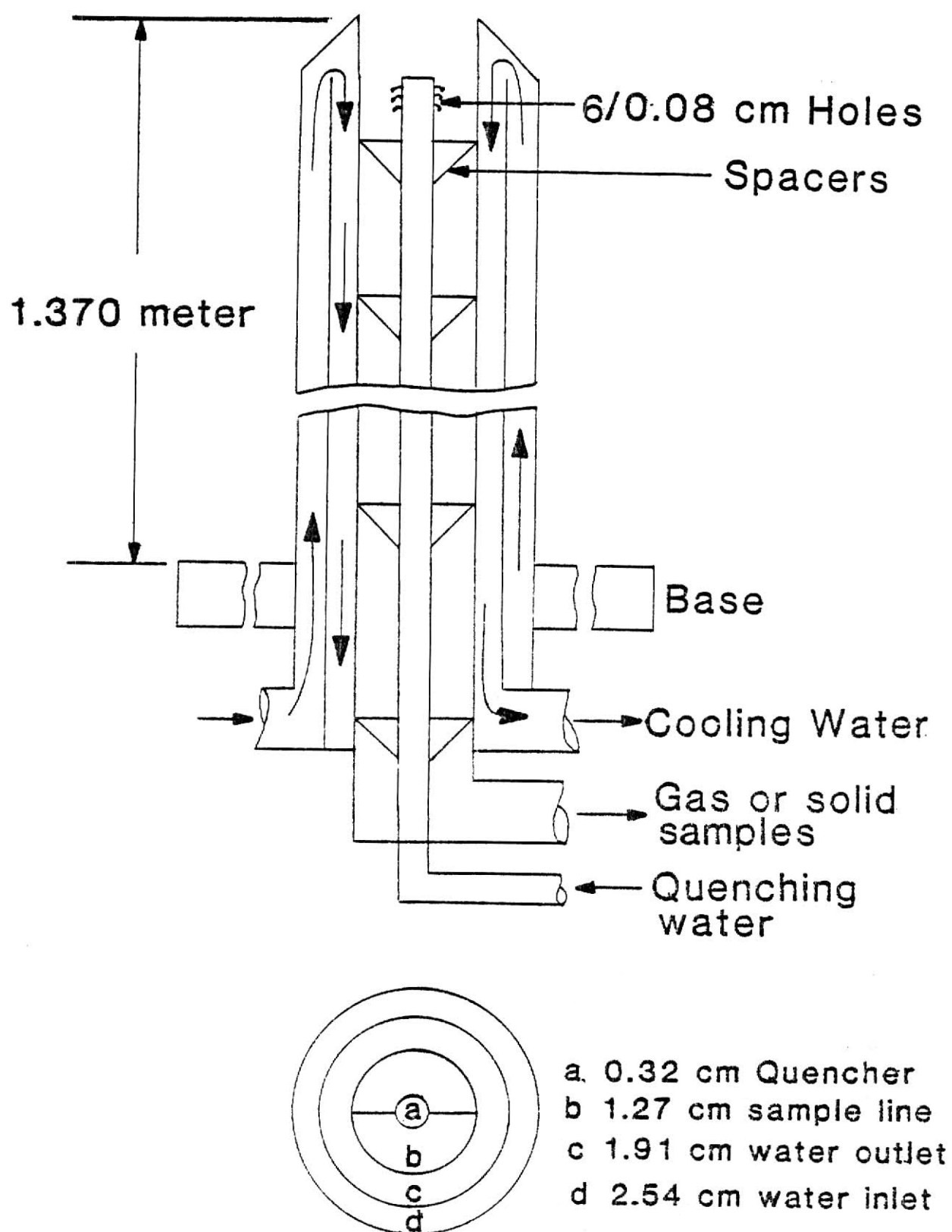


Fig. 2.19 Sampling Probe Cross-Section

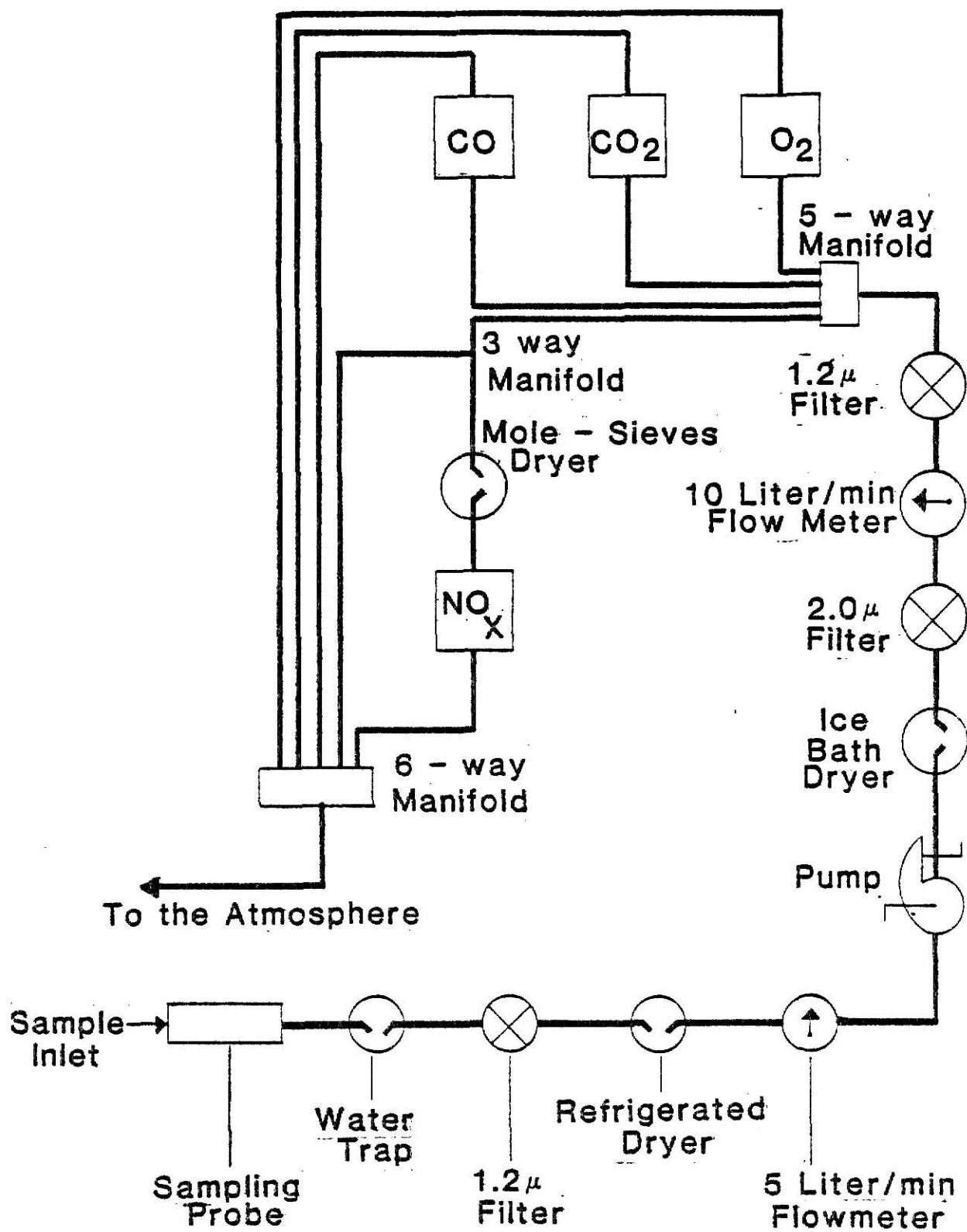


Fig. 2.20 Gas Collection System Schematic

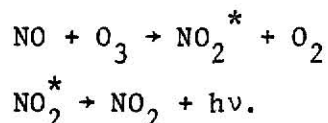
Table 2.1 Components of Gas Sampling System

Component	Manufacturer	Model
Water traps Polypropylene Cylinders	Cole-Palmer	C6652-00
1.2 μ filters	Whatman	GF/C, 7.0 cm
Refrigerated Dryer	J. C. Penny	3305
Flowmeters	Dwyer	VFA2455V
Vacuum Pump	Thomas Ind.	2917CE18TFEL
Ice Bath	Don Schmidt (Ward Hall)	
2 μ S.S. Filter	NUPRO	SS-4F-P4-2
Manifolds	Zamani (Ward Hall)	

Table 2.2 Calibration Gases

Gas/Diluent	Concentration(s)	Bottle Size
O_2/N_2	1.0, 5.0, 10.0%	lecture
CO/N_2	1.0, 3.0, 5.0%	30
CO_2/N_2	3.0%	T
$CO/CO_2/N_2$	1.0%/3.0%	T
NO/N_2	1000 PPM	T
NO_2/N_2	1000 PPM	T
HCN/N_2	1200 PPM	30
NH_3/N_2	1000 PPM	30
H_2S/N_2	1000 PPM	30
SO_2/N_2	1000 PPM	30

ozone from an input of $1.67 \text{ cm}^3/\text{sec}$ of O_2 (Matheson 99.90% purity). The gas sample (flow rate of $3.33 \text{ cm}^3/\text{sec}$) and ozone are introduced into the reactor chamber where they mix and chemically react. The ozone and nitrogen oxide react to produce an excited state nitrogen dioxide molecule (NO_2^*), which deactivates by the emission of a photon ($h\nu$). This sequence is illustrated by the reaction set,



The carbon dioxide and carbon monoxide analyzers are both Beckman model 864 infrared analyzers. Within the analyzer, two equal-energy infrared beams are directed through two optical cells, a flow-through sample cell and a sealed reference cell. Solid state electronic circuitry continually measures the difference between the amount of infrared energy absorbed at a specific wavelength in the two cells. This difference is a measure of the concentration of the carbon monoxide or carbon dioxide in the sample. The output meter has one hundred graduations and three different ranges. For each range, a calibration curve was used to convert the meter reading into a concentration. The analyzers are equipped with a linearizer circuit board to produce a linear output with the concentration.

The Beckman model 755 oxygen analyzer provides continuous readout of the oxygen content of the flowing gas sample. The determination is based on measurement of the magnetic susceptibility of the sample gas. Oxygen is strongly paramagnetic; other common gases, with only a few exceptions, are weakly diamagnetic. The instrument provides a direct readout of the oxygen concentration on a front panel meter.

The gas sampling system was designed to have the flexibility of collecting batch samples in a bag, from where they can be analyzed by gas chromatography as an independent check on O_2 , CO, CO_2 , and the lower hydrocarbons, and by wet chemistry for an analysis of nitrogen and sulfur gases, such as hydrogen cyanide, sulfur dioxide, hydrogen sulfide. Additional details of the batch sampling and subsequent analysis by wet chemical and gas chromatographic techniques may be found in Roenigk.⁽³⁾

2.8.2 Solid Sampling System

Figure 2.21 represents the collection apparatus used for collection of solids. Prior to the experiment, an 18 liter tank of distilled water was provided to quench the gas and solid particles. A varistaltic pump (Monostat Corporation model 72-590-60) is used to pump the distilled water into the gas sample stream through the sampling probe (see Fig. 2.19). The mass flow rate of water was usually about $11.9 \text{ cm}^3/\text{sec}$. The Thomas pump (see Table 2.1) is also used in this configuration. Solid samples are collected on the 1.2μ glass microfiber filters (Whitman, model GF/C) which are located upstream of the water trap, not downstream as was the case in the gas sampling configuration. The flow rate of sample gas is controlled with the flowmeter to assure representative sampling¹⁸ of the solid materials. Details of the sampling rate calculations are discussed in Appendix A.

The solids and other particulate matter remaining on the 1.2μ filter are taken to an oven and dried for at least 24 hours at 400 K before analysis in a Perkin-Elmer elemental analyzer (model 240C). The elemental analyzer determines the carbon, hydrogen, and nitrogen

**THIS BOOK
CONTAINS
NUMEROUS PAGES
WITH MULTIPLE
PENCIL AND/OR
PEN MARKS
THROUGHOUT THE
TEXT.**

**THIS IS THE BEST
IMAGE AVAILABLE.**

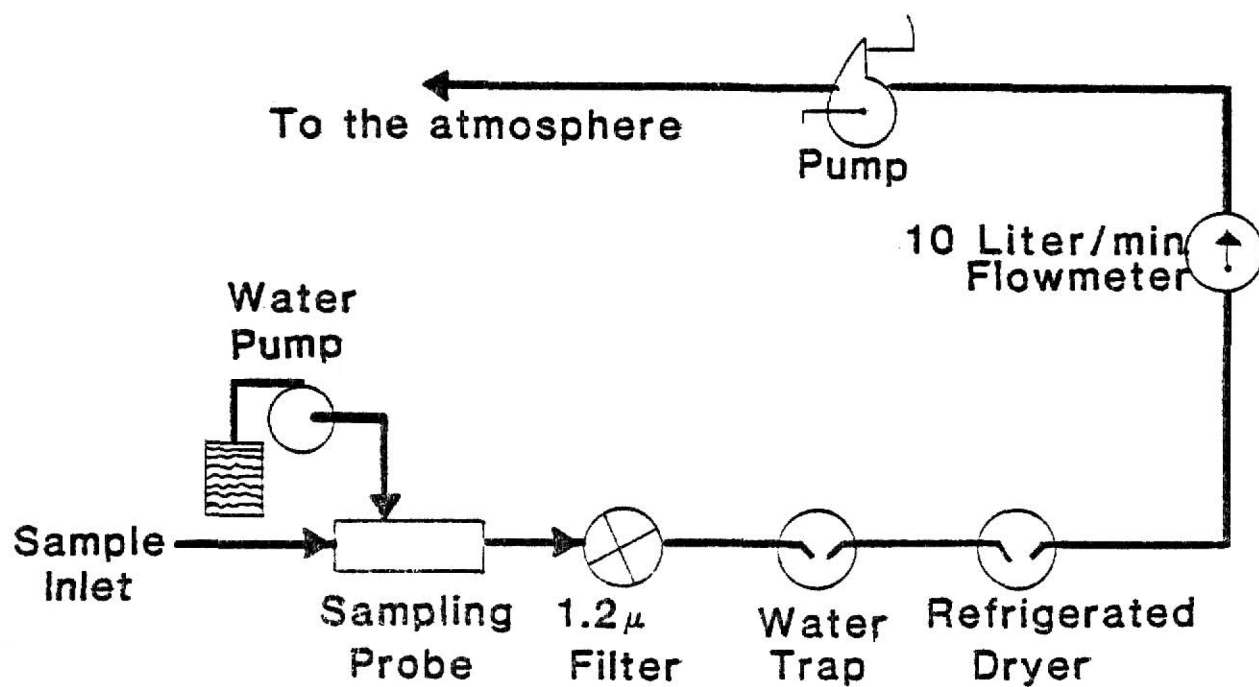


Fig. 2.21 Solid Collection System Schematic

contents of organic compounds by combusting them in pure oxygen (99.995%) under static conditions. The combustion products (CO_2 , H_2O , N_2) are then analyzed automatically in a series of self integrating, steady state, thermal conductivity detectors. Results are recorded in bar graph form on a mV recorder. Three separate systems in the analyzer perform the determinations, the combustion train, the analytical system, and the electronics. Ultra high purity helium is used to carry the combustion products from the combustion train through the analytical system to the atmosphere. Gas flows are determined by solenoid valves, controlled by a cam-operated programmer. A helium bath surrounds the thermal conductivity cells to guard against cracked feed-through or other small leaks. The combustion train includes independently heated combustion and reduction furnaces, each with the appropriate reaction tube. The analytical system consists of a mixing volume (in which the sample combustion products CO_2 , H_2O , and N_2 , are mixed with helium to a homogeneous, equilibrated mixture), a pressure switch, sample volume, detectors, and adsorption traps.

3.0 EXPERIMENTAL PROCEDURE

3.1 Introduction

Because of the complexity of the experimental program, this chapter will detail the experimental methods used and the difficulties encountered in the attainment of the goals set forth in Chapter 1.

The experimental apparatus was designed to simulate the residence time (~ 1 sec) and the firing density (621 KW/m^3) of the primary flame zone of commercial solid fuel furnaces. Thus the results obtained should be correct qualitatively; i.e., the furnace can be used as a fuel screening instrument to uncover trends in emissions from large furnaces. The best measure of consistency, therefore, is to compare the results of the current experimentation to those obtained from similar furnaces. To this end, this study first attempted to repeat some of the previous results documented by Pershing, et al.⁽¹⁴⁾ Many of these results have been compared already, both with larger scale experiments and with utility boiler emissions. The comparisons have been reasonable, both for staged and unstaged combustion.

Once the comparability of the results was assured, the firing of biomass fuels and the co-firing of coal with biomass was undertaken to determine the nitrogeous emissions from the biomass fuels under a range of firing conditions. This included the investigation of not only NO_x formation from the staged and unstaged combustion of these fuels, but also the study of how the elements (H,N,C) evolve from the fuel and form major species and nitrogeous pollutants. The procedure of using the apparatus described in Chapter 2 and the results obtained are the subject of the subsequent sections.

3.2 Unstaged Furnace Operation

The operation of the furnace is detailed in Appendix E. Prior to firing with solid fuel, the furnace was brought to an operating temperature of approximately 1350 K by firing a lean natural gas/air mixture. The time required to reach this temperature was about five hours as shown in Fig. 3.1. During the warm up, the online analyzers were calibrated, the gas sampling lines were put under vacuum to check for leaks (to prevent abnormally high oxygen readings), and the feeder hopper was filled with fuel. Additionally the observation window (see Chapter 2) was replaced if it was coated with soot, the ice in the ice-bath was changed, and the thermocouples were checked to ensure they were positioned properly within the inner refractory layer of the combustion chamber.

After the operating temperature was reached, the furnace was gradually switched from natural gas to solid fuels. It was found that approximately 40 g/min of solid fuel of approximately 60% carbon was sufficient to sustain a stable flame and a wall temperature of about 1350 K. Table 3.1 lists the fuels and their constitution that were used in the study. Fuels were kept in a plastic bag sealed inside a 190 liter barrel which was located in an environment of low relative humidity (~20%). CaSO_4 desiccant was also placed inside the container to absorb any remaining moisture in the barrel. Periodic checks of the fuels' temperature were made, specifically for the biomass with high oxygen content, to prevent any spontaneous chain reaction.

The pilot flame was used to assist in the stabilization of the solid fuel flame for all test conditions. Once the temperature stabilized, the sampling probe was inserted from the bottom of the

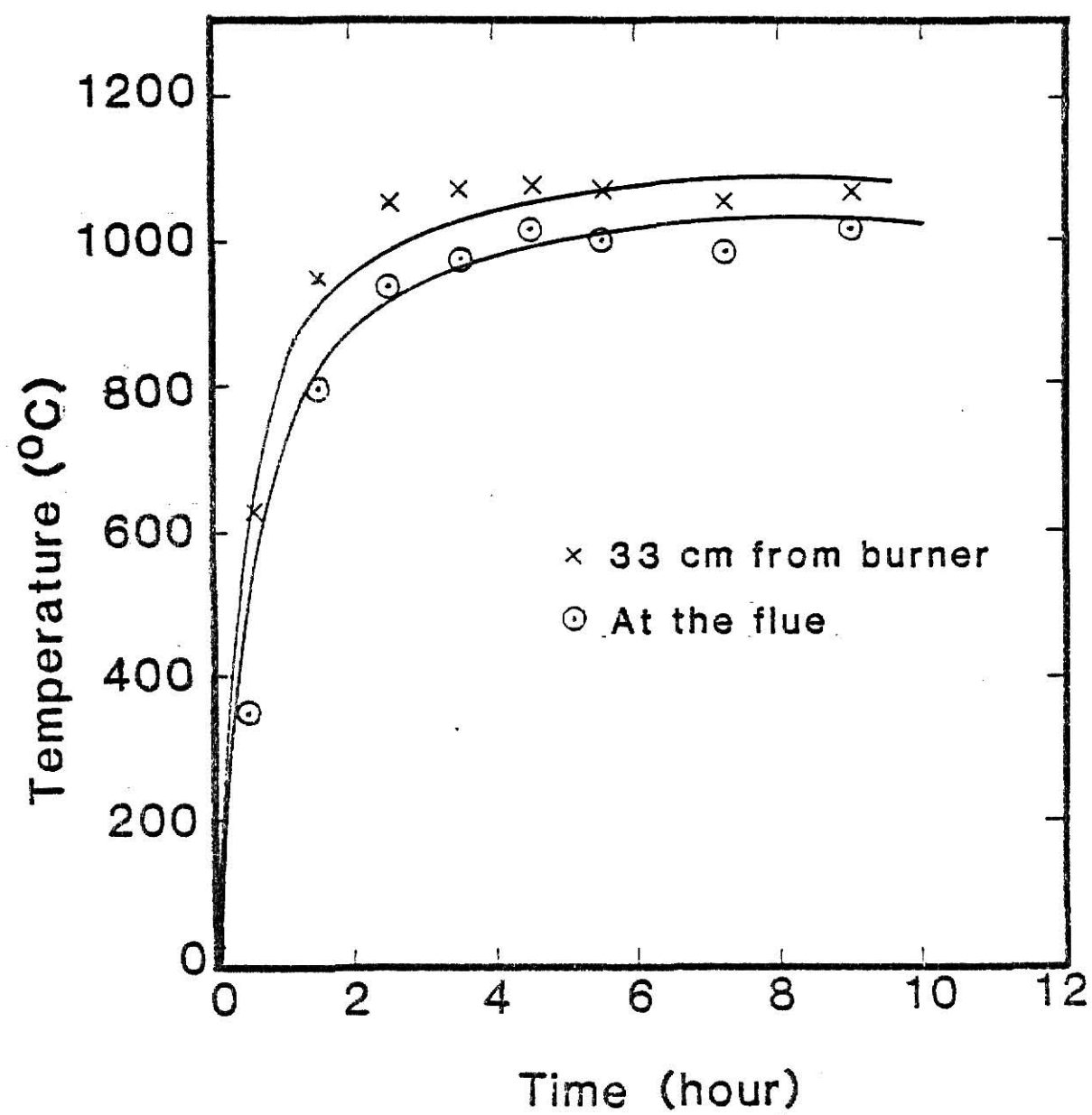


Fig. 3.1 Temperature Profiles During Warm-up

Table 3.1 Analysis of Fuels (Wt%)

Fuel	Ultimate Analysis ^a						Proximate Analysis ^a			
	C	H	N	O	S	Cl	Ash	Molsture	Volatife Matter	Fixed Carbon
Colorado	76.62	6.56	1.86	14.11	0.84	0.01	11.93	6.90	32.52	48.65
Mo-Kan	78.99	6.43	1.31	4.65	8.53	0.08	31.11	5.47	21.29	41.53
Corn Stover	55.21	7.96	2.63	33.86	0.21	0.11	24.88	5.28	59.08	10.76
Wheat Straw	48.23	7.24	1.14	43.07	0.19	0.13	8.16	6.99	68.91	15.94
Colorado + 50% Wheat Straw	69.66	6.73	1.67	21.23	0.68	0.04	11.03	6.92	41.16	40.87
Colorado + 25% Wheat Straw	73.85	6.63	1.73	16.94	0.77	.03	11.58	6.91	29.52	45.57
Colorado + 25% Corn Stover	74.99	6.67	1.92	15.62	0.78	0.02	13.07	6.67	34.86	45.33

^aAnalysis by Galbraith Labs Inc., Knoxville, Tn.

furnace and positioned via the probe drive mechanism from the control room. The sampling system vacuum pump was started (see Fig. 2.20) and the flow rate adjusted to about 2 liters/min. This flow rate was sufficient to provide 0.5 l/min, 0.5 l/min, 0.25 l/min and 0.2 l/min through the CO_2 , CO, O_2 , and NO_x analyzers respectively. The remainder was exhausted to the atmosphere. At stoichiometric conditions the flue gas contained about 1% O_2 and less than 0.5% CO. A higher O_2 reading implied the flame was fuel rich while a CO reading below detectable levels and greater than 1% O_2 indicated fuel lean conditions.

The primary air, which was used to transport the solid fuel from the exit of the auger to the combustion chamber (see Section 2.2), was about 50% of the stoichiometric amount. The remainder was added as swirl air. The flow rate of primary air was held constant and was not preheated. The swirl air was preheated to 450 K and its flow rate was varied to determine variations of flue NO_x with excess air. After adjusting the various flowrates, about five minutes were required to achieve a steady state flame.

3.3 Sampling during Unstaged Combustion

The experimental facility is designed to enable the laboratory personnel to collect data in as short a time as possible and thereby to prolong the life of the furnace and other equipment, to conserve fuel, and most importantly, to accomplish the full complement of runs in a few weeks once testing commenced.

Data were collected in two ways. First, online analysis of the flue permanent gases (O_2 , CO, CO_2) and NO_x was repeated for several different excess air levels. Second, the permanent gases, NO_x and

unburned solids were collected at discrete axial locations at a fixed flue gas O_2 concentration of 3%. The gas sampling line could also be used to collect batch gas samples that were then analyzed for NH_3 and HCN by wet chemical techniques and checked for O_2 , CO, CO_2 and lower hydrocarbons by gas chromatography (see Roenigk⁽³⁾).

Once the flue gas sample measurements were completed the swirl air flowrate was adjusted to give a flue gas oxygen reading of 3%. This step was required because the heat generation rate is insufficient in very lean flames (~6% O_2 in the flue) to sustain the temperature of the furnace at the level comparable to 3% O_2 . Nearly 30 minutes were required to heat the combustion chamber to steady state. At this point measurements were made of combustion gases at six different axial locations from 33 cm below the burner to the flue. The outlet water temperature from the probe as well as the gas outlet temperature were kept constant by adjusting the water flow rate to compensate for the increased outer probe area exposed to the furnace gases. The 2.54 cm o.d. sampling probe served as an effective heat sink. When fully inserted, the probe cooled the lower furnace walls by approximately 500 K. Nonetheless, above the probe (from where samples were extracted), the furnace retained its temperature when the probe was inserted.

After axial measurements of the combustion gas products were completed, the sample probe was removed and furnace temperature was maintained with a natural gas flame. After the lower furnace was heated to steady state (1200 K at the flue) solid fuel was introduced once again. This procedure not only conserved solid fuel, but allowed the

feeder to cool down. Usually the time required to stabilize the solid fuel flame was from 15-20 minutes.

After the fuel/oxidizer flow had been adjusted to give a flue oxygen concentration of 3%, and the CO_2 and NO_x readings had been verified for consistency with previous measurements, solid sampling commenced. To ensure an unbiased sampling of solids, the gaseous flow rate through the probe had to be increased. Appendix A gives details of the flow rate determination. Because of this increased flow rate, the online analyzers could not be used during the solid sampling, and the pump exhaust was ducted directly to the exhaust hood.

Collection of the solid samples was accomplished in the same manner as the gas sampling. However, to insure a rapid quench of the solids in the probe, distilled water was sprinkled from a porous tube inside the probe (see Fig. 2.19) at about 0.25 l/min. Prior to each sample collection, this quencher was operated for two minutes to cleanse the probe of any remaining solids and/or soot from the previous position. Usually, about 10 % of the gas was passed through the fiberglass filter to collect each solid sample. After a filter was removed and dried in an oven for 24 hours at 400 K, the solid samples were analyzed for C, N, H, and ash (see Section 2.8.2).

3.4 Staged Furnace Operation

The combustion process was adjusted by separating the combustion chamber into two zones, shown in Fig. 2.4. In the second zone, a sufficient level of air is supplied through four ports, approximately 5.0 cm below the first stage's throat, to complete the combustion and maintain the flue oxygen concentration at 3%. Once the temperature of

the second stage zone was about 1100 K, the solid fuel was introduced. The time required to stabilize the solid fuel flame was approximately ten minutes.

3.5 Sampling During Staged Combustion

The sampling probe was positioned initially at the exit of the first stage to collect the permanent gases and adjust the first stage stoichiometry ratio $(SR_1)^a$. It was then lowered to the flue position and the second stage combustion air was added gradually until the flue oxygen level attained 3%. The concentration of NO_x was then monitored.

3.6 Miscellaneous Experimental Observations

An unexpectedly high production of slag on the inside wall of the combustion chamber was occasioned by the combustion of high ash fuels such as corn stover and Mo-Kan. Corn stover produced the most slagging. The slag was burned from the furnace walls by firing natural gas prior to the data collection runs in order to prevent the liberation of trapped or adsorbed gases from the slag interfering with the analysis of emissions in subsequent runs. Before the next startup, the solidified slag was removed from both the bottom of the furnace and, to the extent possible, most of the slag remaining on the walls was firmly broken and removed.

Problems encountered during the sample collection were mostly due to plugging of the probe by partially burned solids and soot. These difficulties were observed under fuel rich tests. These runs required

^a ratio of the oxidizer to the oxygen necessary for complete combustion at zero percent excess oxygen.

far longer than the lean runs to complete. For each test condition, the fiberglass filters had to be replaced, the sampling probe was pressurized to insure that the gas line was free of solids accumulation, and the sampling line was checked for leaks.

It was found that ash and some unburned fuel collected in the exhaust flue's long horizontal section. This was not a major impediment since during the entire project (which exceeded 500 hours) it was only necessary to clean the section twice.

During the staged combustion experiments, difficulties were observed in firing fuels of high ash and moisture content. It was not possible to stabilize a flame for the Mo-Kan coal under staged combustion. Possibly this is because nearly 40% of the combustion products at the choke were solids which blocked the passage and created a high pressure in the primary zone. Once the pressure became equal to the pressure of the solid fuel transport air (primary air), the fuel flow was stopped and the flame safeguard shut the system down. In future staging experiments, this problem might be reduced if the choke diameter were to be increased from 5.08 to 7.62 cm.

The high sensitivity of the ozone generator in the chemiluminescent NO_x analyzer to moisture and humidity required that the instrument be shut down every 48 hours of continuous operation for about 10 hours to cool the converter and evaporate the condensate by natural convection. Too much moisture in the ozone generator causes an electrical short circuit between the two high voltage discharge plates and causes the burnout of a fuse.

4.0 RESULTS AND DISCUSSION

Using the procedures documented in Chapter 3, the exit concentration of NO_x from unstaged combustion has been measured as a function of flue gas O_2 content, and the NO_x concentration and unburned solids have been extracted along the furnace axis. The exit NO_x concentration has been determined as a function of first stage stoichiometric ratio (SR_1) under staged combustion. A high nitrogen bituminous Colorado coal and a high sulfur, high ash Missouri-Kansas (Mo-Kan) coal were tested. The high volatile and low fixed carbon biomass fuels, wheat straw and corn stover, were fired separately and in conjunction with the coals.

4.1 Unstaged Combustion

4.1.1 Flue Gas Analysis

The NO_x emissions data from the unstaged experimentation are shown in Figures 4.1 - 4.9. NO_x concentrations are corrected to 0% O_2 and plotted versus % O_2 content at the flue. Details for this correction are provided later in this section. In addition, the percent conversion of fuel nitrogen to NO_x is also indicated.

Let us first turn our attention to the behavior of NO_x , as measured at the flue, versus flue excess oxygen concentration for the Colorado coal, the wheat straw, and the mixture of the two. As shown in Figures 4.1 - 4.5, with an increase in the volumetric percentage of wheat straw the excess oxygen concentration at which the maximum NO_x emissions occur shifts to progressively lower values. For example, the maximum NO_x emissions for the Colorado coal occur at 7.0% excess oxygen (see Fig. 4.1). However, when the Colorado coal is burned in a 75/25 percent by

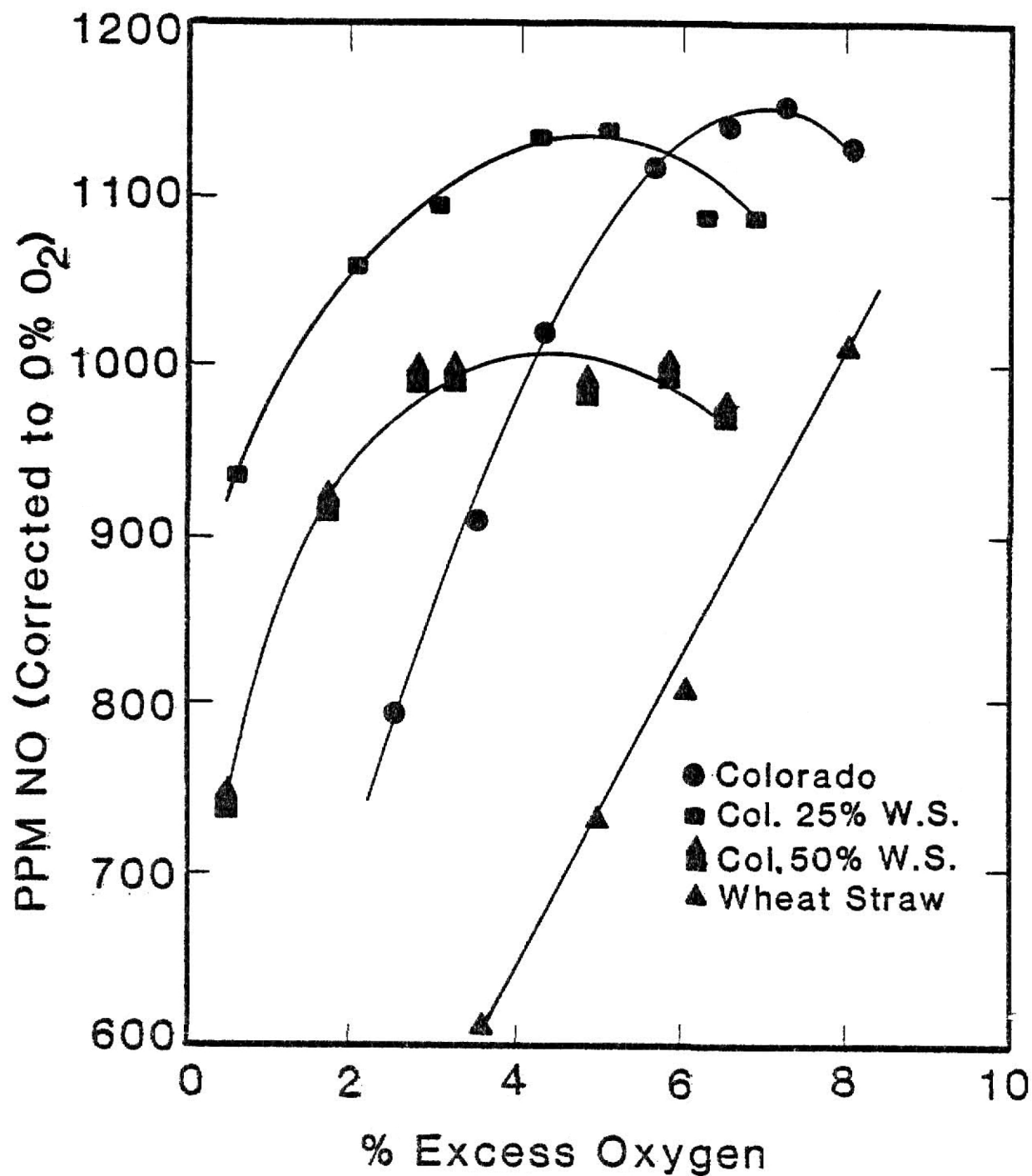


Fig. 4.1 Flue NO_x Concentration for Colorado, Wheat Straw, and Mixtures vs. % Excess Oxygen

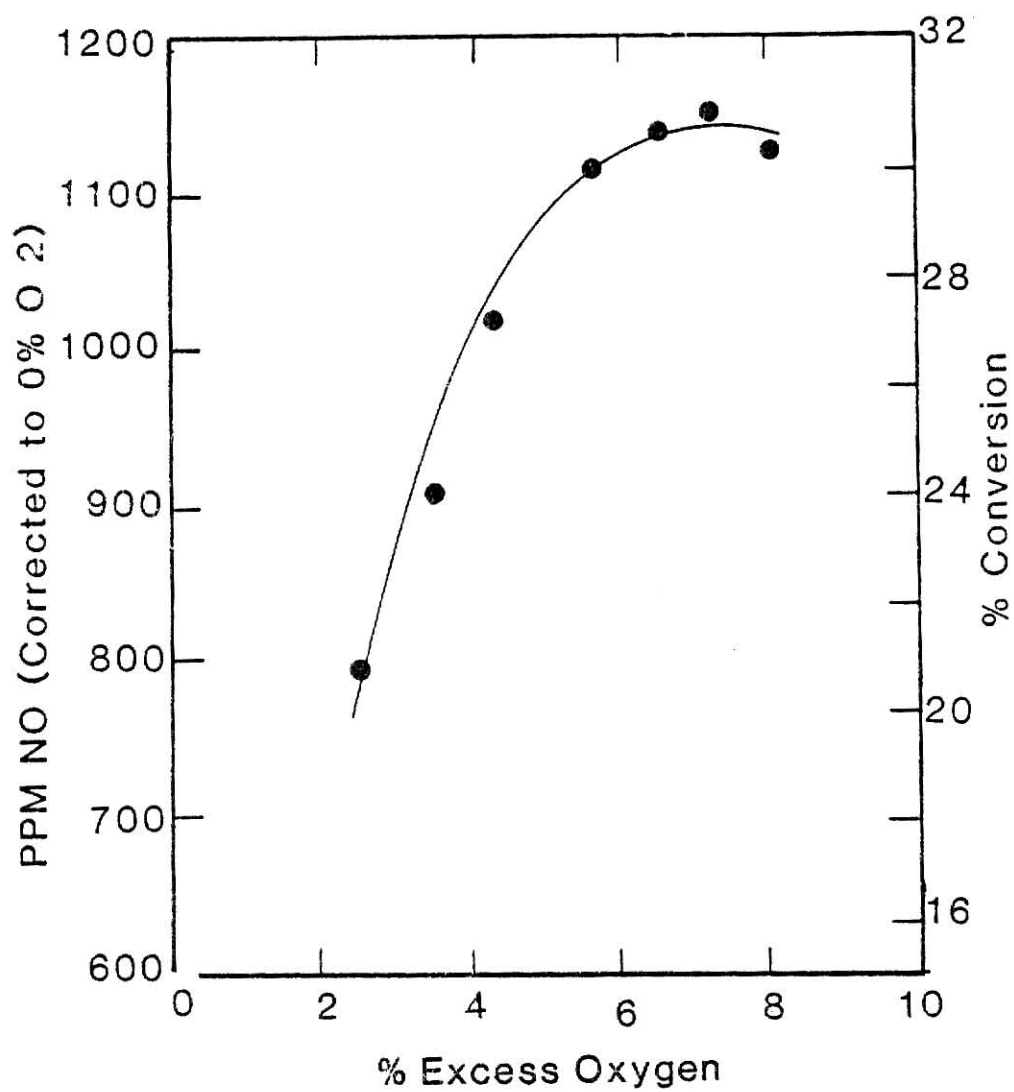


Fig. 4.2 NO_x Emissions and Estimated % Conversion of^xFuel Nitrogen vs. % Excess Oxygen for Colorado Coal

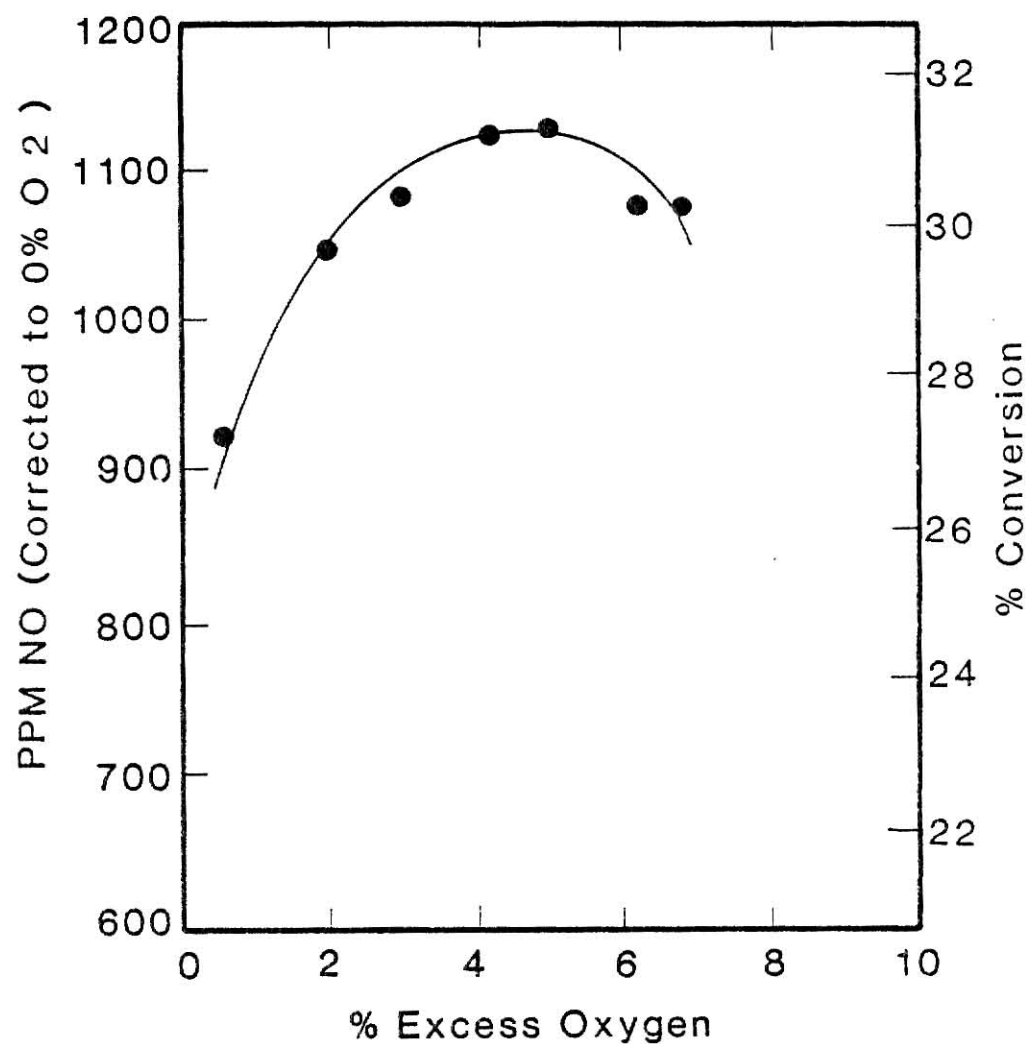


Fig. 4.3 NO_x Emissions and Estimated % Conversion of Fuel Nitrogen vs. % Excess Oxygen for the Colorado/25% Wheat Straw Mixture

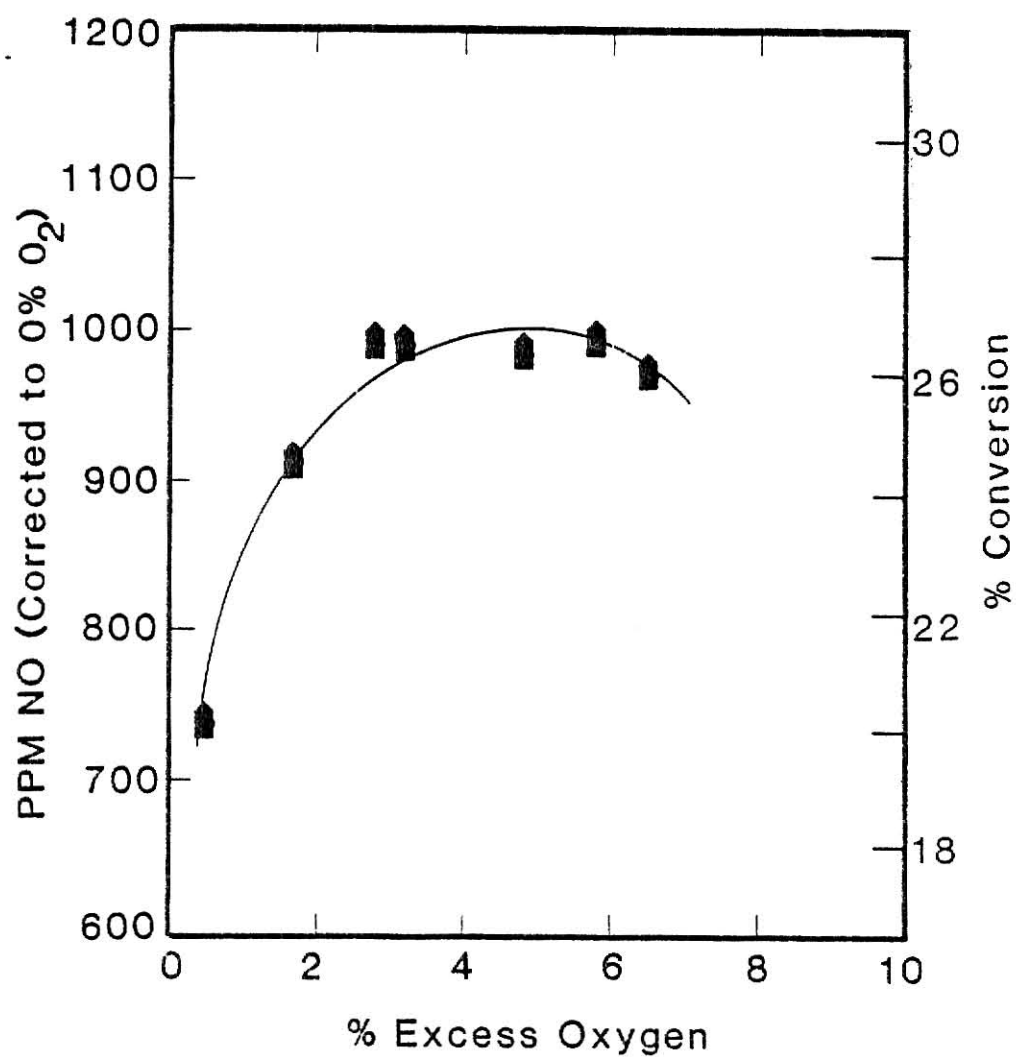


Fig. 4.4 NO_x Emissions and Estimated % Conversion of Fuel Nitrogen vs. % Excess Oxygen for the Colorado/50% Wheat Straw Mixture

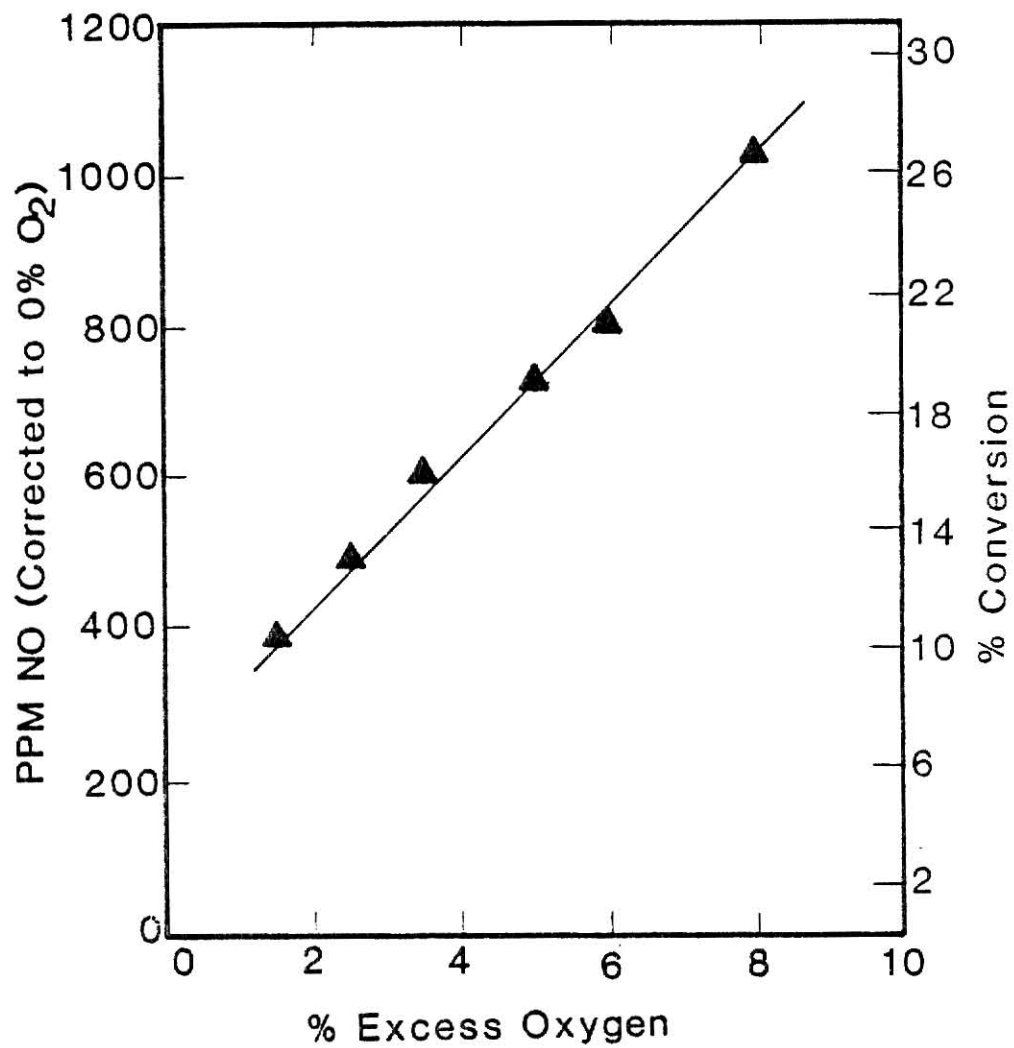


Fig. 4.5 NO_x Emissions and Estimated % Conversion of^xFuel Nitrogen vs. % Excess Oxygen for Wheat Straw

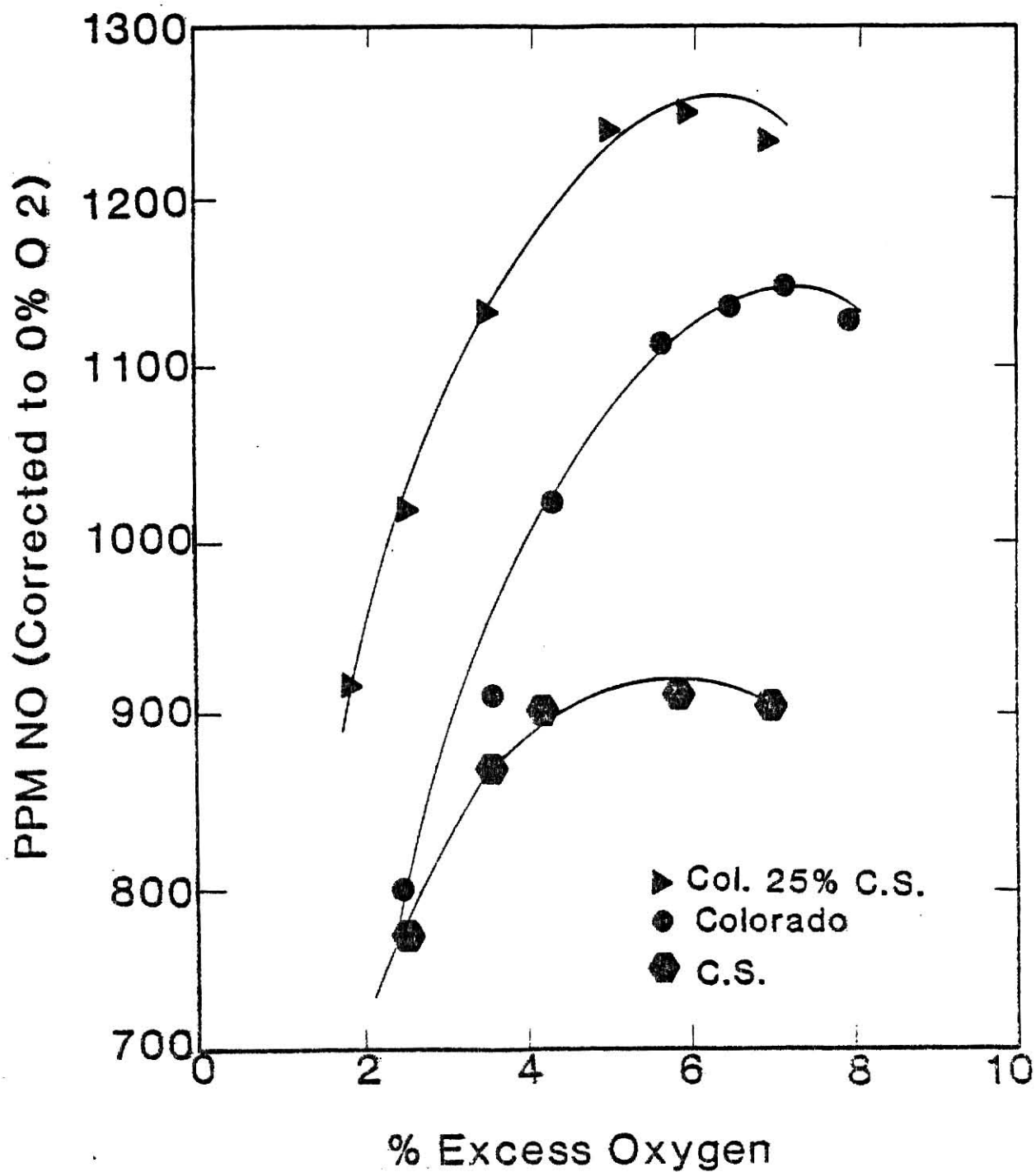


Fig. 4.6 Flue NO_x Concentration for Colorado, Corn Stover, and Mixtures vs. % Excess Oxygen

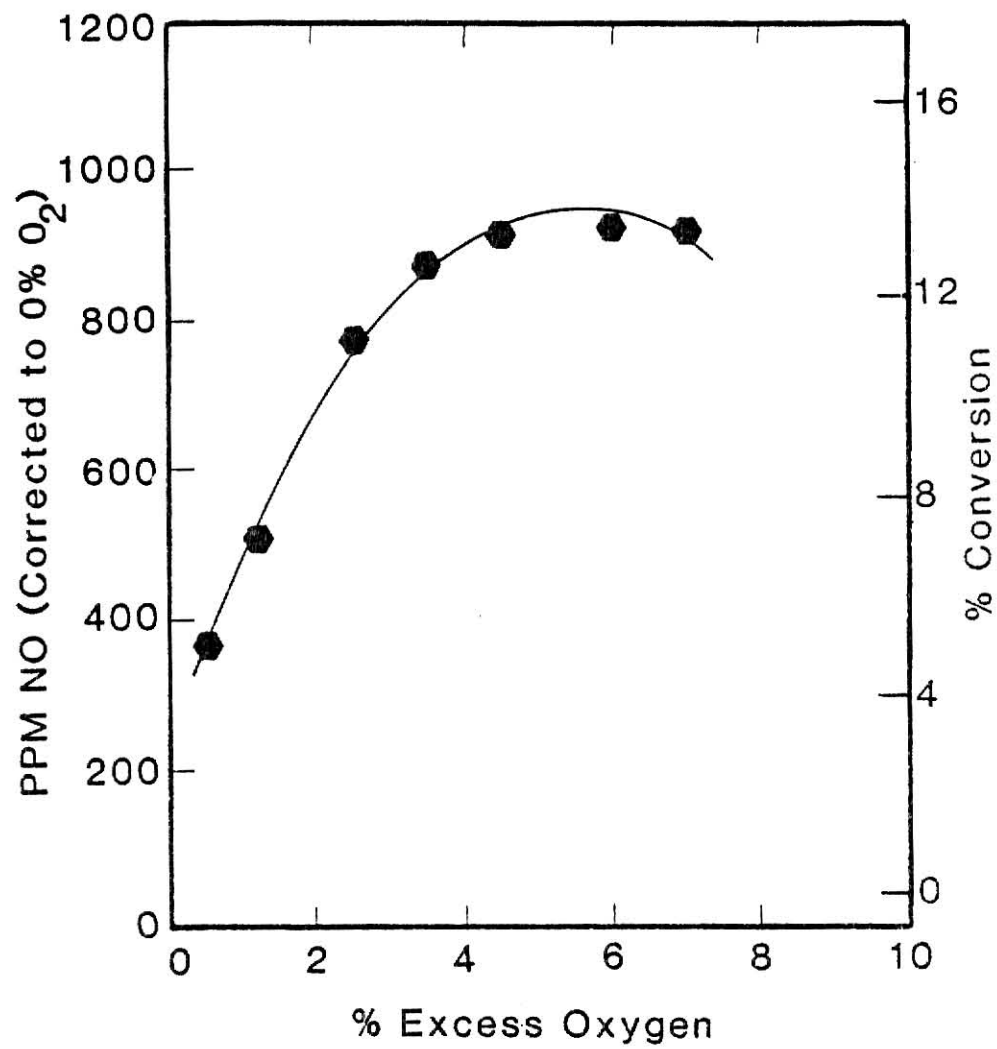


Fig. 4.7 NO_x Emissions and Estimated % Conversion vs. % Excess Oxygen for Corn Stover

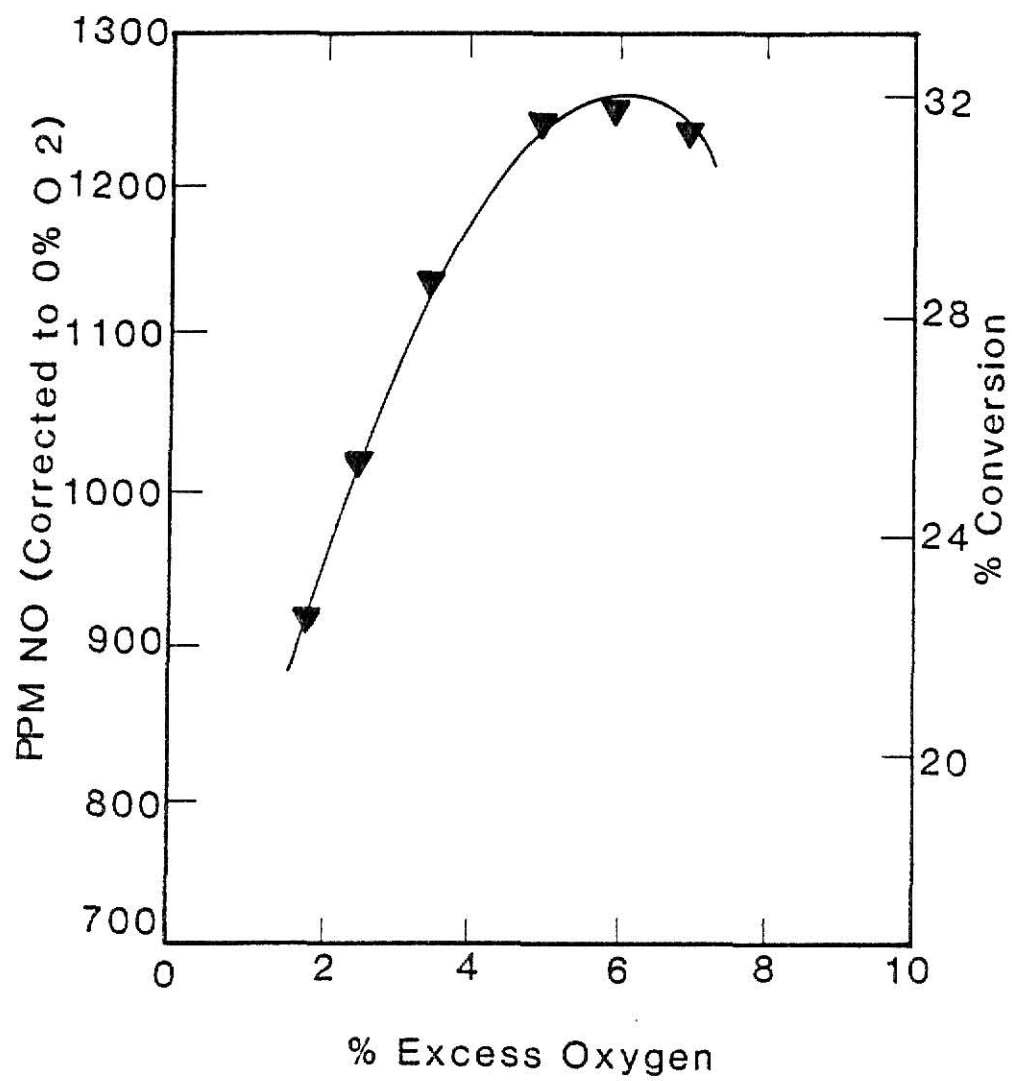


Fig. 4.8 NO_x Emissions and Estimated % Conversion vs. % Excess Oxygen for the Colorado/25% Corn Stover Mixture

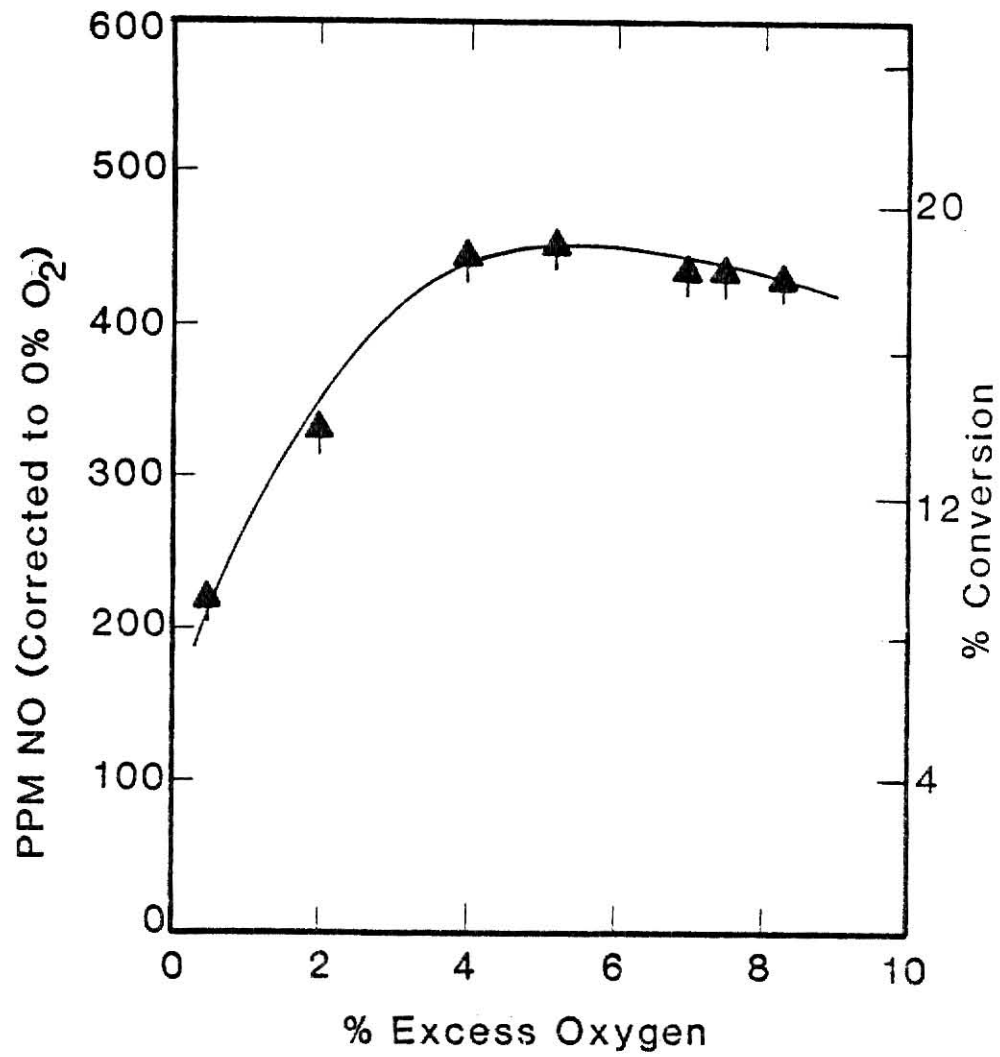


Fig. 4.9 NO_x Emissions and Estimated % Conversion for Mo-Kan Coal

volume mixture with wheat straw, the maximum NO_x occurs at 4.5% flue excess oxygen. Furthermore, when Colorado coal mixed with 50% by volume wheat straw is burned, the maximum NO_x occurs over a broad plateau between 3% and 6% flue excess oxygen.

If it is assumed that about 80% of the NO_x is due to fuel-bound nitrogen,⁽⁹⁾ the maximum conversions remain in line with those typically measured from solid fuels. Hence, the maximum conversions for both the Colorado coal and 75/25 coal/straw mixture are about 31% (see Figs. 4.2 and 4.3). For the 50/50 coal/straw mixture, the maximum conversion is nearly 27% (see Fig. 4.4). Of importance is the fact that while the maximum NO_x emissions decline with the decreasing amounts of fuel-bound nitrogen, at modest levels of excess air (less than about 5% flue gas O_2) the NO_x levels from the 75/25 volume percent mixture of Colorado coal and wheat straw are appreciably higher than those resulting from the Colorado coal. In fact, the NO_x emissions from the 50/50 mixture are greater than those from the coal for excess oxygen concentrations of about 4% or less. Interestingly, the NO_x emissions from wheat straw (shown in Figs. 4.1 and 4.5) display no maximum over the range of stoichiometries studies. The maximum conversion of about 27% of the fuel-bound nitrogen to NO_x is similar, however, to that of the other fuels and mixtures studied.

To eliminate the influence of dilution of N_2 on the results, these data have been normalized to 0% O_2 at the flue by the use of the relation

$$C_c = \left(\frac{21}{21 - C_{\text{O}_2}} \right) C_m \quad , \quad (4.1)$$

where C_c and C_m denote the corrected and measured concentrations of the sample, respectively, and C_{O_2} represents the concentration (in percent) of oxygen. This relation is widely used to aid comparison of data, and C_c is reported as the pollutant concentration reduced to stoichiometric conditions. (9)

The second biomass used in this investigation was corn stover. The flue NO_x levels as a function of excess oxygen are shown in Figs. 4.6 - 4.8. A behavior similar to that of coal/wheat straw mixtures is evidenced. The maximum emissions again occur at increasingly less excess oxygen as the biomass fuel is added.

As with the wheat straw/coal mixtures, there exists a range of excess oxygen concentrations for which the corn stover/coal mixtures yield higher NO_x emissions. In fact, this occurs over the entire range of oxygen concentrations studied for the 75/25 volume mixture. Thus, the influence of corn stover on the NO_x emissions is even more pronounced than is that of the straw.

Because of its importance locally, a high sulfur, high ash Mo-Kan coal was also used in this study. The NO_x emissions versus flue excess oxygen are shown in Fig. 4.9. While the conversion of fuel nitrogen is quantitatively the same versus flue excess oxygen as for the other fuels and mixtures, the NO_x levels and the percentage conversion of the fuel nitrogen are both much less. Because of the higher ash content (3x%), equivalent feeding ranges (g/min) of the solid fuels resulted in a lower flame temperature from the Mo-Kan coal (see Fig. 4.10). Thus only 17% of the fuel nitrogen was converted to NO_x compared to 23% conversion from Colorado coal at 3% flue excess oxygen.

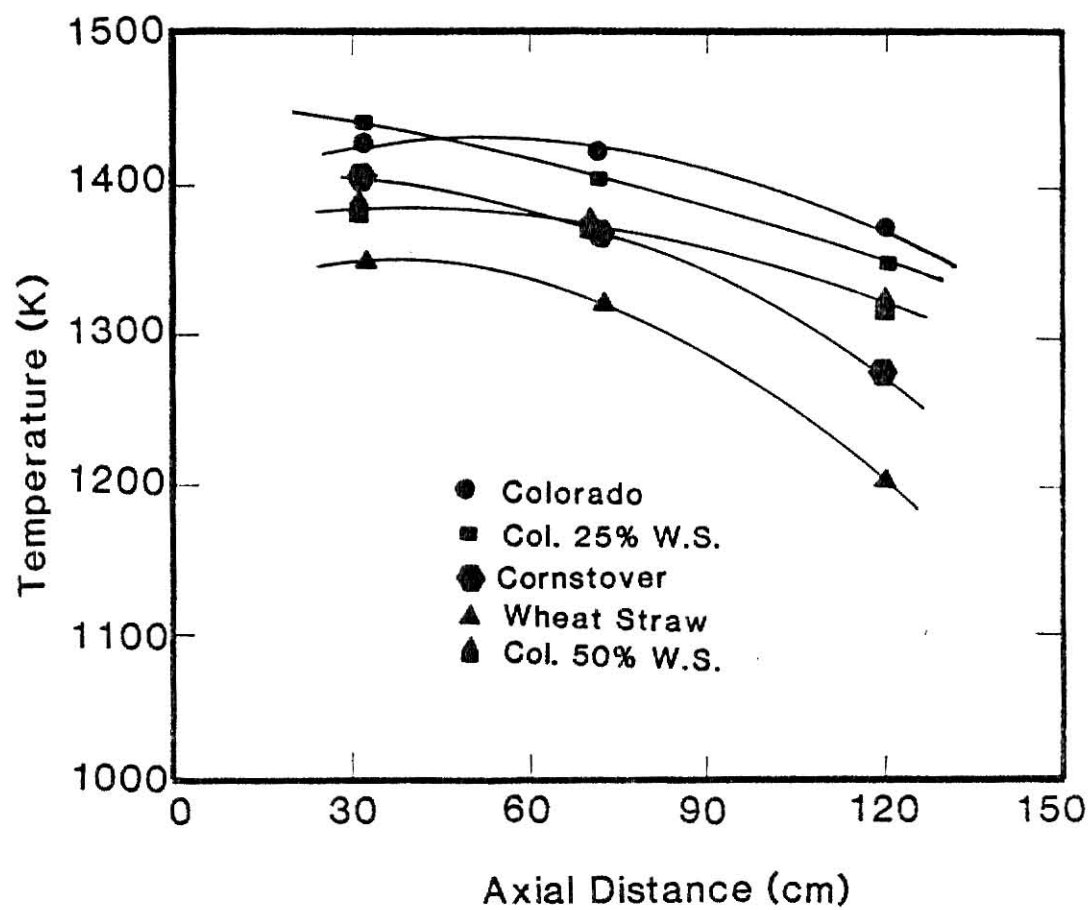


Fig. 4.10 Axial Temperature Profiles for Fuels Tested

The question arises, why does the 75/25 volume percent mixture of the Colorado coal/wheat straw yield higher NO_x emissions than either fuel alone at any percent excess oxygen? As indicated in Fig. 4.10, the temperature profiles in the furnace are quite similar for the coal and the mixture. However, the straw burns at a much lower temperature by itself. As noted by Soloman⁽¹⁵⁾ the release of fuel-bound nitrogen is highly temperature dependent. To what extent can the fuel nitrogen release be expected to increase in the early stages of the flame if the temperature increases from 1350 to 1450 K? Since the nitrogen in the biomass fuels is probably more loosely bound than that in coal, its release can be approximated by Soloman's first order kinetics for loosely-bound nitrogen,

$$K = 200 \exp [-7600/T] \text{ sec}^{-1} \quad . \quad (4.3)$$

The ratio of loosely-bound nitrogen release at 1450 to 1350 K, at the residence times typical of the first 30 cm of the furnace (~ 0.8 sec.), is only 1.88. This increase in release of nitrogen bound in wheat straw is not enough to explain the increase in nitrogen conversion at any percent excess oxygen. For example, at 4% excess oxygen, the observed NO_x emission from the mixture was about 1120 ppmV, where Colorado alone emitted about 1000 ppmV. At the same percent excess oxygen, but with a flame cooler by at least 100 K, the wheat straw emitted only 620 ppmV. The 100 K increase in temperature would increase the release of its loosely-bound nitrogen by 88%. However, not all of this nitrogen will be converted to NO_x . Pershing et al.⁽¹⁴⁾ (see Fig. 4.11) found that the ammonia conversion to NO_x at about 4% excess oxygen in the stack is approximately 65%. Based on these arguments, if it has been assumed

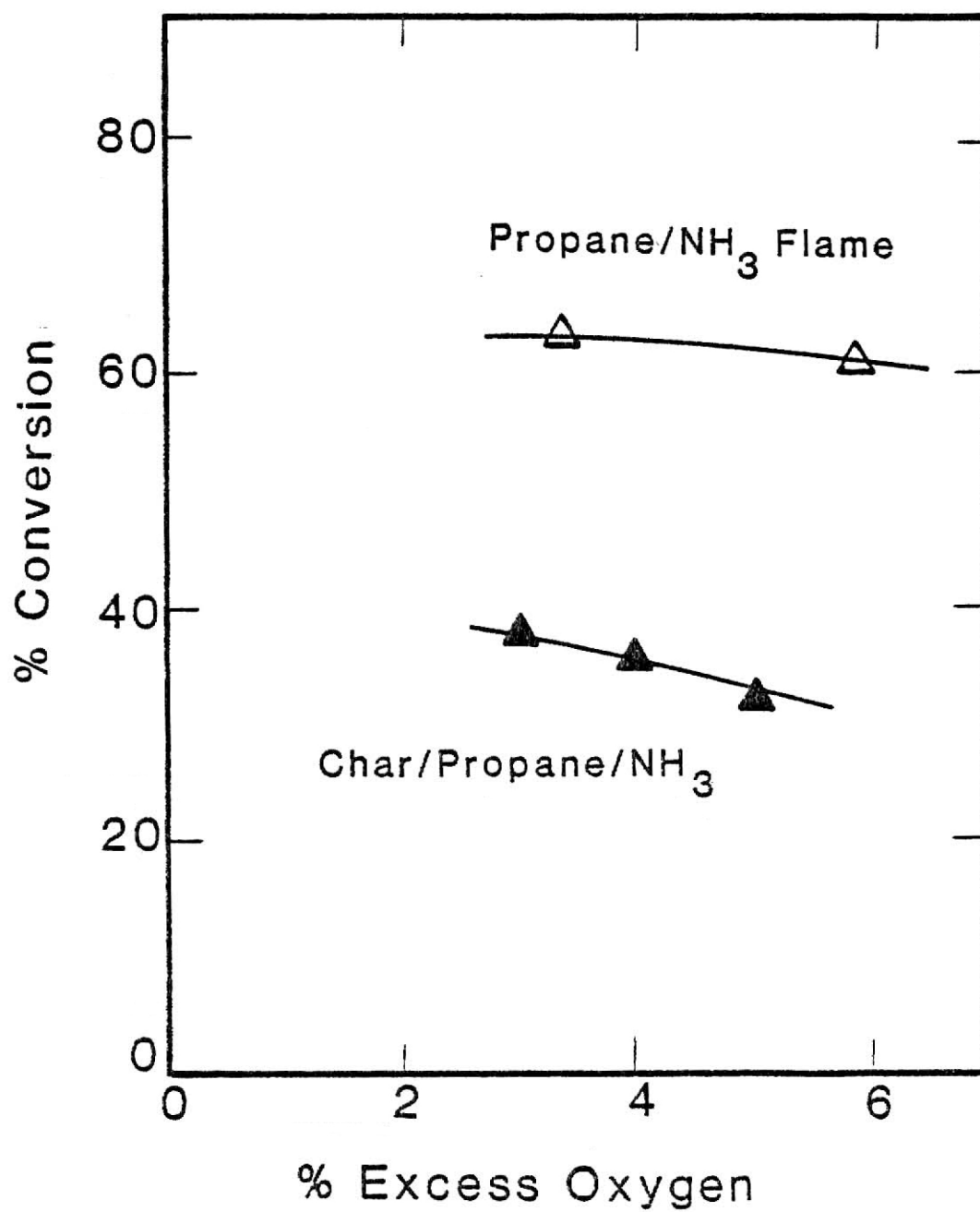


Fig. 4.11 Ammonia Conversion to NO_x in Propane/ NH_3 Flame, and Char/Propane/ NH_3 Flame (after Pershing et al.¹⁴)

that all the nitrogen in the wheat straw is converted to NH_3 , then the limiting conversion of fuel-bound nitrogen to NO_x is predicted to be 65%. Therefore, the maximum increase of NO_x formation from wheat straw at 1450 K is 57% ($88\% \times .65$) more than the level observed at 1350 K. This value is approximately 975 ppmV. If the extent of conversion of fuel-bound nitrogen in the two fuels were the same in the mixture as they are alone, one would expect $1000 \text{ ppmV} \times .91^a + 975 \text{ ppmV} \times .09 = 998 \text{ ppmV}$, where the observed value was 1120 ppmV. Therefore, the addition of wheat straw apparently provides another kinetic pathway for NO_x production besides those present with either fuel alone.

The availability of fuel-bound oxygen of the wheat straw in mixture could increase the conversion of fuel nitrogen in Colorado coal. Habelt⁽¹⁶⁾ has suggested that fuel nitrogen conversion in slowly mixed diffusion flames can be correlated in terms of the fuel/oxygen/nitrogen ratio. Fuel oxygen was believed to affect fuel NO_x formation because it is immediately available, it may be associated with the volatile fuel nitrogen fragments, and it can, therefore, readily form NO_x .

Since the fuel properties of corn stover are similar to wheat straw, and the data shown in Fig. 4.6 behave qualitatively the same as the data shown in Fig. 4.1, similar arguments can be advanced for the influence of the high volatile, high oxygen cornstover on NO_x formation.

^aThe mass fraction of Colorado and wheat straw in 75/25 mixtures is based on the bulk densities and volume fractions of each fuel.

$$\rho_{\text{Colorado}} = 0.68 \text{ g/cm}^3, \rho_{\text{W.S.}} = 0.21, \rho_{\text{C.S.}} = 0.20$$

$$0.25 \times 0.21 + 0.75 \times 0.68 = 0.56 \text{ g/cm}^3$$

$$(\text{wt}\%) = \frac{0.05}{0.56} \times 100 = 9.0\%, (\text{wt}\%) = \frac{0.51}{0.56} \times 100 = 91.0\%.$$

4.1.2 Axial Gas Analysis

The NO_x variation along the length of the furnace is shown in Figs. 4.12-4.14. Qualitatively the axial profiles are quite similar with one exception, corn stover. The NO_x formation occurs, primarily, in the upper half of the furnace, as shown by the plateaus reached in NO_x concentration between 60 and 90 cm from the burner for the various fuels. However, as noted in Section 4.1.1, the NO_x emissions for the Colorado coal/25% wheat straw mixture are higher than the sum of the individual contributions for lower excess O_2 concentrations. So, too, are the axially resolved NO_x concentrations higher for the mixture than they are for the weighted sum of the fuels throughout the furnace.

The one exception to the NO_x profiles is the axial distribution of NO_x from corn stover combustion. It was observed that the NO_x decreased from 820 to 720 ppmV over a 50 cm length, but at the flue the concentration of NO_x was about 800 ppmV. Since this variation is only about 100 ppmV, it can be assumed, without additional evidence, that the NO_x peaks very early in the flame and remains nearly constant throughout the remainder of the furnace. Suffice it to say that the combustion of corn stover was effected with difficulty due to its high ash content.

4.1.3 Axial Solids and Gas-Phase Compositions

To assist in the understanding of the combustion of the solid fuels of the axial compositions, the major gas-phase species and the elemental compositions of partially burned solids have been determined. Of particular interest is the question of how wheat straw and corn stover influence the NO_x formation along the length of the furnace.

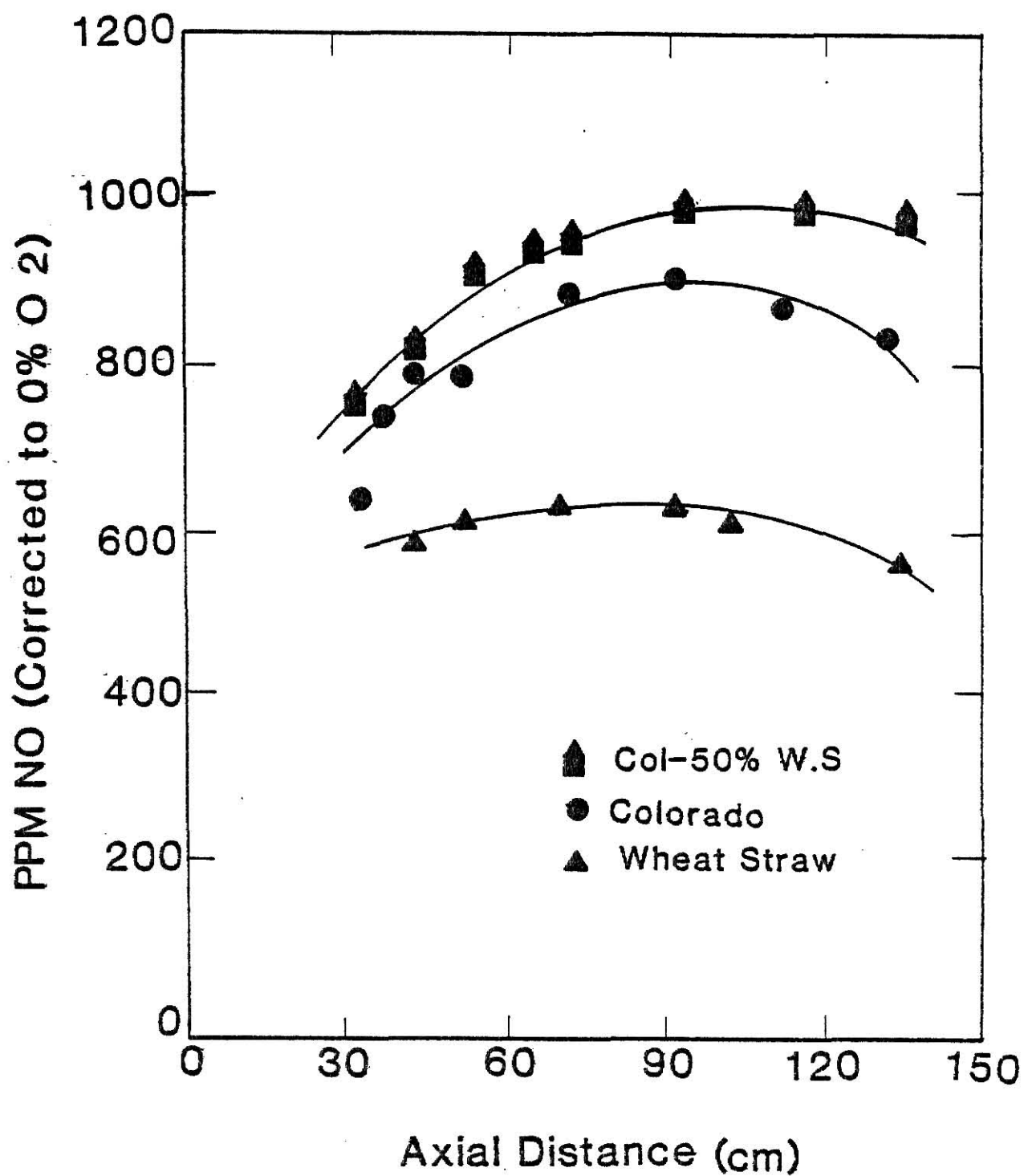


Fig. 4.12 Axial NO_x Distribution for Colorado, Wheat Straw, and Colorado/Wheat Straw Mixture

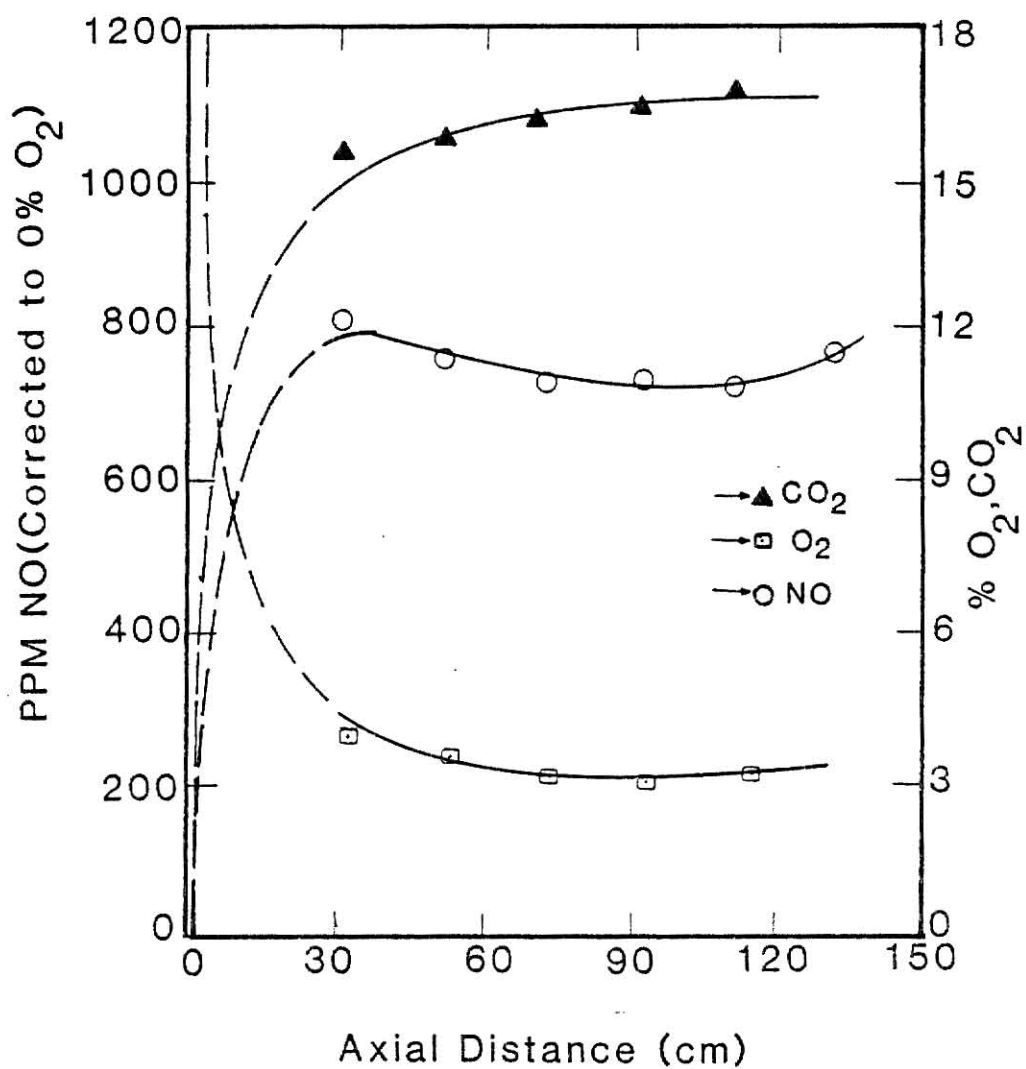


Fig. 4.13 Axial NO_x Distribution from Corn Stover

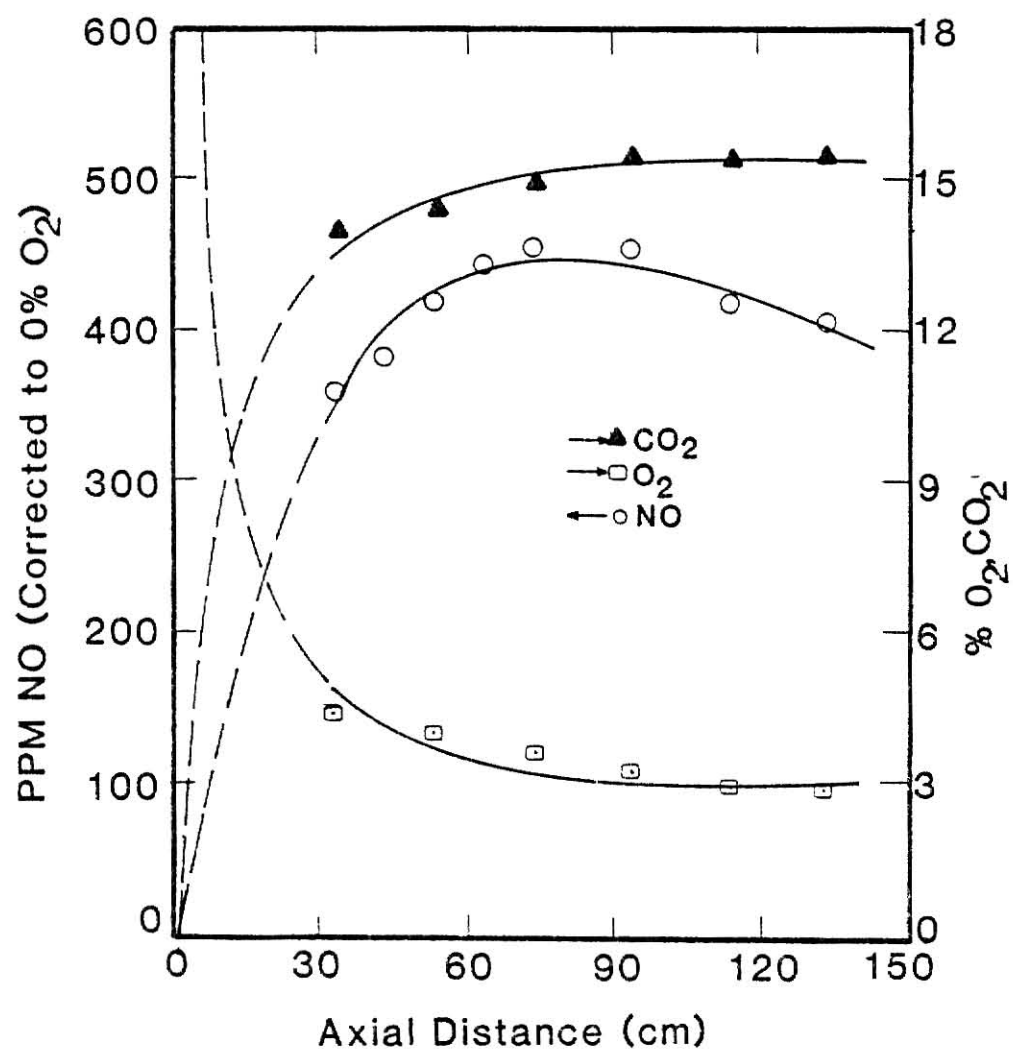


Fig. 4.14 Axial NO_x Distribution from Mo-Kan Coal

Figs. 4.15 through 4.19 show the percent burnout of the fuels as a function of axial location. The loss of each component is calculated using the ash as a tracer for weight loss; thus the loss of each component can be determined as

$$\% B = \left[1 - \frac{b}{b_o} \frac{a_o}{a} \right] \times 100 \quad (4.3)$$

where,

B = burnout,

b = the concentration of each component,

a = ash concentration,

o = denotes the initial concentration (dry basis).

In all the fuels used, hydrogen is lost preferentially to either nitrogen or carbon. The hydrogen burnout exceeded 99.1% for each fuel, while the nitrogen and carbon burnout exceeded 98.7% and 96.6%, respectively. Since the coal particle size (200 mesh) was nearly (4x) smaller than biomass, it is not surprising that the solid phase disappearance, by both devolatilization and heterogeneous combustion, occurs more quickly for the coals. What is surprising is that at 75 cm, the nitrogen loss exceeded 90% for all fuels, and yet the percentage conversion of fuel-bound nitrogen varied considerably among the fuels. Obviously, the relative tightness with which the fuel nitrogen is held in the solid fuel is but one determinant of what percentage fuel-bound nitrogen is ultimately converted to NO_x . A principal factor must remain the temperature, which is much lower for the biomass fuels and the Mo-Kan coal. Other factors could be the reduction of NO_x by gaseous intermediates or mineral matter or possibly soot, and the availability of oxygen in the region of most rapid nitrogen evolution.

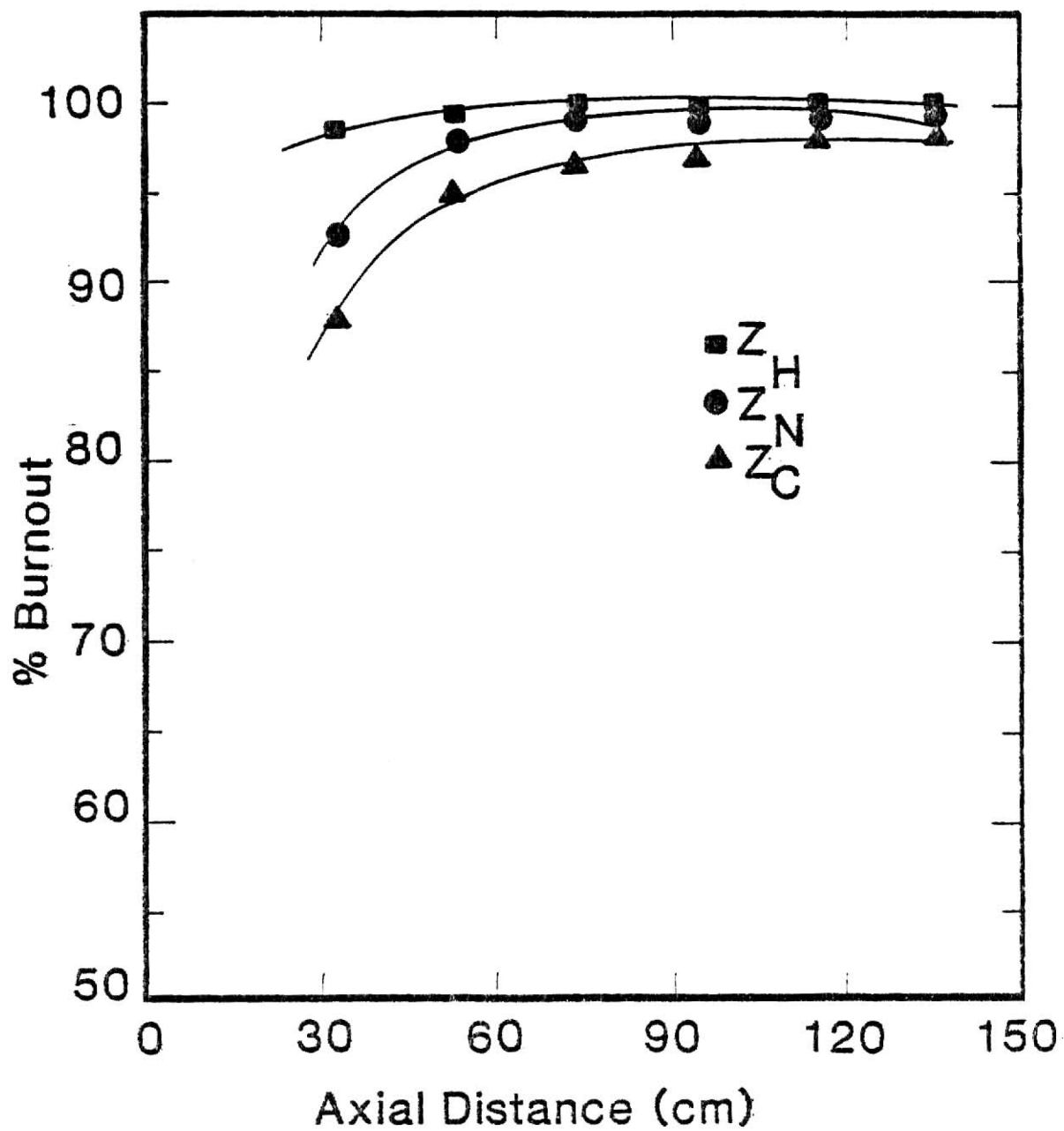


Fig. 4.15 Axial % Burnout of Hydrogen, Nitrogen and Carbon for Colorado Coal

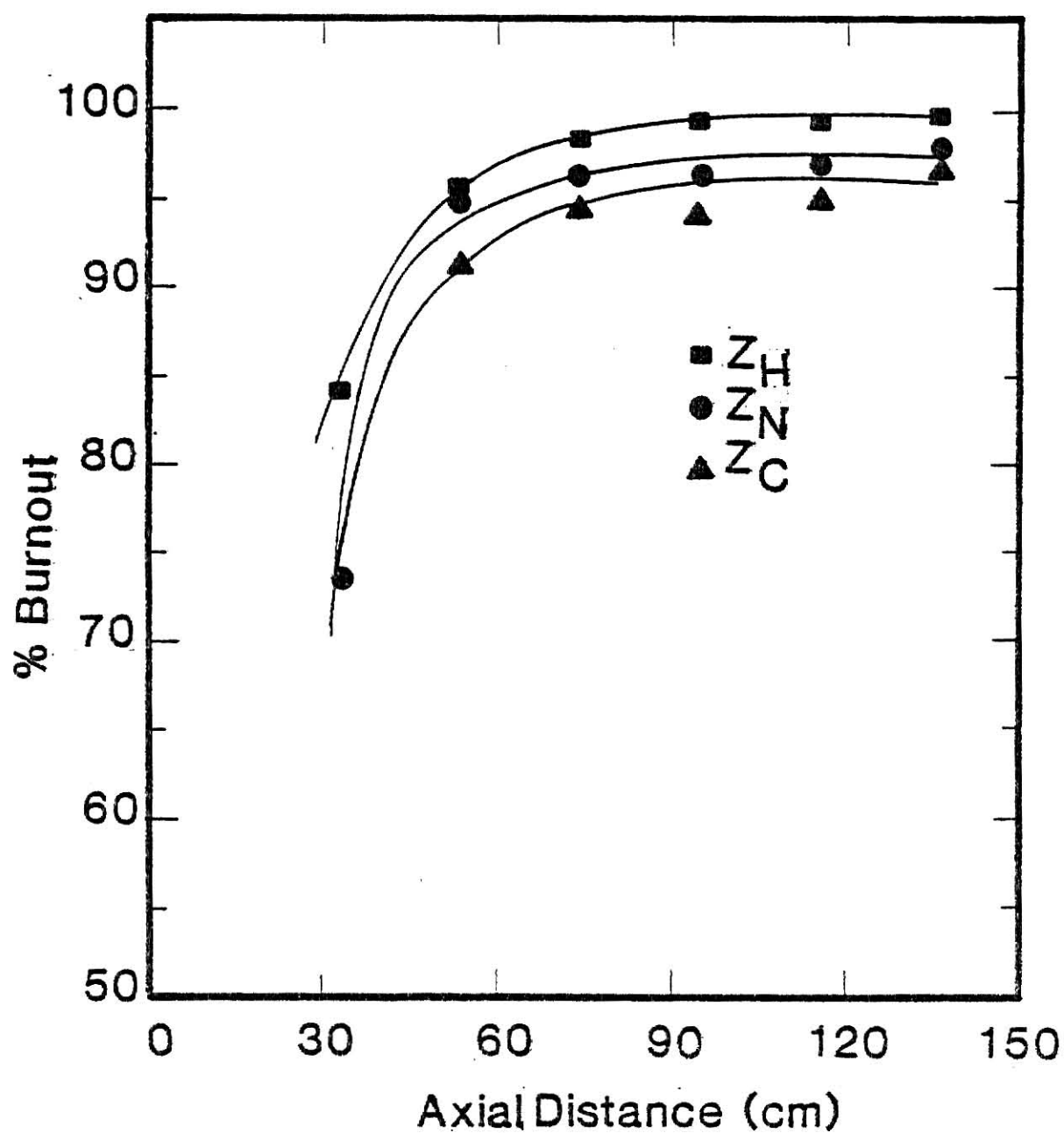


Fig. 4.16 Axial % Burnout of Hydrogen, Nitrogen, and Carbon for the Colorado/50% Wheat Straw Mixture

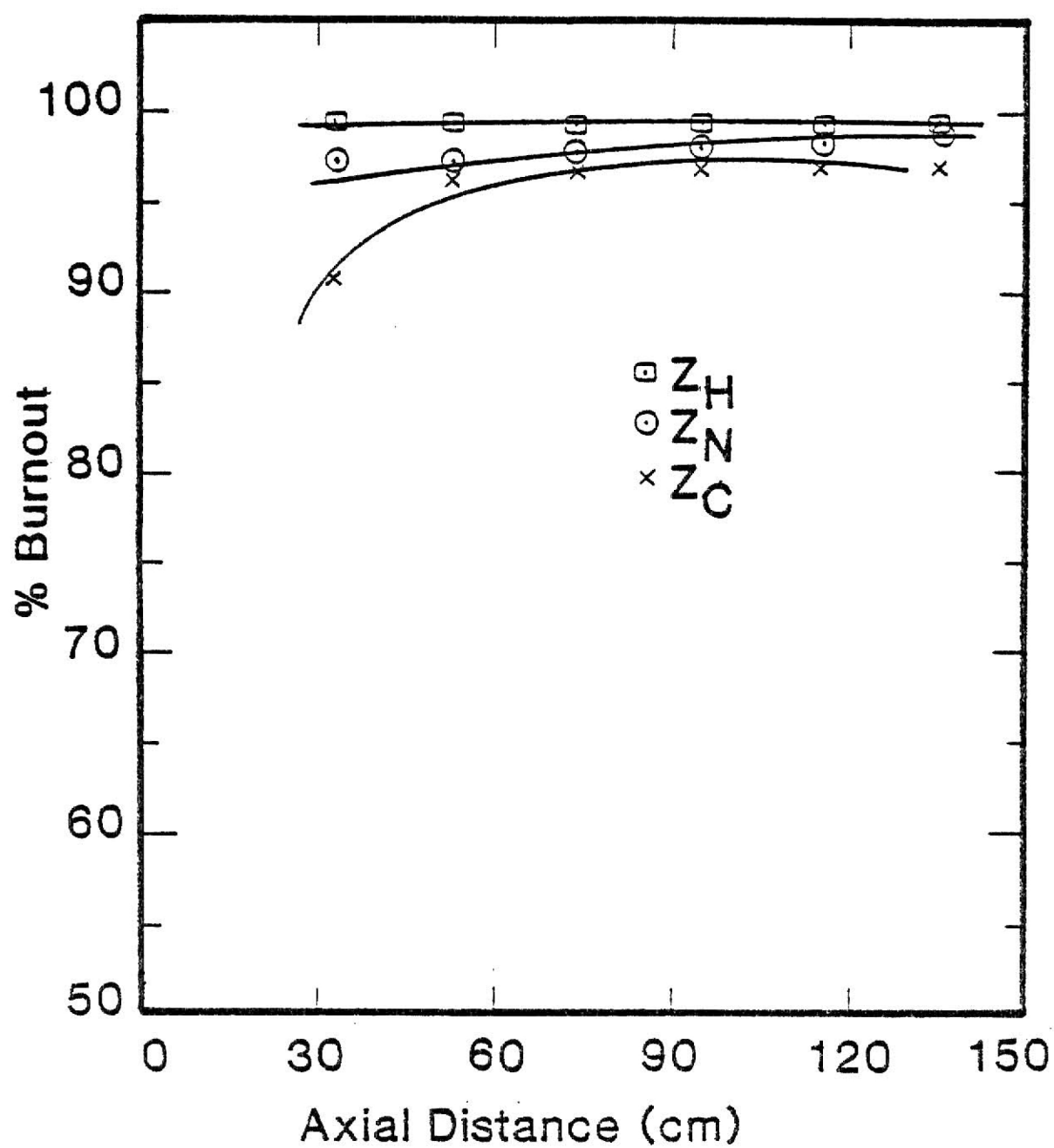


Fig. 4.17 Axial % Burnout of Hydrogen, Nitrogen and Carbon for the Mo-Kan Coal

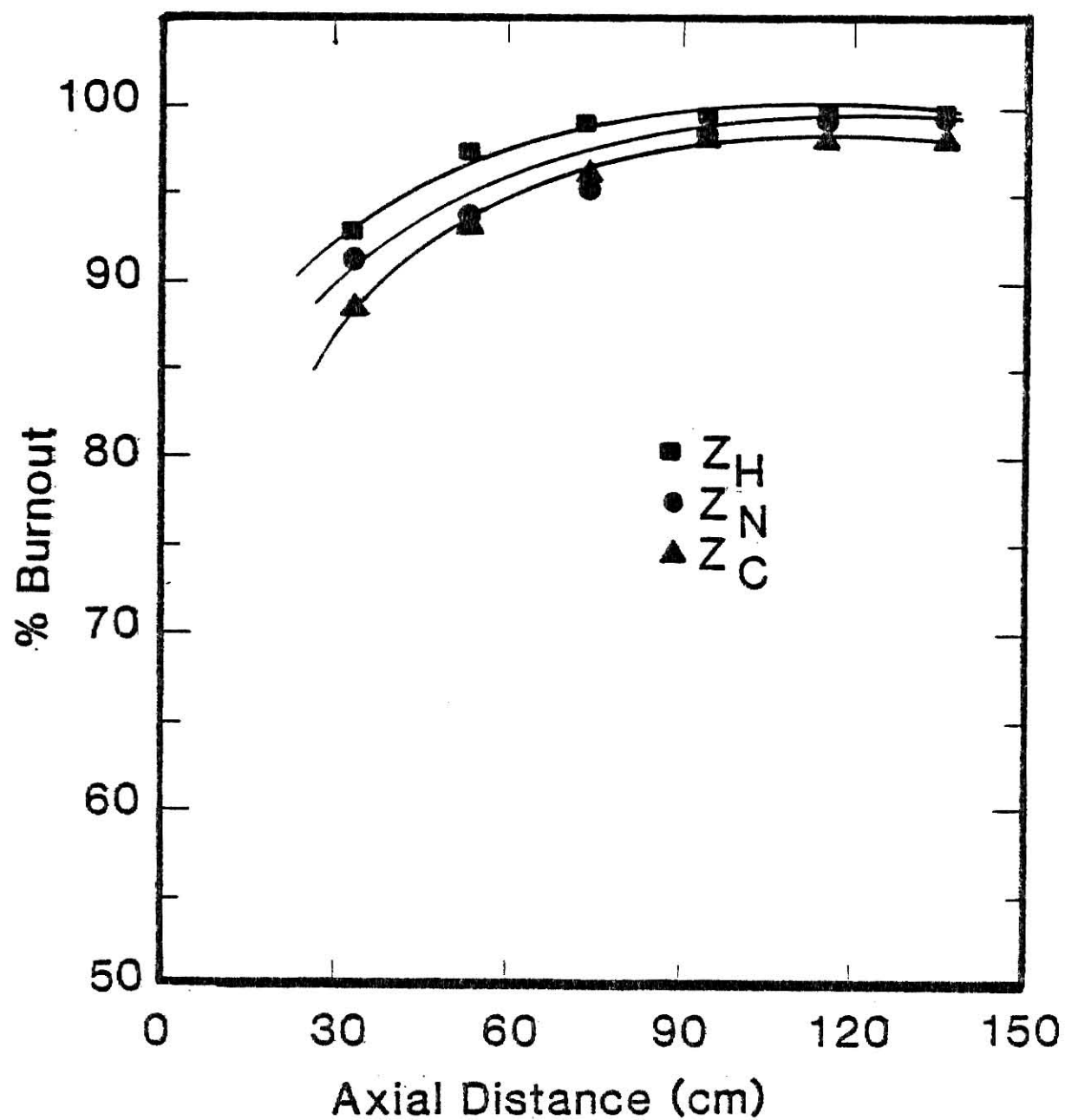


Fig. 4.18 Axial % Burnout of Hydrogen, Nitrogen, and Carbon for Wheat Straw

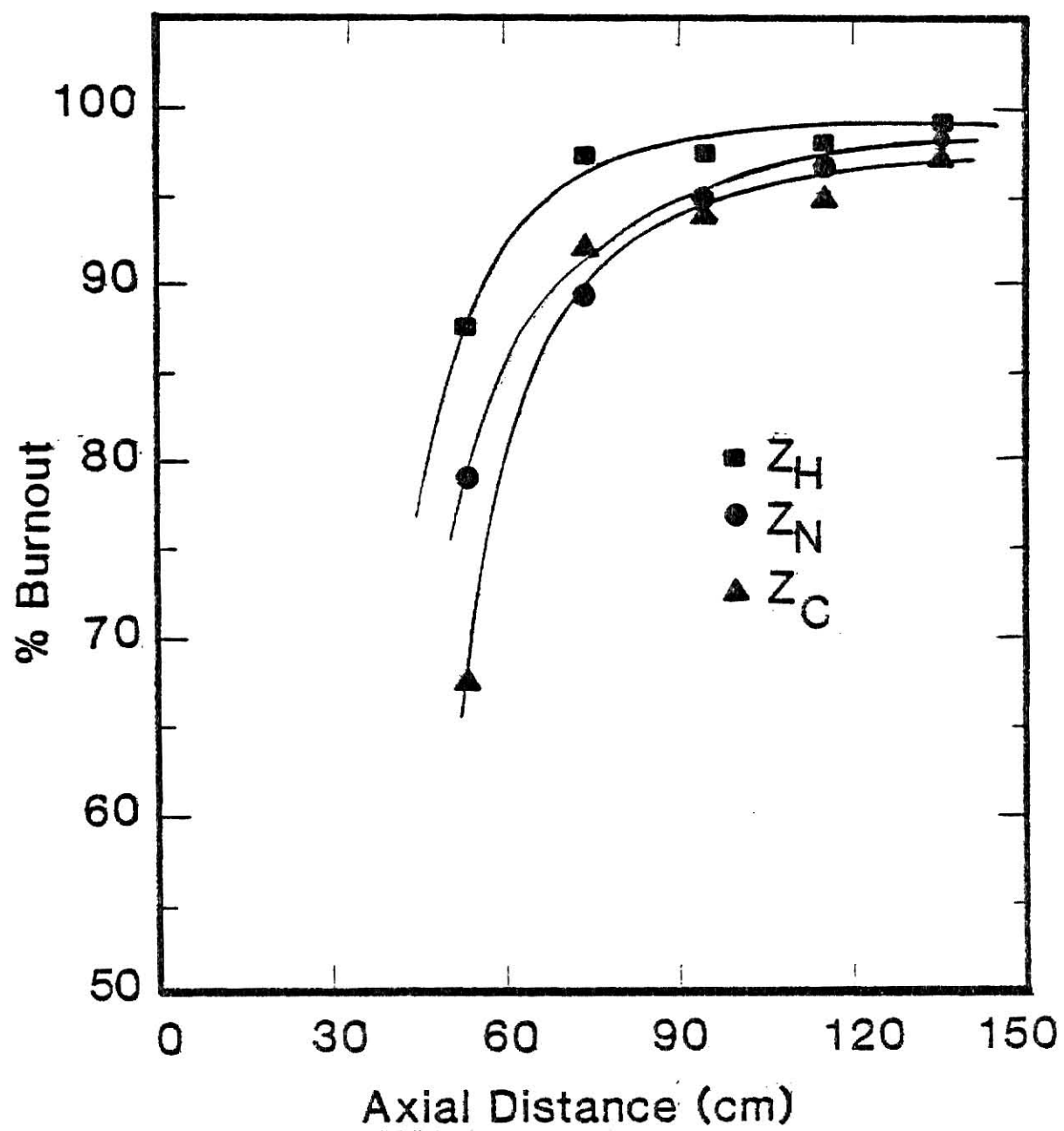


Fig. 4.19 Axial % Burnout of Hydrogen, Nitrogen, and Carbon for Corn Stover

Although more detailed study is required to truly understand these trends, they are consistent with the hypothesis that the greater oxygen content of the straw is assisting the conversion of the flue-bound nitrogen at richer apparent stoichiometries. For instance, the ratio of the flue excess oxygen concentrations for maximum NO_x for Colorado coal/25% wheat straw mixture is approximately the same as the ratio of their initial oxygen contents. A similar observation may be made for Colorado coal/50% wheat straw mixture. The ratios of the initial oxygen concentration are about 1.55 for Colorado/25% wheat straw and 2.12 for Colorado/50% wheat straw mixtures respectively.

The NO_x emissions from unstaged combustion are actually in agreement with those reported by Pershing et al.⁽¹⁴⁾ for a wide range of U.S. coals. Fuel NO_x formation as a function of percent nitrogen in the fuel (on a dry ash-free basis) is shown in Fig. 4.20. The shaded area represents the NO_x emissions for 26 different coals burned in an axial diffusion flame with a solid's feeding rate of approximately 2.2 Kg/hr and with a 5% excess O_2 . The particle size distribution was 65% through 200 mesh, similar to that used in the current study. In general, fuel NO_x emissions increased with increasing fuel nitrogen content. Lower rank coals usually contain less nitrogen and produce less NO_x than the higher volatile bituminous coals. The Mo-Kan coal and corn stover produced NO_x emissions lower than those typical of the Pershing study. The reasons for this lower conversion have been speculated on above.

The gas-phase composition measurements as a function of axial position in the combustion chamber are shown in Figs. 4.21-4.25. To show the same flue gas compositions as described in Section 4.1.1, the

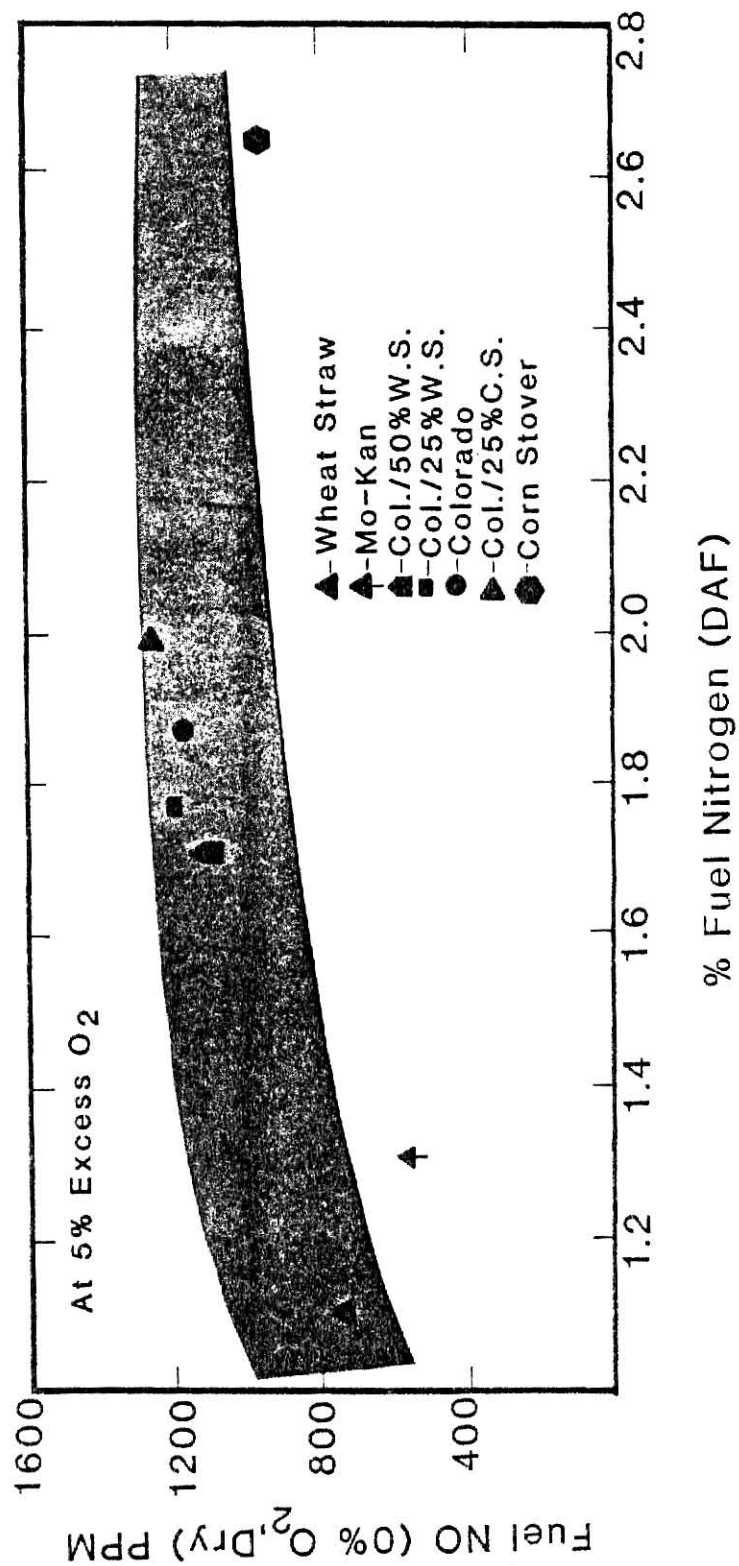


Fig. 4.20 Comparison of NO_x Emissions vs. % Fuel Nitrogen (DAF) with Pershing, et al.¹⁴

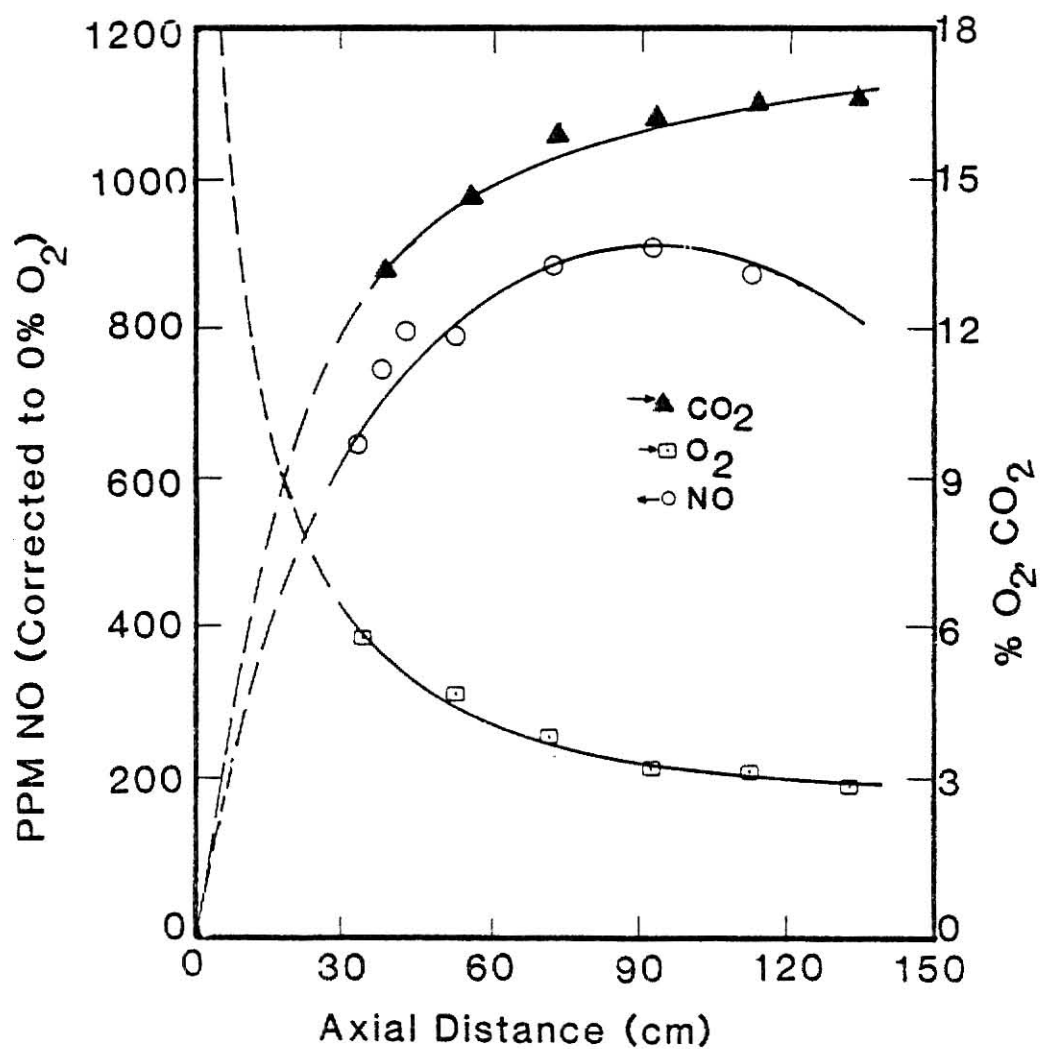


Fig. 4.21 Axial Gas-Phase Composition for Colorado Coal

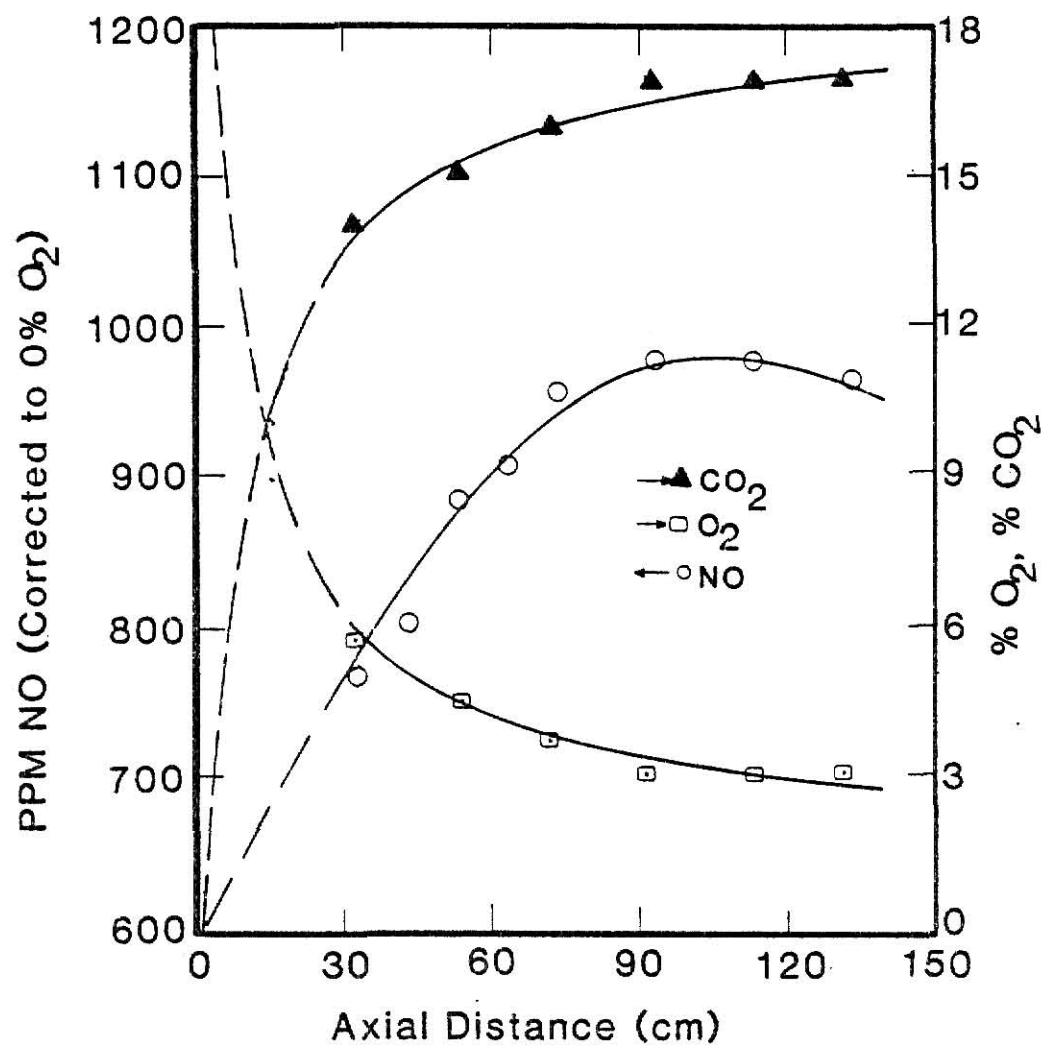


Fig. 4.22 Axial Gas Phase Composition for the Colorado/50% Wheat Straw Mixture

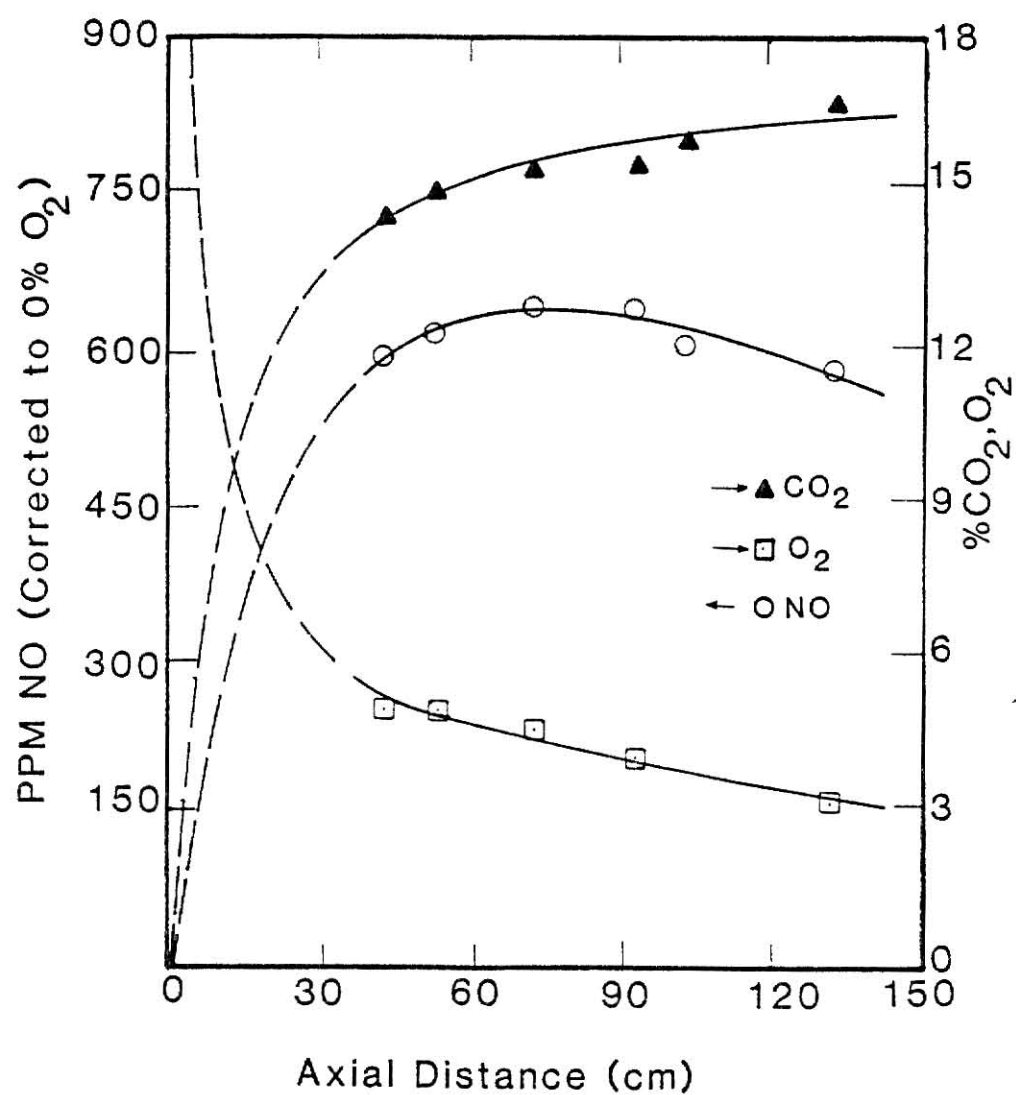


Fig. 4.23 Axial Gas Phase Composition for Wheat Straw

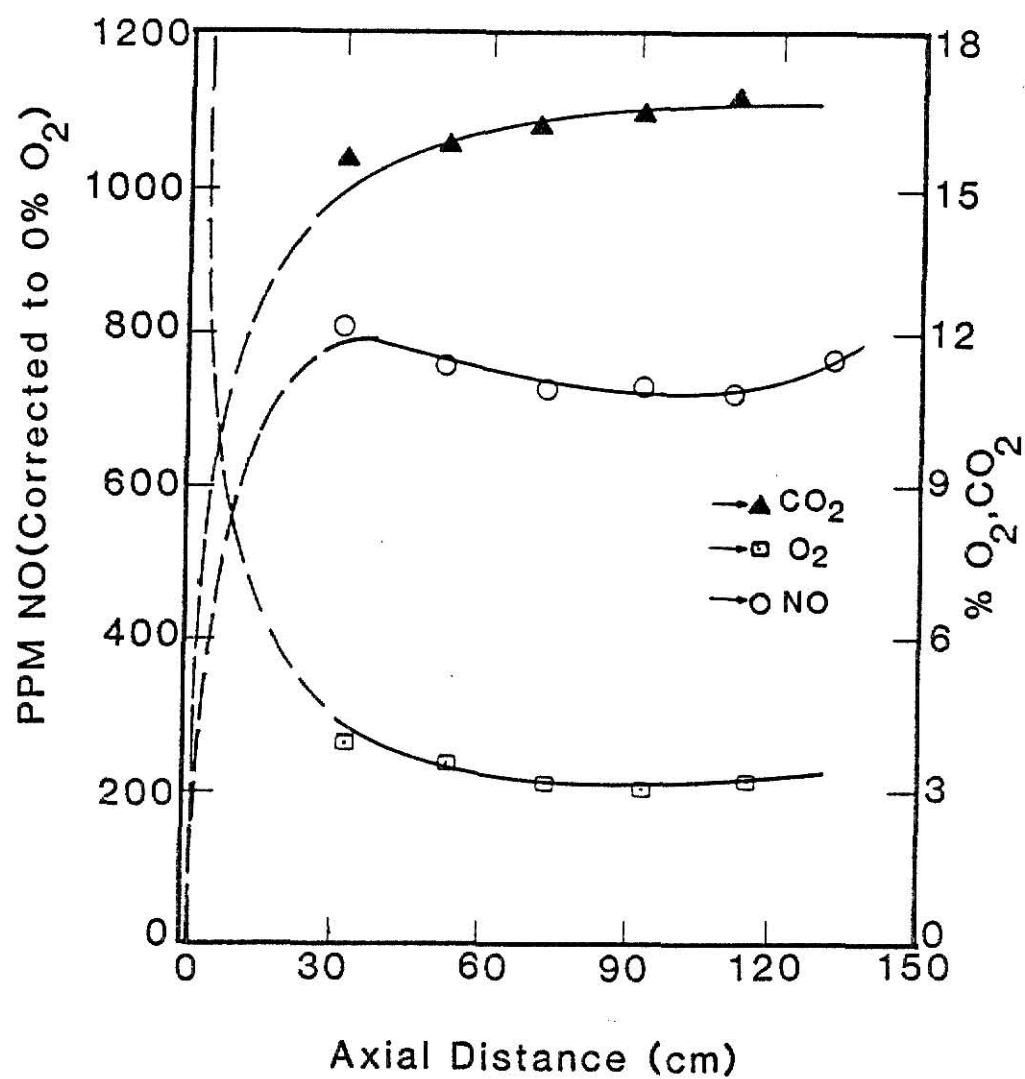


Fig. 4.24 Axial Gas Phase Composition for Corn Stover

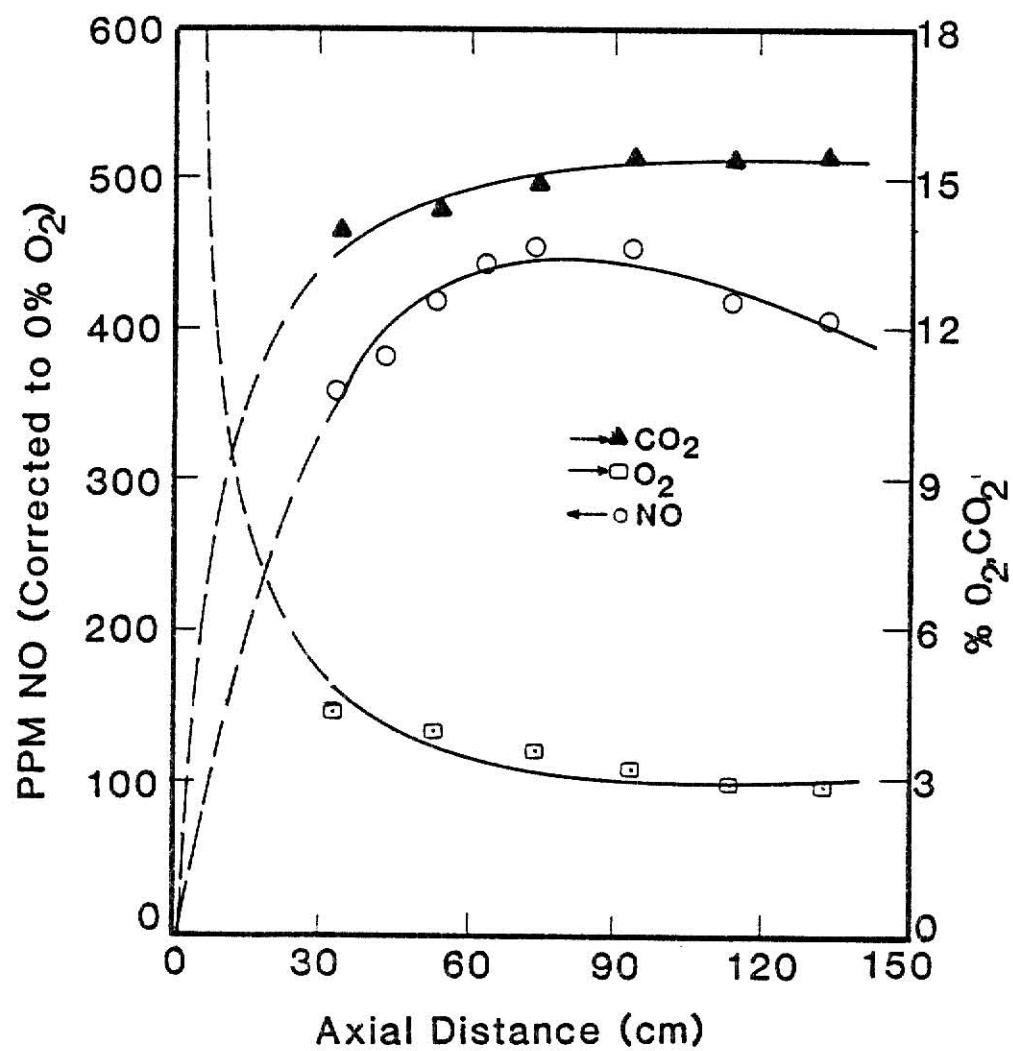


Fig. 4.25 Axial Gas Phase Composition for Mo-Kan Coal

NO_x concentrations are corrected to 0% O_2 . The axial measurements of the gas-phase composition for the Colorado coal approached their limiting values earlier in the flame than did the same concentrations for the Colorado coal/50% wheat straw mixture, a behavior expected from the solid-phase composition data shown in Figs. 4.16-4.20.

The concentration of O_2 decreases while the CO_2 and NO_x levels increase. This may reflect the axial burnout of solids. The nitrogen loss from solid fuels occurs faster than carbon; thus, NO_x peaks even as CO_2 continues to increase due to fixed carbon burnout.

4.2 Staged Combustion Gas Analysis

Previous studies (9,17) have shown that one of the effective techniques for controlling fuel NO_x formation is staged combustion, whereby the availability of oxygen is reduced during the period of rapid evolution of fuel-bound nitrogen. As noted in Sections 4.1.1 and 4.1.2, the loss of fuel nitrogen from the solid is greater than 90% completed for all the fuels in the first 75 cm of distance in the furnace. Based on these measurements, a staging collar was installed in the fourth section of the furnace, approximately 94 cm below the burner (see Section 2.1). Solid fuel was fired in the same fashion as before; however, addition of a portion of the combustion air was delayed until most of the fuel nitrogen had evolved.

The resulting NO_x emissions at the flue, when the overall excess oxygen is maintained at 3%, are presented in Figs. 4.26-4.30. It can be seen that for all the fuels tested, as the first stage stoichiometric ratio, SR_1 , was increased (i.e., the first stage made progressively more rich), the exhaust NO_x emissions decreased, reached a minimum, and then

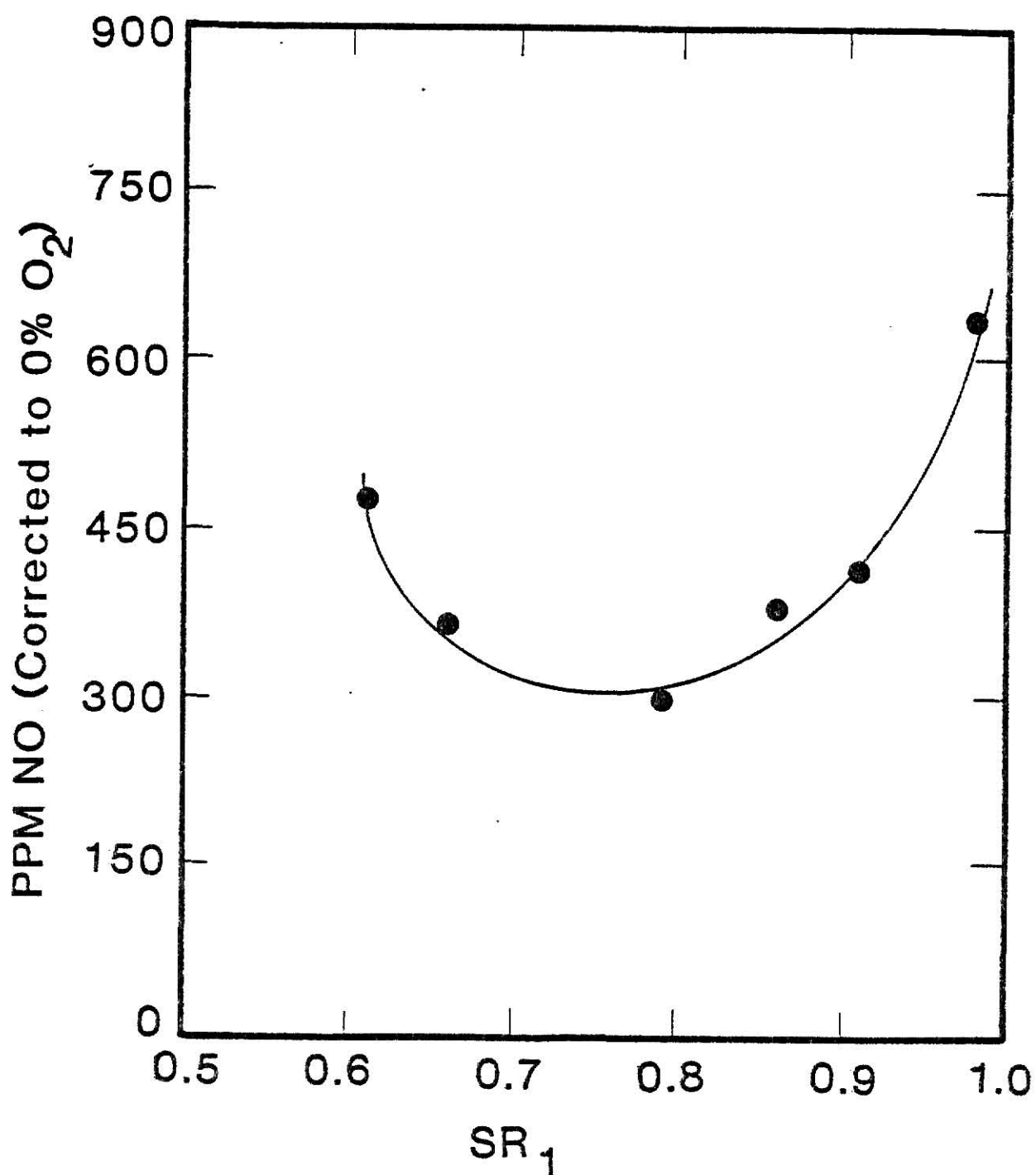


Fig. 4.26 NO_x Emissions vs. First Stage Stoichiometric Ratio (SR_1) for Colorado Coal

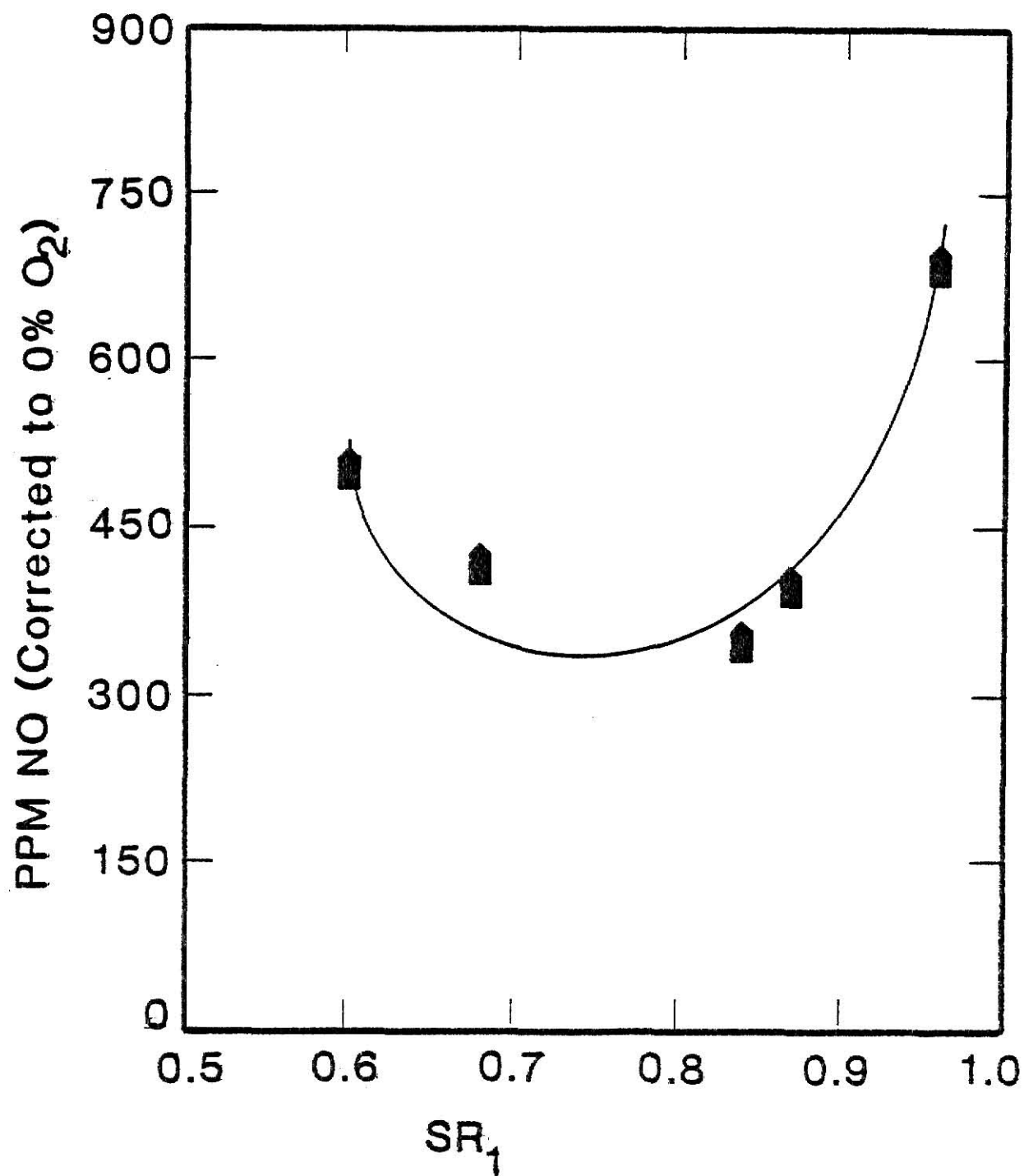


Fig. 4.27 NO_x Emissions vs. First Stage Stoichiometric Ratio (SR_1) for the Colorado/50% Wheat Straw Mixture

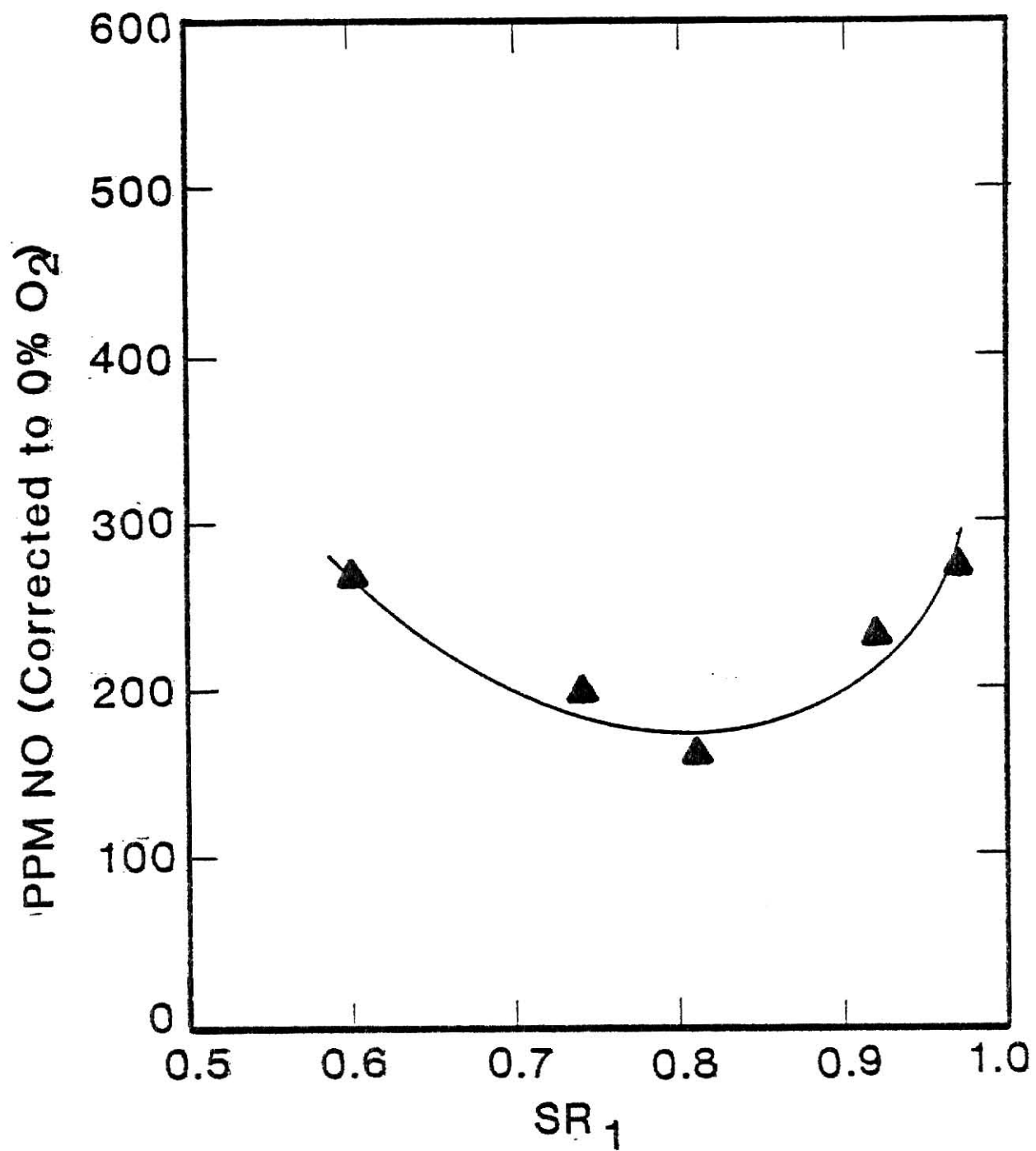


Fig. 4.28 NO_x Emissions vs. First Stage Stoichiometric Ratio (SR_1) for Wheat Straw

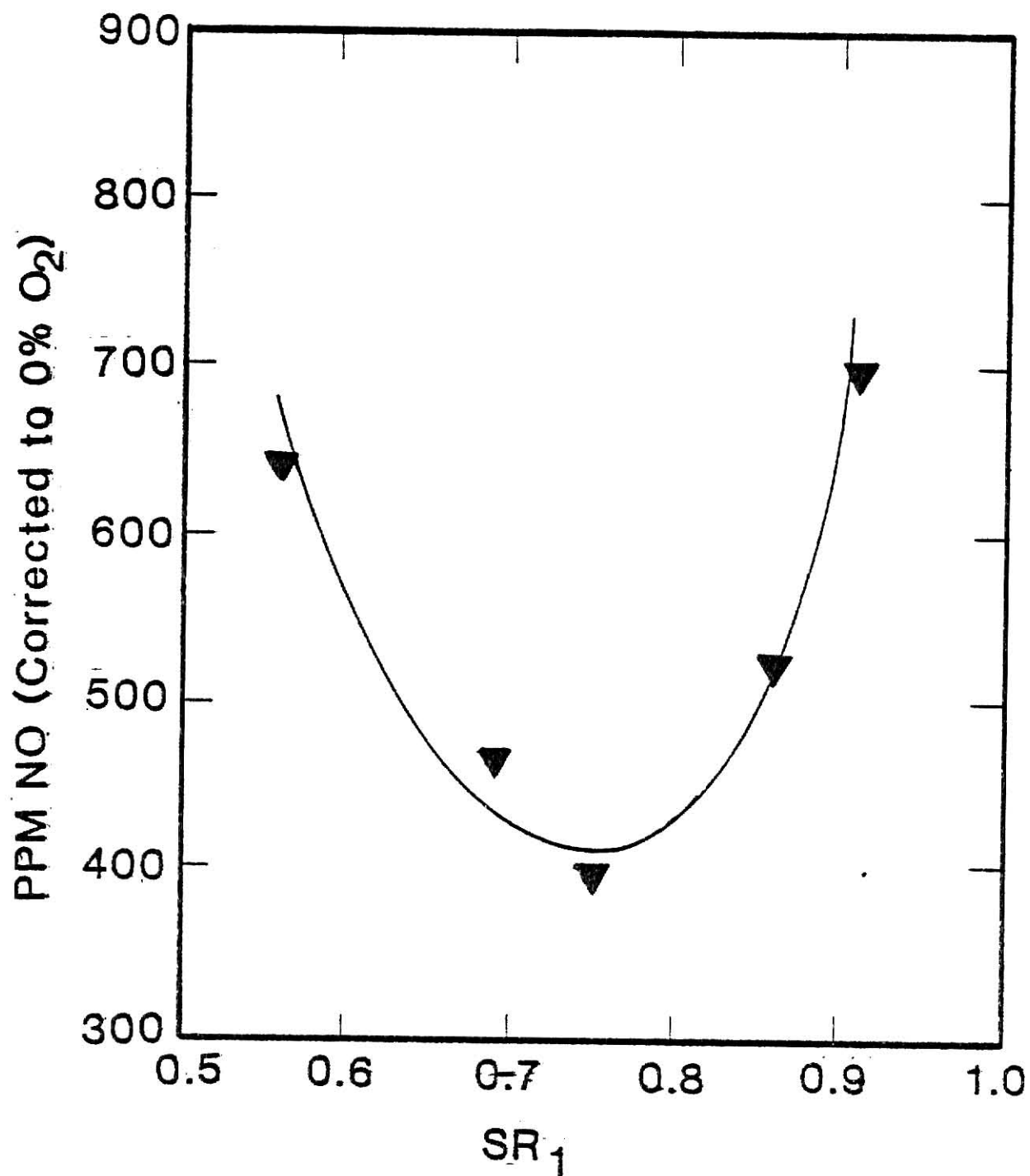


Fig. 4.29 NO_x Emissions vs. First Stage Stoichiometric Ratio (SR_1) for the Colorado/25% Corn Stover Mixture

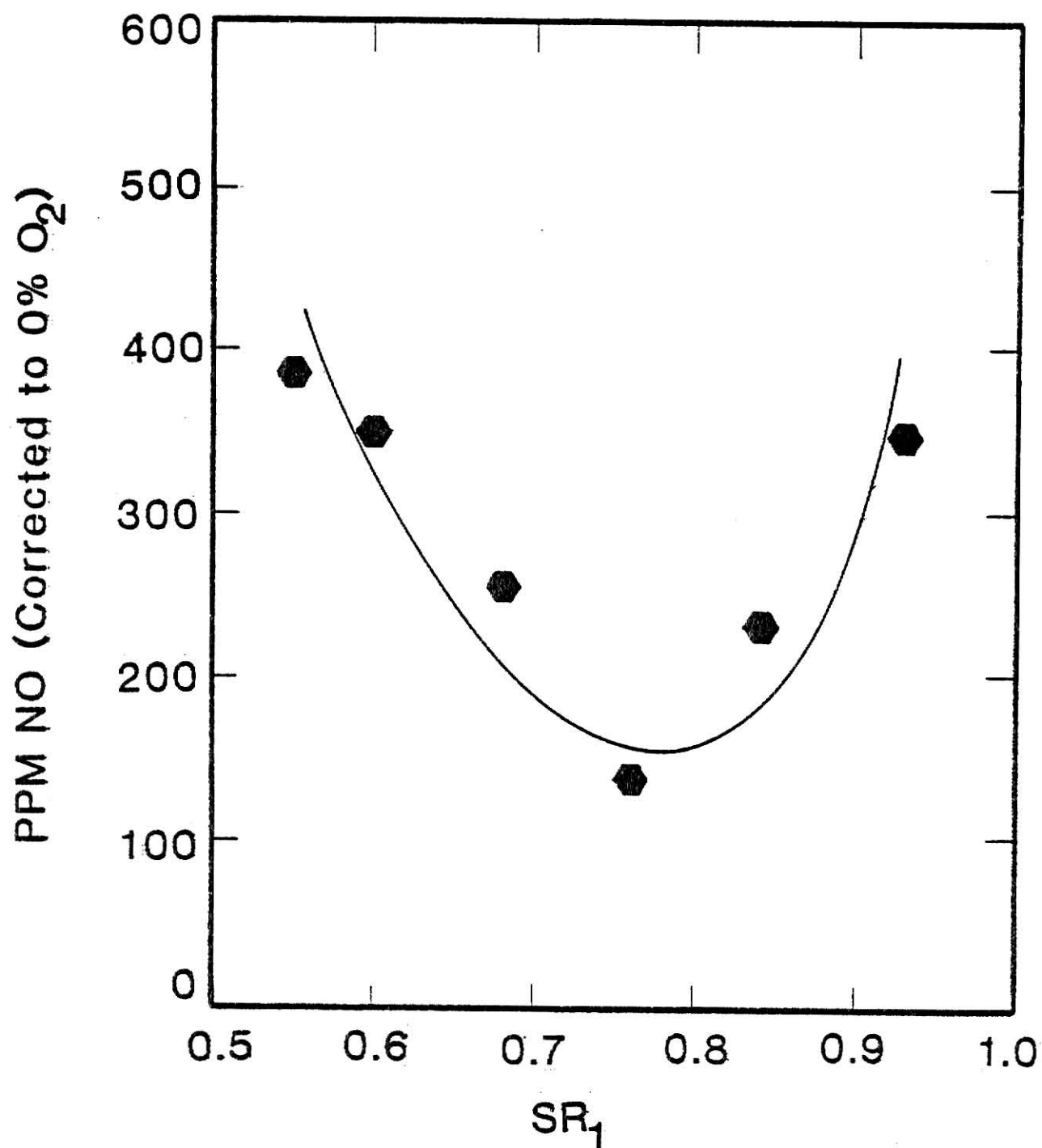


Fig. 4.30 NO_x Emissions vs. First Stage Stoichiometric Ratio (SR_1) for Corn Stover

increased. The minimum exhaust NO_x emissions for the Colorado coal and its mixtures with biomass correspond to about a 10% conversion of total fuel nitrogen, compared to a 23% conversion of fuel nitrogen under unstaged combustion at 3% excess oxygen at the flue.

Why does the concentration of fuel NO_x at the flue reach a minimum and then increase as the SR_1 approaches 1.0? To answer this question, one needs to know that the reactants at the exit of the first stage contain oxidizable nitrogen species in both the gas (NO , HN_3 , HCN) and solid (char nitrogen) phases. Also, the fraction of coal nitrogen converted in the first stage to NO_x decreases and the fraction converted to HN_3 increases with decreasing rank. The conversion of coal nitrogen to HCN appears to be less dependent upon the rank for the coals studied by Pershing.⁽¹⁴⁾

Fig. 4.31 summarizes the influence of coal composition on the distribution of nitrogen species in the gas phase at the exit of the first stage. The data are plotted on a cumulative $\text{NO}+\text{HCN}+\text{NH}_3$ basis and have been corrected to 0% O_2 , dry, neglecting the influence of hydrogen on the total flue gas volume. For bituminous coals (Fig. 4.31a), the HCN concentration in the first stage exceeded the NH_3 concentration at all stoichiometries. Data are shown also for a high volatile bituminous Utah coal (38% volatile matter compared with 33% in Colorado). For lower rank coals (high oxygen content, low fixed carbon), typical data are shown in Fig. 4.31b. At all stoichiometries, the NH_3 concentration exiting the first stage was high, while HCN concentrations were significantly less than NH_3 levels.

Pershing et al.⁽¹⁴⁾ suggests that the ultimate conversion of coal nitrogen to NO_x in the exhaust is independent of the original coal

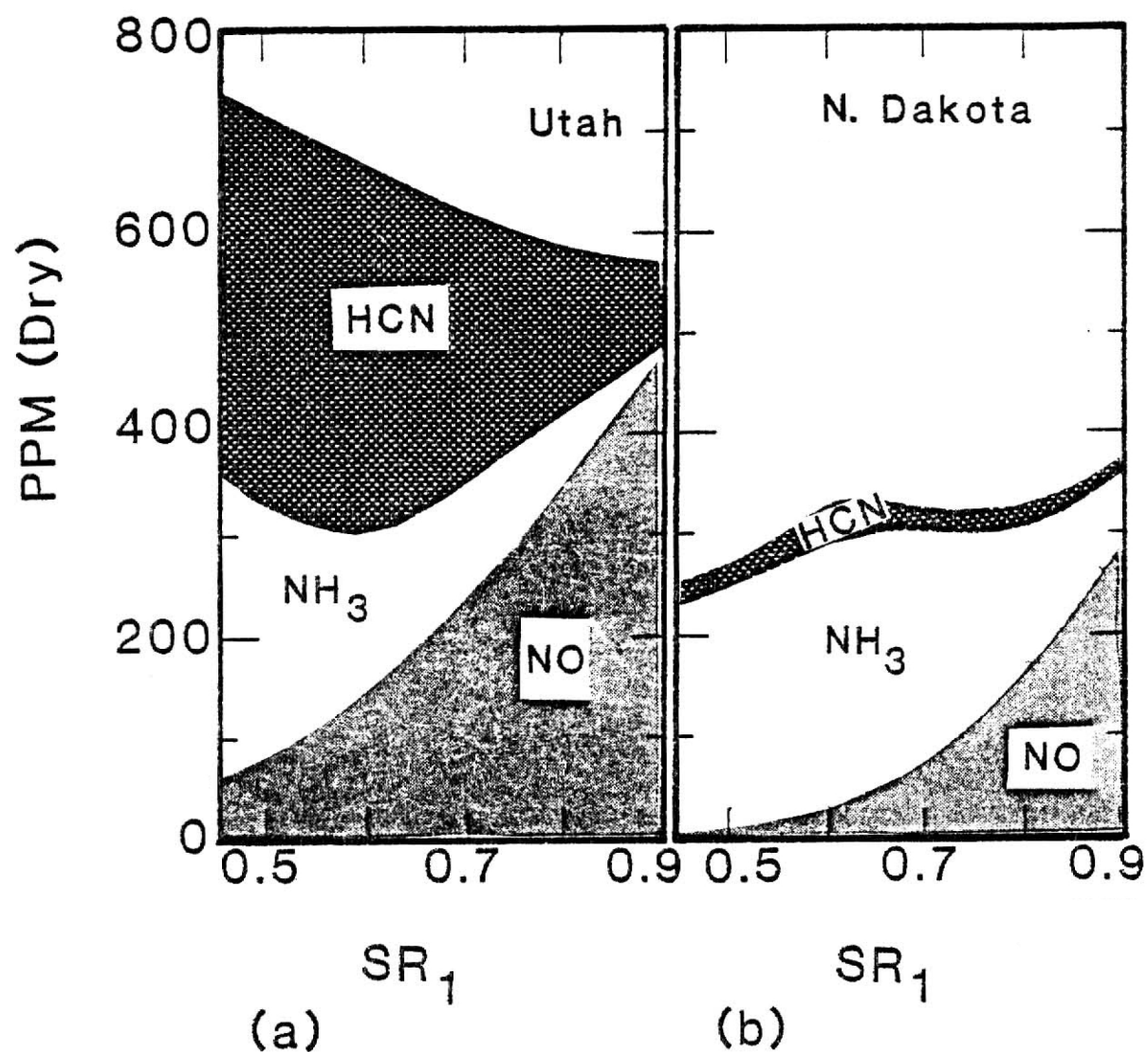


Fig. 4.31 Gas-Phase Distribution of Volatile Nitrogen Species at the Exit of the First Stage for a High Volatile B Bituminous Coal and a Lignite A (after Pershing, et al.¹⁴)

nitrogen remaining at the exit of the first stage. Therefore the increase in NO_x formation in the second stage is due to gas-phase nitrogen species ($\text{HCN} + \text{HN}_3$, NO). The NH_3 and HCN are summed because these species normally occur together under very fuel-rich conditions.

It can also be seen in Fig. 4.32 that as the first stage stoichiometric ratio decreases, the NO_x entering the second stage decreases; however, this is compensated for by an increase in other oxidizable nitrogen gases (HCN , HN_3). The ammonia curve intercepts the curve drawn through the NO_x data at about a SR_1 of 0.8. At a first stage stoichiometric ratio of 0.65, HCN intercepts NO_x . Since HN_3 and HCN exiting the first stage convert to NO_x in the second stage, the NO_x concentration at the flue is large for the $\text{SR}_1 \leq 0.65$. For first stage stoichiometric ratios greater than 0.8, the flue NO_x concentration is high, as expected (see Section 4.1.1). Therefore, the minimum NO_x concentration may occur in the ranges $0.65 \leq \text{SR}_1 \leq 0.8$ for the bituminous coals tested by Pershing. This minimum probably occurs because of the difference in the conversion efficiencies of the oxidizable nitrogen species exiting the first stage.

The minimum NO_x concentrations for fuels used in this research occur for first-stage stoichiometries between 0.7 and 0.8. The minimum NO_x concentration for Colorado coal occurs at $\text{SR}_1 \approx 0.78$. The level of NO_x emissions and the trends with rank under staged combustion from this work are also compared with those of Pershing et al.,⁽¹⁴⁾ as shown in Fig. 4.33. Both the Colorado and Utah coals are high rank high volatile bituminous. On the other hand, biomass fuels with their low fixed carbon, relatively high oxygen, and high volatile matter contents, should behave more as lignite fuels. Indeed, this appears to be the case.

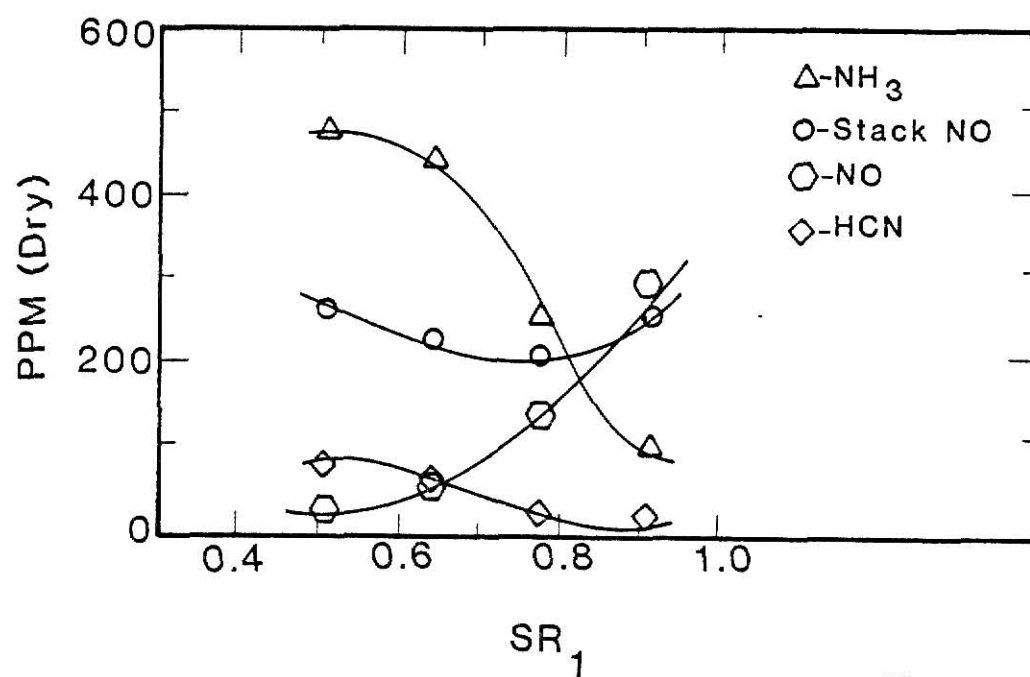


Fig. 4.32 Gas-Phase Distribution of Volatile Nitrogen Species Entering the Second State vs. SR₁ for a North Dakota Lignite Coal (after Perhsing, et al.¹⁴)

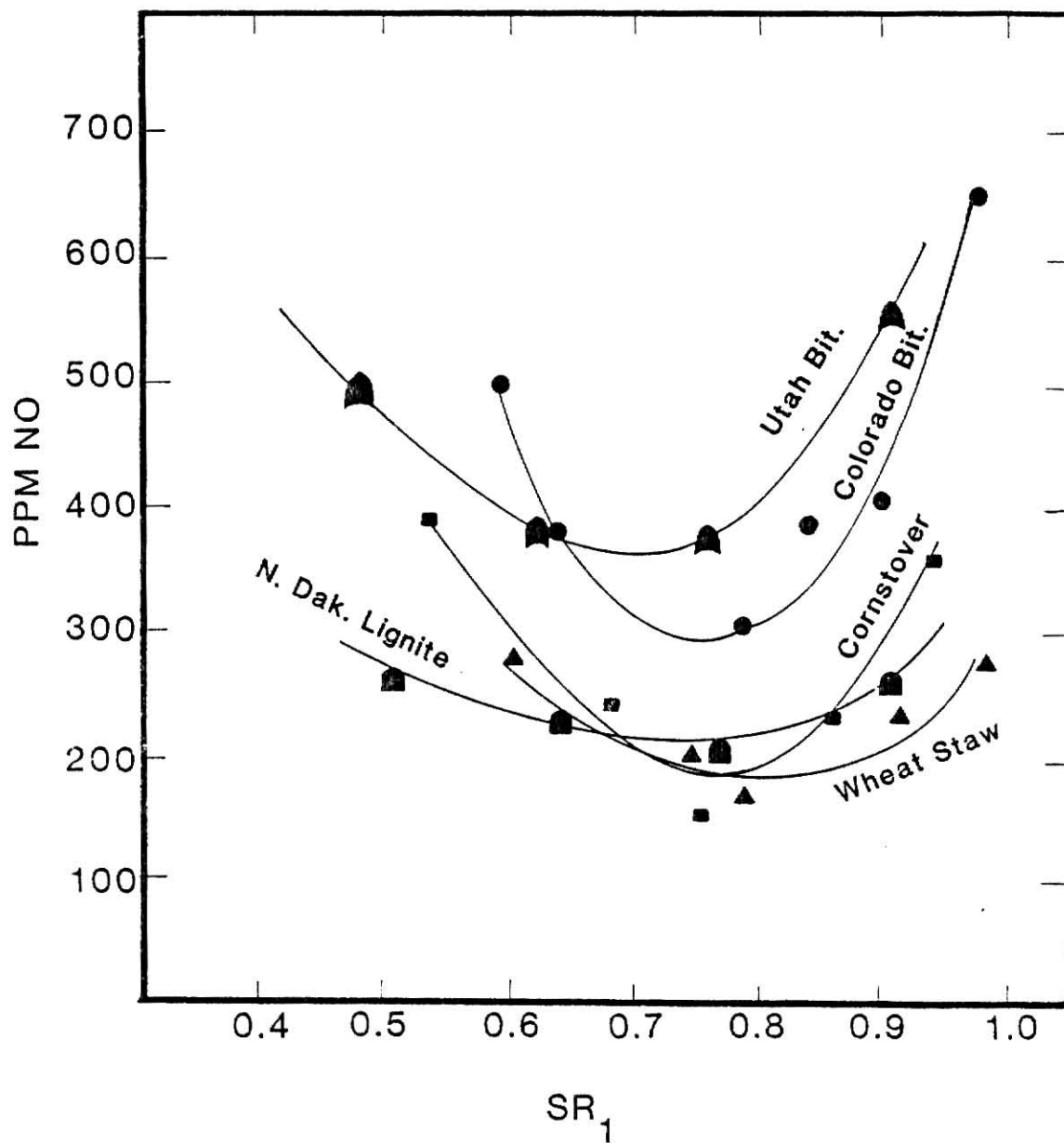


Fig. 4.33 Comparison of Staged NO_x Emissions vs. SR_1 with data of Pershing, et al.¹⁴

4.3 Summary

The NO_x emissions resulting from the suspension firing of agricultural residue and pulverized coal have been examined for the first time. In general, NO_x at the flue increases as the flue excess oxygen increases, reaches a maximum and then decreases for very high O_2 levels. The trends were observed for all fuels tested except wheat straw. When the Colorado coal was mixed with 25% wheat straw by volume, the flue NO_x emissions were greater than expected based on the emissions from each fuel and corrected for mass fraction and furnace temperature. It is suggested that the increased availability of volatile oxygen from the wheat straw facilitates the increased NO_x formation. Similar behavior was observed when corn stover was mixed with coal. The decrease in NO_x emissions for very lean conditions is explained by the corresponding drop in the furnace temperature, Fig. 4.34.

Qualitatively, the axial profiles of the major gaseous species (CO_2 , CO , O_2 , and NO_x) were quite similar except for corn stover. Primarily, NO_x forms in the upper half of the furnace, then its concentration remains approximately constant through the lower half of the combustion chamber. The axial compositions of solids were also determined. It was found that at 75 cm from the burner, more than 90% of the carbon, 95% of the nitrogen, and 97% of the hydrogen of the fuel had been consumed. Any variations in the NO_x emissions from the individual fuels does not reflect a lack of nitrogen evolution from the fuel or incomplete carbon burnout.

In staged combustion, for all fuels tested, as the first stage stoichiometry increased from 0.5, the exhaust NO_x emissions decreased, reached a minimum, and then increased. This minimum was less than 50%

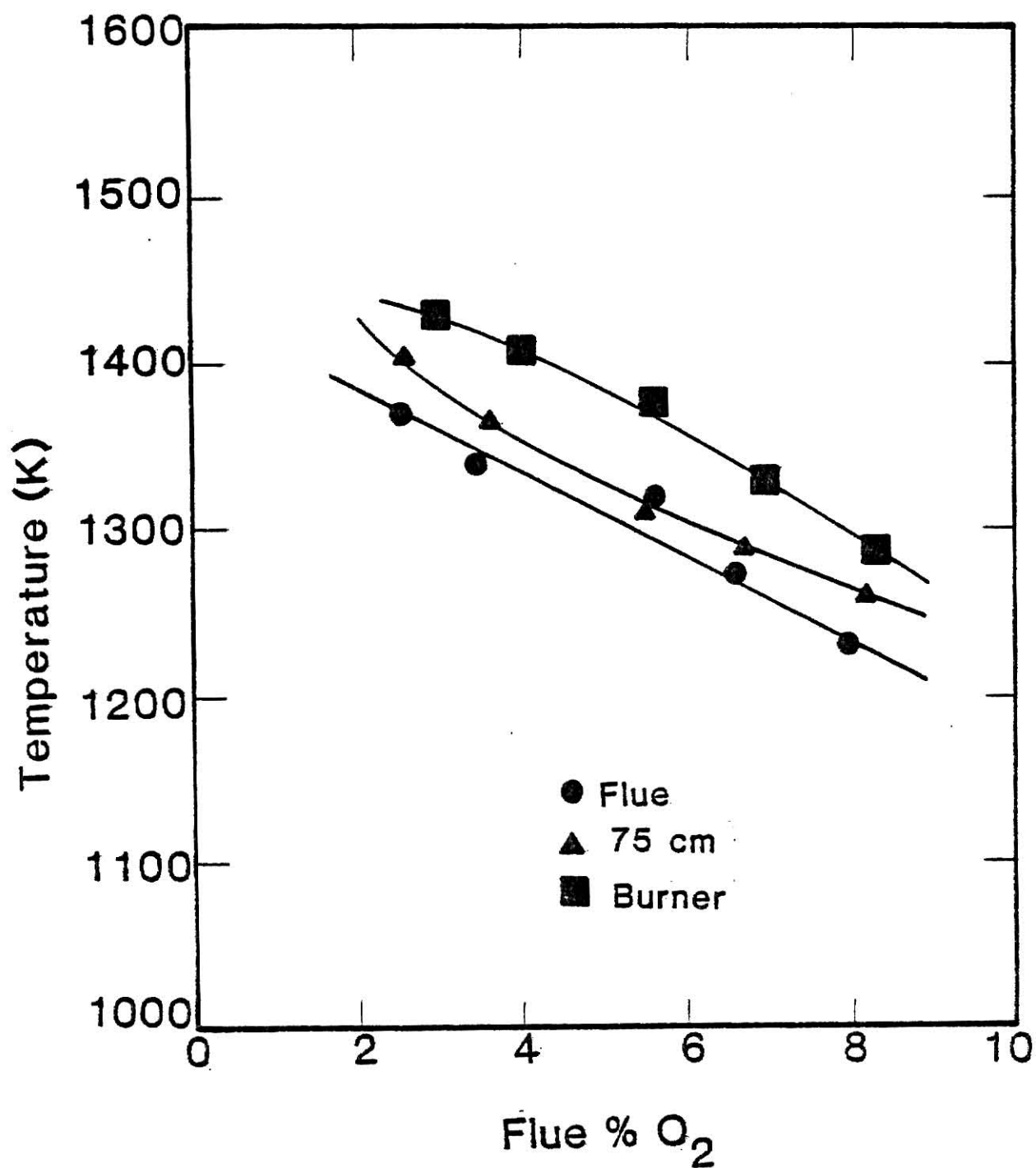


Fig. 4.34 Wall Temperature Profiles vs. Flue % O₂ at the Flue, Mid-Section of the Furnace, and below the Burner

of the NO_x level observed under unstaged combustion at 3% excess oxygen for all fuels. The behavior of the NO_x emissions evidenced from this study suggest that NO_x control strategies using staged combustion can be applied successfully to high volatile nitrogen fuels, provided slagging in the first stage can be avoided. This latter problem may be controlled, perhaps, by proper control of flame temperature, but more likely, through fuel preparation.

References

1. N. Dean Eckhoff, "Use of Crop Residue to Support a Municipal Electric Utility." Center for Energy Studies Report CES 41, Kansas State University, 1979.
2. Energy Technologies and the Environment. U.S. Department of Energy, DOE/EP-0026, June 1981.
3. Richard A. Roenigk, M.S. Thesis, Kansas State University 1983.
4. Electric World, p. 88. April 1981.
5. "Acid Rain," pp. 24-27. EPA-600/9-79-036, July 1980.
6. A.F. Sarofim and J.M. Beér, in The Combustion of Pulverized Coal: Pollutant Formation and Control, edited by A.F. Sarofim, G.B. Martin, W.S. Lanier, and T.W. Lester, (EPA Project Decade Monograph, in press), Chap. 4.
7. Ya.B. Zeldovich, P.Ya. Sadovnikov, and D.A. Frank-Kamenetskii, Moscow-Leningrad: Academy of Sciences of the USSR, Institute of Chemical Physics. Translated by M. Shelef, Scientific Research Staff, Ford Motor Co., 1947.
8. K.A. Bueters, W.W. Habelt, C.E. Blakeslee, and H.E. Burbach, presented at 66th Annual AIChE Meeting, 1973.
9. D.W. Pershing, G.B. Martin, and E.E. Berkau, AIChE Symposium Series 71, (148), p. 19 (1975).
10. J.O.L. Wendt, and D.W. Pershing, Combustion Science and Technology 16, 111 (1977).
11. D.W. Pershing, and J.O.L. Wendt, in Sixteenth Symposium (International) on Combustion, (The Combustion Institute, Pittsburgh, 1976) p. 389.
12. M.P. Heap, T.J. Tyson, and T.M. Lowes, presented at 68th Annual AIChE Meeting, 1975.
13. M.P. Heap, D.W. Pershing, G.C. England, J.W. Lee, and S.L. Chen, in Proceedings of the Third Stationary Source Combustion Symposium, (EPA-600/7-79-050b, 1979), Vol. 2, p. 3.
14. D.W. Pershing, M.P. Heap, and S.L. Chen, in The Combustion of Pulverized Coal: Pollutant Formation and Control, edited by A.F. Sarofim, G.B. Martin, W.S. Lanier, and T.W. Lester, (EPA Project Decade Monograph, in press), Chap. 9.
15. P.R. Soloman, ibid, Chap. 3.

16. W.W. Habelt, presented at 70th Annual AIChE Meeting, New York, NY, 1977.
17. J.O.L. Wendt, Prog. Energy Combust. Sci., 6, 201 (1980).
18. T.J. Howells, J.M. Beér, and I. Fells, Journal of the Institute of Fuel, 33, 521 (1960).
19. William C. Hinds, Aerosol Technology, (Wiley, New York, 1982).
20. J.M. Coulson and J.F. Richardson, Chemical Engineering, (Pergamon Press Ltd., Oxford, 1965).
21. Frank Kreith, Principals of Heat Transfer, 2nd ed. (International Textbook Co., Scranton, PA., 1975).
22. P.W. Atkins, Physical Chemistry. (Oxford University Press, Oxford, 1978).
23. D.R. Stull, and H. Prophet, JANAF Thermochemical Tables, 2nd ed. (National Bureau of Standards, Washington, 1971).
24. Steam/Its Generation and Use. (Babcock & Wilcox Co., New York, 1978).

APPENDIX A

Sampling Flowrate Calculations

Isokinetic sampling is a procedure to ensure that a representative sample of aerosol enters the inlet of a sampling tube when sampling from a moving aerosol stream. This statement is only true if the walls of the sampling probe are infinitely thin. In any real system a damming effect occurs upstream from the probe head⁽¹⁸⁾ (see Fig. A.1).

Experiments conducted by Howells et al. on sampling in pulverized fuel and luminous hydrocarbon flames show that isokinetic sampling gives neither the correct concentration of solid particles nor the correct particle size distribution. It was found for a probe with rounded shoulders that the sampling stream velocity must be 5.5 times the mainstream velocity in order to give a concentration value which is correct to within ± 5 percent.

In this research the inlet of the sampler was aligned parallel to the gas streamlines. The gas velocity entering the probe was adjusted to be approximately 5.0 times the free stream average velocity.

For a free stream velocity V_o and a gas velocity V in the probe, the isokinetic condition for a properly aligned probe is $V_o = V$. To meet this condition, the flowrates in the duct and tube must be directly proportional to their respective cross-sectional areas. For steady, incompressible flow, the relationship between the volumetric flowrates in the sampling probe and in the duct is⁽¹⁹⁾

$$\frac{w_s(T)}{w_o(T)} = \frac{A_s - A_o}{A_o} \quad (A-1)$$

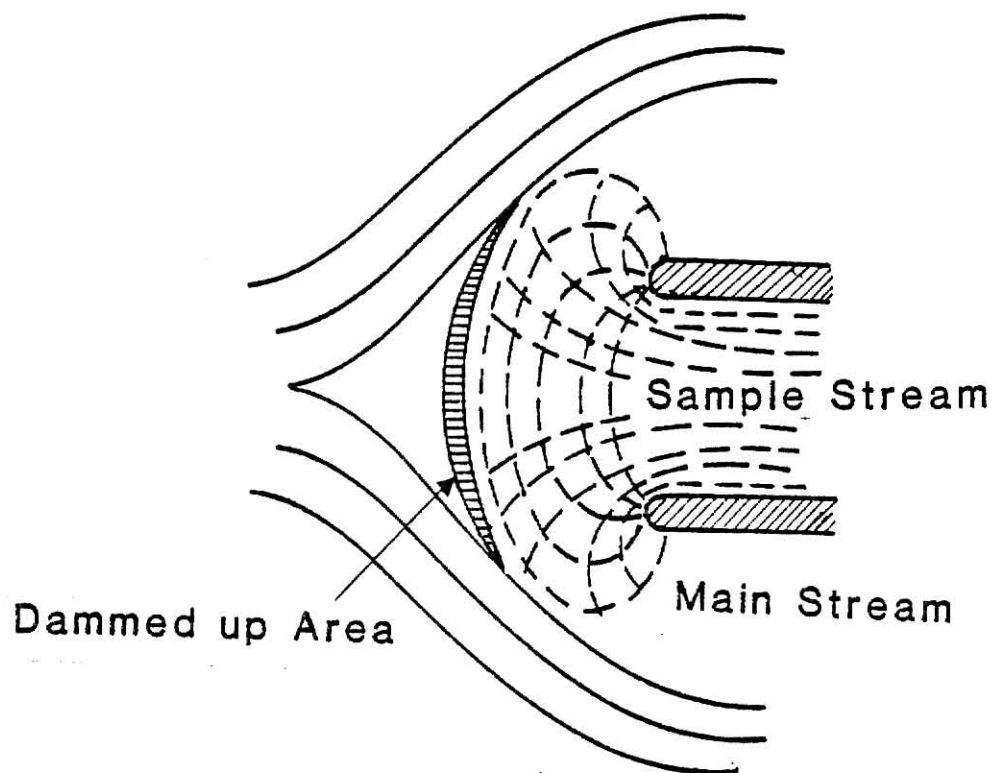


Fig. A.1 Effect of Sampling Probe on Flow Streamlines

where

$w_s(T)$ = sampling probe volumetric flowrate,

$w_o(T)$ = duct volumetric flowrate,

A_s = probes cross-sectional area,

A_o = duct cross-sectional area,

A_Q = quencher cross-sectional area.

The duct volumetric flowrate can be determined to a rough approximation from

$$w_o(T) = \left[\frac{\text{Air}}{\text{Fuel}} + 1 \right] \left[\frac{\dot{m}_o}{\rho(T)} \right] \quad , \quad (\text{A-2})$$

where

$\left(\frac{\text{Air}}{\text{Fuel}} \right)$ = the ratio of the mass flowrate of air compared to the mass flowrate of the solid fuel,

\dot{m}_o = mass flowrate of the solid fuel,

$\rho(T) = \frac{\sum_i m_i x_i}{RT}$ = density of the gaseous products at temperature T and atmospheric pressure,

$\sum_i m_i x_i$ = sum of the products of molecular weights and the percentages of combustion product gases,

R = ideal gas constant.

Substitute equation (A-2) into (A-1),

$$w_s(T) = \left[\frac{\text{Air}}{\text{Fuel}} + 1 \right] \left[\frac{\dot{m}_o}{D_o^2} \right] \left[\frac{D_s^2 - D_Q^2}{D_o^2} \right] \left[\frac{RT}{\sum_i m_i x_i} \right] \quad (\text{A-3})$$

where D_s , D_Q , and D_o are the inside diameters of probe, quencher, and duct respectively.

Since the temperature of the combustion chamber was approximately at the steady state, the axial temperature variation is assumed to be negligible. The combustion products are assumed to 17% CO_2 and 83%

inert nitrogen at 1400 K and atmospheric pressure. Therefore,

$$\begin{aligned}\sum_i M_i X_i &= .17 \times 44 + .83 \times 28 \\ &= 30.72 \text{ gr/mole} \quad .\end{aligned}$$

Substitute all the constants into equation (A-3), and simplify, and one obtains

$$w_S(1400K) = 0.024 \left(\frac{\text{Air}}{\text{Fuel}} + 1 \right) \left(\frac{\dot{m}}{\dot{m}_o} \right) \quad . \quad (\text{A-4})$$

Table (A-1) shows the results for this work.

Table (A-1) Sampling flowrates for fuels tested

Fuel	Air/Fuel (DAF)	$\dot{m}_o \left(\frac{\text{Kg}}{\text{sec.}} \right)$	$w_s \left(\frac{\text{m}^3}{\text{sec.}} \right)^a$
Colorado	10.64	5.40×10^{-4}	1.53×10^{-4}
Mo-Kan	11.61	6.33×10^{-4}	1.92×10^{-4}
Corn stover	7.91	4.60×10^{-4}	0.98×10^{-4}
Wheat straw	6.31	3.75×10^{-4}	0.66×10^{-4}
Colorado/ 50% W.S.	9.62	3.68×10^{-4}	0.94×10^{-4}
Colorado/ 25% W.S.	10.26	4.85×10^{-4}	1.31×10^{-4}
Colorado/ 25% C.S.	10.50	5.04×10^{-4}	1.39×10^{-4}

^aFlowrate measured at 298K at sampling probe outlet.

APPENDIX B

Energy Balance on Furnace System

The consistency of the wall furnace temperature measurements, the fuel and air flow rates can be provided by an energy balance on the furnace. The overall energy balance can be written as,

$$(q)_{\text{gen.}} - (q)_{\text{cond.}} - (q)_{\text{out}} = 0 \quad (\text{B.1})$$

where

- $(q)_{\text{gen.}}$ = The enthalpy of the reaction within the furnace, W;
- $(q)_{\text{cond.}}$ = conduction heat transfer, W;
- $(q)_{\text{out}}$ = enthalpy convected out the flue, W.

These terms are now calculated separately.

B.1 Conduction Heat Transfer Through Furnace Walls.

To calculate the steady state temperature distribution through the furnace wall, it is assumed that the heat flow through the composite structure is one-dimensional, steady state, and the material properties are constant. The thermal conductivities of the different materials used in the furnace construction were provided by the manufacturers. The inside wall temperature was monitored at different locations of the furnace. Fourier's law; equation (B.1.1) is valid in general. Or,

$$q = -KA \frac{dT}{dx} \quad , \quad (\text{B.1.1})$$

where

- q = rate of heat flow by conduction, W;
- K = thermal conductivity of material, W/m-K;

A = the cross-sectional area perpendicular to the heat flow by conduction, m^2 ;

$\frac{dT}{dx}$ = the temperature gradient in the direction of heat flow x , K/m .

Since the length of the furnace is relatively long compared to the wall thickness, it can be assumed the heat flow through the walls is in the radial direction only. Therefore in Eq. (B.1.1), the area is $2\pi r_1 \ell$ where r_1 is the radial location within one of the layers and ℓ is the length of the combustion chamber. It was assumed that to a first approximation, the resistance to heat transfer between the hot combustion gases and the inside wall was negligibly small because of the presence of both forced convection and radiation. The conduction heat transfer through the first layer of the furnace is then,

$$q = -2\pi K_1 r_1 \ell \frac{dT}{dr_1} \quad (B.1.2)$$

Integrating, one obtains,

$$q = \frac{2\pi K_1 \ell}{\ln\left(\frac{r_2}{r_1}\right)} (T_1 - T_2) \quad (B.1.3)$$

where T_1 , the inside wall temperature, was measured during furnace operation to be approximately 1170 K. Likewise, a similar relation can be obtained for the heat transfer in the other two refractory layers and in the outer steel shell of the furnace, thus,

$$q = \frac{2\pi K_2 \ell}{\ln\left(\frac{r_3}{r_2}\right)} (T_2 - T_3) \quad (B.1.4)$$

$$q = \frac{2\pi K_3 \ell}{\ln\left(\frac{r_4}{r_3}\right)} (T_3 - T_4) \quad (\text{B.1.5})$$

$$q = \frac{2\pi K_4 \ell}{\ln\left(\frac{r_5}{r_4}\right)} (T_4 - T_5) \quad (\text{B.1.6})$$

The heat transfer from the outer steel shell to the ambient air occurs via natural convection, primarily, and can be represented by Newton's Law of Cooling as,

$$q = 2\pi r_5 \ell h_\infty (T_5 - T_\infty), \quad (\text{B.1.7})$$

where T_∞ is the room temperature monitored continuously to be approximately 308K and h_∞ is the natural convection heat transfer coefficient ($\text{W/m}^2 \cdot \text{K}$). h_∞ was determined for the vertical surfaces from Coulson.⁽²⁰⁾ The simplified equation for natural convection to air is

$$h_\infty = 1.58 \left(\frac{\Delta T_o}{D_o} \right)^{.25}, \quad (\text{B.1.8})$$

where $\Delta T_o = T_5 - T_\infty$, K;

D_o = outside furnace diameter, m.

One obtains $h_\infty = 6.20 \text{ W/m}^2 \cdot \text{K}$.

At steady state, the heat flow through all the elements must be the same. These equations can be expressed in terms analogous to Ohm's Law and combined to yield a series of resistances to the heat flow.⁽²¹⁾

The result is,

$$q = 2\pi l(T_i - T_\infty) / \left[\ln\left(\frac{r_2}{r_1}\right)/K_1 + \ln\left(\frac{r_3}{r_2}\right)/K_2 + \ln\left(\frac{r_4}{r_3}\right)/K_3 + \ln\left(\frac{r_5}{r_4}\right)/K_4 + \right. \\ \left. 1/r_5 h_\infty \right] \quad . \quad (B.1.8)$$

The thermal conductivities and radii are listed in Table (B-1).

For an inside surface temperature of 1170 K and an ambient temperature of 300 K, the heat loss through the furnace walls is 1.25 kW. The temperature profile of the furnace wall, determined using equation (B.1.9), is shown in Fig. B.1.

B.2 Heat Generation Rates

In this investigation natural gas from the building was used to heat up the combustion chamber. Pipeline quality natural gas was analyzed by a Carle Model 311 gas chromatograph. This analysis was performed repetitively over several days because of the slight daily variations in the natural gas contents. The average gas compositions determined from this procedure were used to determine the heat generation rate.

The amount of energy liberated in the combustion chamber during the reaction of natural gas and air is identified as ΔH , where an exothermic reaction is defined as negative. The energy added to the system at constant pressure is just the change of enthalpy $\Delta H(T)$, which is, (22)

$$\Delta H(T_f) = \Delta H(T_i) + \int_{T_i}^{T_f} \Delta C_p(T) dT \quad (B.2.1)$$

where $\Delta C_p(T)$ is the change in heat capacity of the products and reactant

Table B-1

Layer Geometry and Thermal Conductivities

Thermal Conductivity (kw/m-K)	Radius (m)
$K_1 = 7.09 \times 10^{-4}$	$r_1 = .076$
$K_2 = 2.08 \times 10^{-4}$	$r_2 = .102$
$K_3 = 1.01 \times 10^{-4}$	$r_3 = .123$
$K_4 = 5.19 \times 10^{-2}$	$r_4 = .194$

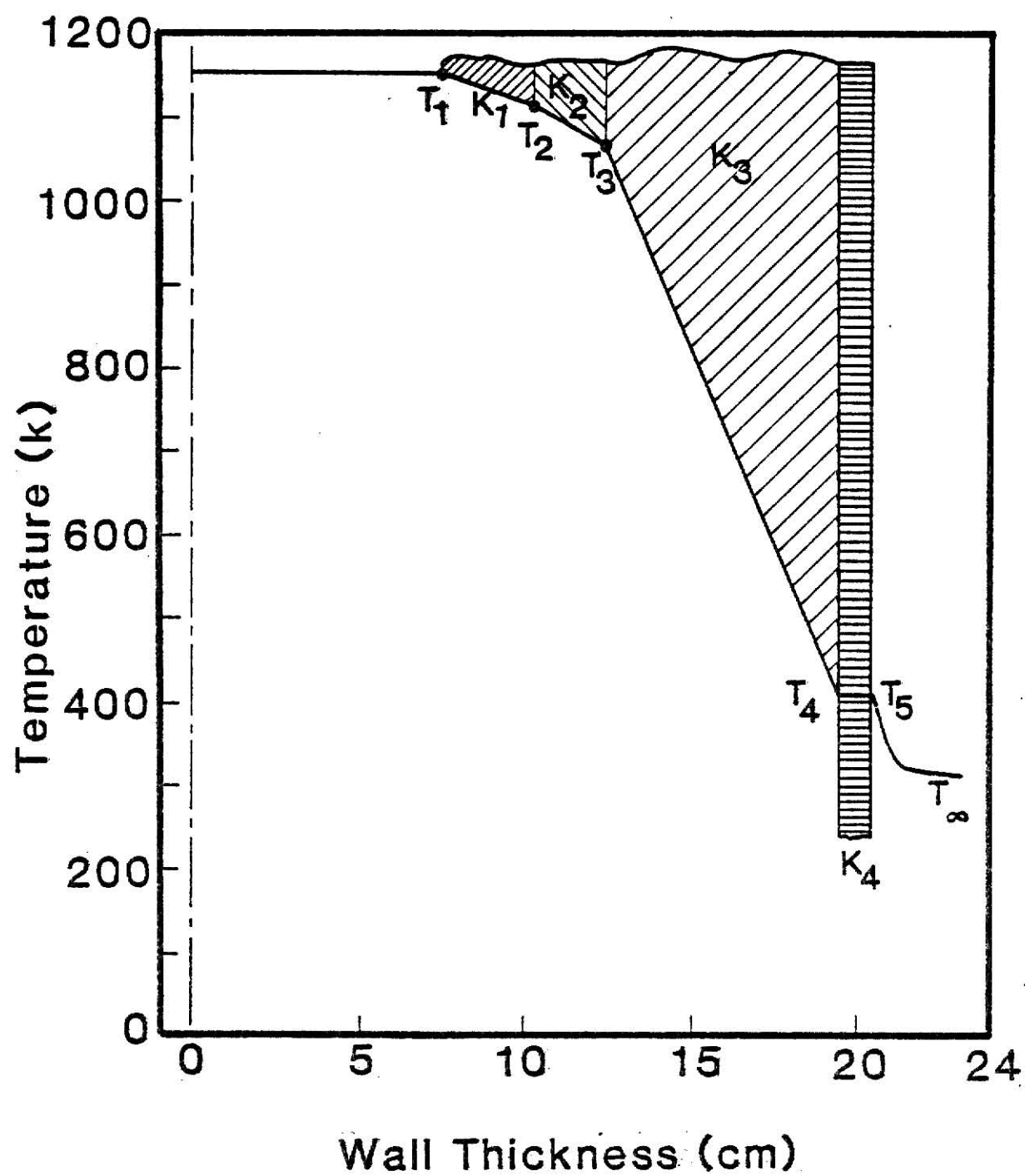


Fig. B.1 Calculated Temperature Profile Through Furnace Wall

over a narrow range of temperatures dT . Often the molar heat capacity can be expressed adequately as,

$$C_p(T) = a + bT + cT^{-2} \quad (\text{B.2.2})$$

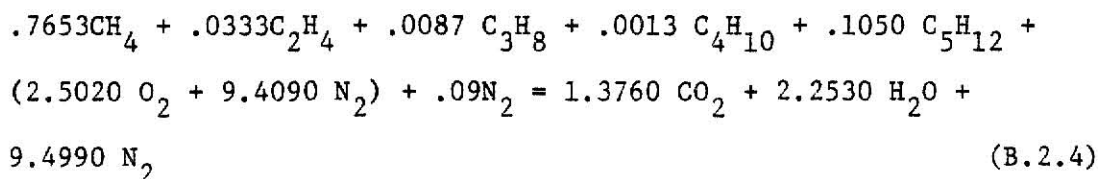
where the constants a , b , and c are determined experimentally at a reference temperature of 298 K. These constants were found from Atkins⁽²²⁾ and are listed for major species of interest in Table B.2.

It has been assumed that the combustion products are formed at 298 K and that the products are then heated to the steady state temperature of the combustion chamber; thus, $\Delta C_p(T)$ in Eq. (B.2.2) is assumed to be $C_p(T)$ for the combustion products CO_2 , H_2O and the inert, N_2 .

Substituting Eq. (B.2.2) into (B.2.1) and integrating over the temperature range of 298-1170 K, it is obtained that

$$\begin{aligned} \Delta H(T_f) &= \Delta H(T_i) + \int_{298 \text{ K}}^{1170 \text{ K}} (9 + bT + cT^{-2}) dT, \\ &= H(T_i) + 875 a + 6.4 \times 10^5 b + 2.5 \times 10^{-3} c. \end{aligned} \quad (\text{B.2.3})$$

Complete combustion of natural gas with air results in the following stoichiometric equation,



For the complete combustion of .0161 moles natural gas/sec, approximately .192 moles of air/sec are required, and 0.208 moles/sec of products are produced.

Table (B.2)
Thermochemical Data

Species	ΔH_f° (298) KJ/moles	a JK mole	JK^{-2} ^b mole	c JK mole
CH ₄	-17.86			
C ₂ H ₄	-20.00			
C ₃ H ₈	-25.07			
C ₄ H ₁₀	-30.05			
C ₅ H ₁₂	-34.98			
CO ₂	-94.26	44.23	8.79×10^{-3}	-8.62×10^5
H ₂ O	-57.79	30.54	10.29×10^{-3}	0
N ₂	0	28.58	3.77×10^{-3}	$-.5 \times 10^5$

The heat of reaction or heat evolved at the reference temperature can be determined as follows,

$$\Delta H(298) = \sum_{i \text{ prod.}} n_i (\Delta H_f^\circ)_{298,i} - \sum_{j \text{ react.}} n_j (\Delta H_f^\circ)_{298,j} \quad (\text{B.2.5})$$

where the ΔH_f° are heats of formation of the various products and reactants. These data are tabulated in the JANNAF Tables⁽²³⁾ and are listed in Table (B.2). Substituting Eq. (B.2.5) into (B.2.3) and using the constants from Table (B.2), it is found that the heat evolved at 298 K is 1012.0 KJ/mole of natural gas. The heat required to increase the temperature of the products to 1170 K is about 392 KJ/mole of natural gas; thus, the net heat release in the combustion chamber is 619.0 KJ/mole of natural gas. Finally, firing .0161 moles/sec of natural gas yields a power output of 9.97 kW.

B.3 Convective Heat Loss

In steady state, the difference in the average bulk temperature between the inlet and outlet of the furnace is a direct measure of the rate of the net convective heat transfer loss from the combustion chamber.⁽²¹⁾ Thus,

$$q = \dot{m} C_p T \quad (\text{B.3.1})$$

where

q = rate of heat transfer, W;

\dot{m} = mass flowrate, (kg/sec);

C_p = specific heat at constant pressure, J/kg·K;

T = gas temperature (K).

The heat capacity of the combustion products at 1170 K and constant pressure was determined for CO_2 , H_2O , and inert N_2 to be 5.39×10^{-2} , 4.26×10^{-2} and 3.29×10^{-2} KJ/moles-K⁽²²⁾ respectively. The combustion products contain 10.50% CO_2 , 17.16% H_2O and 72.36% N_2 ; thus, the convective loss from the combustion chamber is

$$\begin{aligned}
 & 0.208 \frac{\text{moles}}{\text{sec}} \times \left(0.105 \frac{\text{moles } \text{CO}_2}{\text{moles}} \times 5.39 \times 10^{-2} \frac{\text{KJ}}{\text{mole} \cdot \text{K}} + \right. \\
 & \quad 0.172 \frac{\text{moles } \text{H}_2\text{O}}{\text{moles}} \times 4.26 \times 10^{-2} \frac{\text{KJ}}{\text{mole} \cdot \text{K}} + \\
 & \quad \left. 0.724 \frac{\text{moles } \text{N}_2}{\text{moles}} \times 3.29 \times 10^{-2} \frac{\text{KJ}}{\text{mole} \cdot \text{K}} \right) \times 1170 \text{ K} \\
 & = 8.96 \text{ kW} .
 \end{aligned}$$

The summation of the energy terms is thus,

$$q_{\text{cond}} + q_{\text{out}} = q_{\text{gen.}}$$

$$1.25 + 8.96 = 9.97$$

$$10.21 \approx 9.97 .$$

Thus, the system energy balance is closed to within 3%.

B.4 Heat Generation from Solid Fuel

In the case of solid fuels, the approximate heating value can be determined if the ultimate chemical analysis of the fuel is known. Dulong's formula⁽²⁴⁾ gives reasonably accurate results (within 2-3%) for most coals and is often used as a routine check for values determined by calorimeter:

$$q\left(\frac{\text{J}}{\text{gr}}\right) = [14544 \text{ C} + 62028 (\text{H}_2 - \text{O}_2/\text{B}) + 4050 \text{ S}] \times 2.326, \quad (\text{B.4.1})$$

where C, H₂, O₂, and S are the percentage of each species by ultimate analysis. Table (B-3) shows the heating value for the fuels used in this investigation.

Table (B-3)
Calculated Heating Values

Fuel	q (KJ/gr)
Colorado	32.92
Mo-Kan	35.96
Corn stover	24.07
Wheat straw	19.01
Colorado + 50% Wheat straw	29.51
Colorado + 25% Wheat straw	31.57
Colorado + 25% Corn stover	32.25

APPENDIX C

Calculation of Air Flowrate Through the Funnel

Solid fuel is transported to the combustion chamber by the primary air flowrate (see Fig. 2.5). Along a stream line, for steady, incompressible, frictionless flow, according to Bernoulli's equation, at a choke where the velocity of the flow is maximum, the pressure is minimum. Therefore, the negative pressure with respect to atmosphere at the throat will produce a flow of air through the funnel. This flowrate may be determined from cold flow measurements via

$$.21w_1 = a(w_1 + w_2) \quad (C-1)$$

where,

w_1 = unknown volumetric flowrate of air through the funnel,

a = measured percent oxygen in the furnace,

w_2 = primary air volumetric flowrate.

To determine a , N_2 was used instead of air in the primary leg of the air supply system to the burner. The sampling probe was used to extract gas samples that were analyzed by the Beckman O_2 analyzer. Results of this test are shown in Fig. C.1 where the volumetric flowrate of air through the funnel is plotted versus the volumetric flowrate of N_2 through the primary leg.

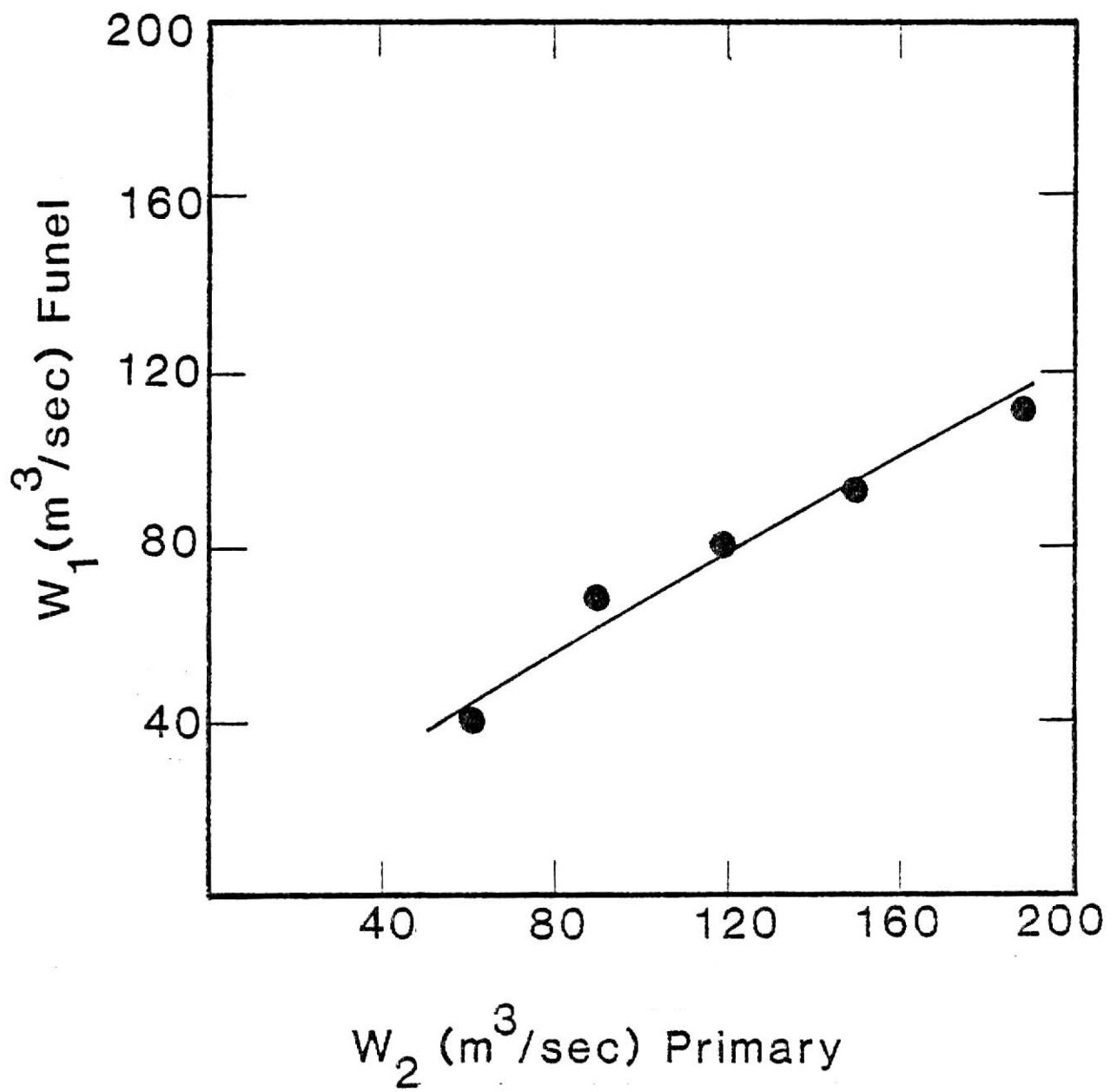


Fig. C.1 Funnel Air Flowrate as a Function of Measured Primary Air Flowrate

APPENDIX D

D.1 Flame Safeguard Unit

The flame safeguard unit diagram is shown in Fig. D.1. The purpose of the unit is to disconnect the power supply to the systems supplying fuel to the furnace if a potentially dangerous situation arises. Line voltage is applied through the power switch on the control panel, through three other safety cutoffs, through the flame safeguard switch on the control panel, and to terminals 1 and 6 of the unit. The unit has a total of 10 terminals. Terminal 2 grounds the unit, while 1 and 6 provide the power for the safeguard. The two terminals marked T are connected to each other and F and G accommodate the leads from the ultraviolet flame detector. These can be denoted signal terminals, and they enable other terminals whenever T and T are connected and the proper signal (corresponding to a flame in the detector's line of sight) is fed to F and G. The remaining terminals 3, 4 and 5 are output terminals, but the signal timing at each is not identical.

Terminal 3 accommodates the leads for the pilot gas and pilot air solenoid valves and is at ground except when the unit is enabled or in the startup mode. Terminal 4 is attached only to the pilot assembly ignition transformer, and is held at ground except during startup. Terminal 5 supplies line voltage to the main gas supply line solenoid valve and to a solenoid actuated relay that controls the application of the 220 V., three phase power for the feeder. This terminal is closed to line voltage only when the flame safeguard is enabled. Each of the circuits mentioned has a separate switch on the control panel so that in addition to the flame safeguard, manual control is also required.

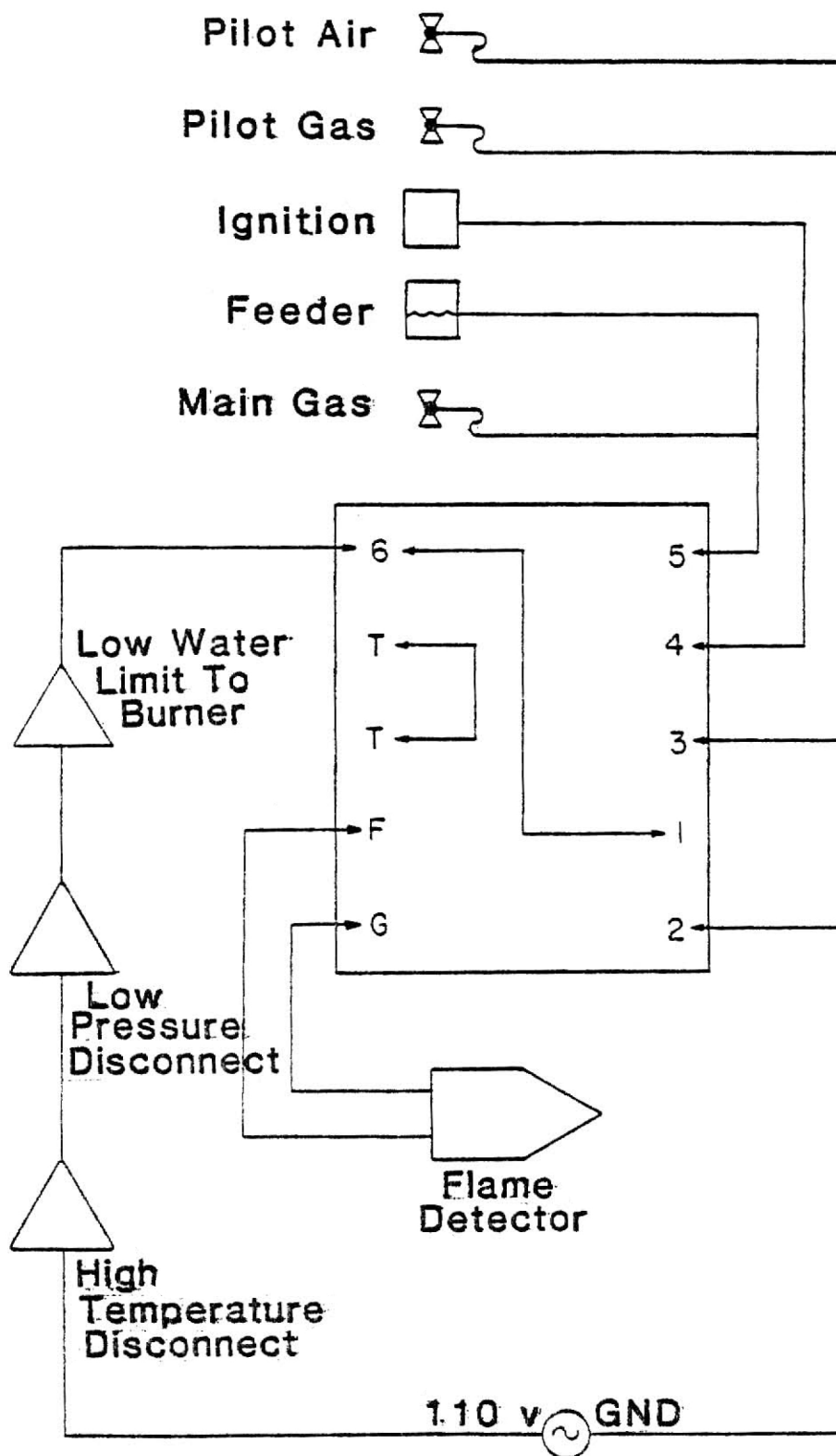


Fig. D.1 Wiring Diagram for Flame Safeguard

As indicated above, there are two operational modes for the flame safeguard unit. When the proper signals appear at the input terminals and power is applied at terminals 1 and 6 the unit is in the enabled mode. If no flame is present, but a manual signal is received, (either by turning on the power to the unit or operating the unit's RESET button) the unit is in the startup mode. The enable state is a steady state which remains until some external impetus is received, i.e., either the power to the unit is disconnected or a required signal is lost. The startup mode is finite and lasts only as long as a self-contained thermistor's resistance is below a certain level or a signal is received at terminals F and G. If the thermistor's resistance exceeds the limit, the RESET button pops out and breaks the connection of line voltage to terminals 1 and 6. If a flame is achieved, i.e., a signal is received at F and G, the unit automatically enters the enabled mode.

During the startup, power is applied to the pilot gas, the pilot air, and the ignition transformer. As soon as the pilot flame lights, the flame detector signals the flame safeguard, which shuts down the ignition transformer and applied line voltage to the main gas line and feeder. Under normal operation, the manual switches for these two systems are kept open until the pilot is lit. Then, the main gas switch is closed to light the gas flame or the feeder is started to ignite the solid fuel flame. Since these are achieved in the enabled mode, this continues until either the flame is extinguished or the system is manually shut down.

APPENDIX E

Furnace Operating Procedure

To protect the operator, instrumentation, and other equipment used in this experiment, the following procedures should be strictly followed. A sketch of the equipment control panel is given in Fig. E.1, to help in the interpretation of the instructions.

A. EMERGENCY PROCEDURE: In case of an emergency with a hot furnace, the following steps will shut off the fuel supply system.

1. Turn off the flame safeguard;
2. turn off both pre-heaters;
3. lower the sampling probe.

B. PRE-STARTUP:

1. Check the compressor oil level and its safety pressure release valve;
2. blow out air through the spit valve located on the bottom of the compressor;
3. check the refrigerator line to make sure it is not frozen solid;
4. turn the compressor on and open the main air valve located at the end of the tank;
5. turn on cooling water for,
 - 5.1 burner (check the water flow rate limit switch),
 - 5.2 sample probe, and
 - 5.3 flue gas jacket;

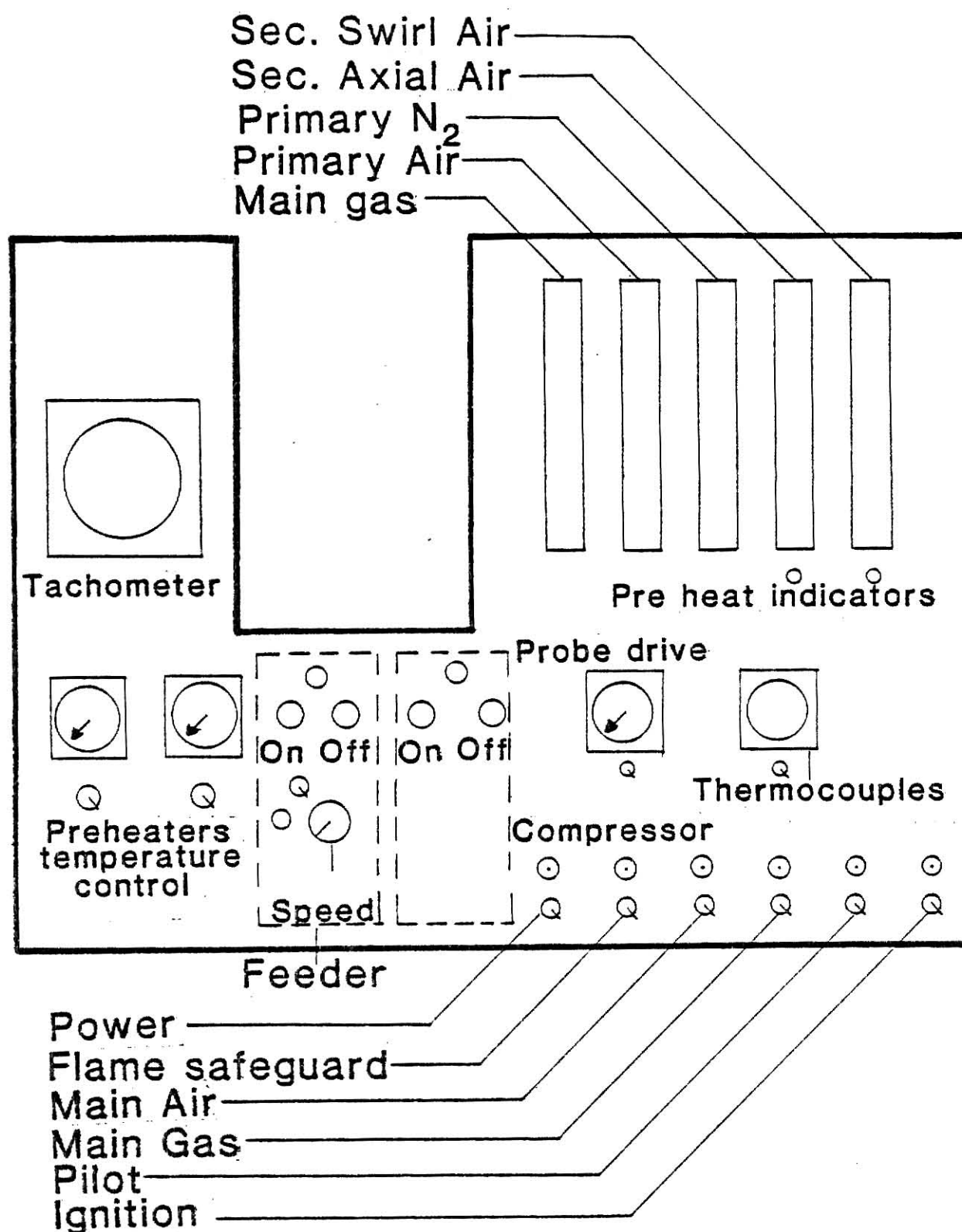


Fig. E.1 Control Panel Configuration

6. clean the observation port;
7. reset the low pressure switch (80 psig);
8. check the high temperature limit switch (390 K);
9. open main gas, pilot gas, pilot air valves (located on top of the furnace);
10. make a visual check of thermocouples;
11. turn on power breaker boxes for feeder and preheaters;
12. replace all air filter elements;
13. fill the ice bath with ice.

C. STARTUP:

1. Shut off all the flowmeters;
2. open the manual main air and main gas valves (located under the control panel);
3. turn on the following switches on the control panel,
 - 3.1 power,
 - 3.2 thermocouple indicator (check the thermocouples electronically),
 - 3.3 flame safeguard,
 - 3.4 pilot gas,
 - 3.5 ignition,
 - 3.6 main air.

NOTE: If the flame safeguard indicator does not remain on, then repeat steps 5.1, 7, 8 of Section B and push the safeguard box button. If the flame safeguard cycles off, on, and finally off, then the pilot could be oxidized, and needs to be replaced.

At this stage the control panel should show the following indicator lamps on:

compressor,
power,
flame safeguard,
pilot,
main air, and
thermocouple indicator.

4. Adjust the two secondary flow meters to 300 SCRH;
5. turn on the main gas switch;
6. adjust the gas flow meter to 50 SCFH;
7. turn on the air pre-heaters and set the temperature to 500 K.

NOTE: Wait 5-10 minutes, then turn off pilot and ignition and remove the pilot from the combustion chamber to within the furnace wall. This protects the tip of the pilot from oxidation. The following indicator lights should now be on:

compressor,
power,
flame safeguard,
main air,
main gas,
thermocouple indicator, and
pre-heaters # 1 & # 2.

8. Turn on the exhaust fan;

9. calibrate the on-line analyzers by:

- 9.1 opening the hand pressure valve of the calibration bottle (be sure the low pressure valve is closed),
- 9.2 opening the corresponding valve on the manifold (mounted on the wall above the calibration gas bottles,
- 9.3 adjusting the total gas flowrate at ~ 2 liter/min (furnace room),
- 9.4 setting the flow rates for the analyzers as follows,
 - CO, 0.5 liter/min,
 - CO₂, 0.5 liter/min,
 - O₂, 0.25 liter/min, and
- 9.5 waiting 2-5 minutes for the purge of the calibration gas to be sufficient for the analyzers to stabilize.

D. SOLID FUEL COMBUSTION:

After a furnace temperature of about 1270 K is reached, solid fuel can be injected while the main gas is still on. Gradually the solid fuel to natural gas ratio should be increased until a stable and a more luminous flame is produced. In addition, the pilot now can be moved into the combustion chamber and ignited to insure the stability of the flame.

The following precautions should be taken:

- 1. Check for enough solid fuel;
- 2. adjust the primary air to about 250 SCFH;
- 3. turn on the motor for the flexible rod at the top of the funnel;

4. turn on the feeder. The following should be observed:
 - 4.1 tachometer should read 25 RPM;
 - 4.2 the feeder speed control should be zero psig.
5. Increase the feeder speed control very slowly. Under no cases should it exceed 10 psig.

NOTE: If the feeder does not start after pushing the start button on the control panel, check the following:

- a. power breaker box in furnace room;
- b. if a is checked but still feeder does not stay on, the air pressure to the feeder may not be enough to crank the feeder motor; thus, turn off all air flow meters momentarily, and start the feeder. Increase the air flowrate until the oxygen analyzer indicates 3.0%.

E. SHUT-DOWN PROCEDURE:

1. Short term shut-down:
 - 1.1 shut the feeder off;
 - 1.2 lower the main gas flowrate to 10 SCFH;
 - 1.3 turn off the pre-heaters;
2. Long term shut-down:
 - 2.1 Shut down the following,
 - 2.11 feeder;
 - 2.12 pre-heaters;
 - 2.13 main gas;
 - 2.14 flame safeguard;
 - 2.2 increase the primary and secondary air flow rates;

- 2.3 turn off the pump to the analyzers and connect the analyzer inlets to the atmosphere;
- 2.4 turn the refrigerator temperature control to the minimum position.

NOTE: After the furnace temperature is down to about 400 K, the following procedures should take place:

- 2.5 turn off the compressor and shut off its valve;
- 2.6 turn off the flow meters and main air switch;
- 2.7 shut off the manual main air and main gas valves;
- 2.8 shut off the water cooling line;
- 2.9 turn off power breaker boxes;
- 2.10 turn off the thermocouple end power switches.

ACKNOWLEDGEMENTS

The author would like to express his deep gratitude to Dr. Thomas W. Lester, major advisor, and Dr. Josef F. Merklin, an expert in gas chromatographic and mass spectrometric analysis, for their guidance and support throughout this study. Their professional manner in solving many problems to their true level of significance will always be remembered.

Thanks is extended to Dr. Galen King for his assistance and sharing his great experience in trouble shooting of instrumentations. The help of Richard Roenigk in construction of furnace was appreciated. Thanks is also extended to Don Schmidt whose help in maintaining and operation of the facility and collection of data was beyond our expectations. The contribution of Mr. Bill Starr, who maintained the equipment and provided troubleshooting support cannot be neglected. The inconspicuous but vital contributions of Connie Schmidt, who typed the manuscripts and Barbara Wieliczka, who performed the drafting work, are gratefully acknowledged.

Finally, an inestimable amount of credit is due to the author's wife, Rebecca, for her love, encouragement, and unnatural ability to occupy herself and raising our lovely daughter Mariam during the long hours the author was engaged with the project.

SUSPENSION FIRING OF RESIDUE/COAL MIXTURES:
NO_x FORMATION AND CONTROL

by

Hossein Sadeghi Zamani

B.S., Kansas State University, 1980

AN ABSTRACT OF
A MASTER'S THESIS

Submitted in partial fulfillment of the
requirements for the degree

MASTER OF SCIENCE

Department of Nuclear Engineering

KANSAS STATE UNIVERSITY

Manhattan, Kansas

1983

ABSTRACT

Suspension Firing of Agricultural Residue/Coal Mixture: NO_x Formation and Control

The combustion of readily available agricultural and forest residues is one alternative to increasingly interruptable natural gas supplies for municipal utilities and small industries in the Great Plains. Since the agricultural residues, in particular, contain between 1 and 2% nitrogen on an as fired basis, the potential exists for greatly enhanced release of NO_x from these stationary units. Furthermore the nitrogen exists primarily in labile moieties; thus, the conversion of fuel-bound nitrogen could be considerably greater than for coal. To study this possibility, a cylindrical, refractory lined, down-fired furnace firing up to 5 kg/hr of pulverized fuel has been employed. On-line monitoring of major gaseous products of reaction and NO_x , and batch sampling with subsequent wet chemical analysis of NH_3 and gas chromatographic analysis of HCN, were used to follow the conversion and reduction of NO_x . The percentage conversion of the fuel-bound nitrogen was found to be greater than that observed in pulverized coal combustion, but less than the percentage conversion for liquid fuels. The efficacy of staging in suppressing NO_x emissions has been determined by using a staging choke midway along the axial dimension of the flame. The results of such control techniques were found to be variable with respect to pulverized coals because of the large amounts of fuel-bound oxygen in the agricultural fields.